Archive Copy
36274

UM-HSRI-76-26-1

Predicting the Braking Performance of Trucks and Tractor-Trailers

Phase III Technical Report

C.B. Winkler
J.E. Bernard
P.S. Fancher
C.C. MacAdam
T.M. Post

Project 360932

Truck and Tractor-Trailer Braking and Handling Project

June 1976

Highway Safety Research Institute/University of Michigan

Technical Report Documentation Page

1. Report No. UM-HSRI-76-26-1	2. Government Accession No.	3. Recipient's Catalog No.
4. Title and Subtitle PREDICTING THE BRAKING PERFORMANCE OF TRUCKS AND TRACTOR-TRAILERS Phase III Technical Report		5. Report Date June 15, 1976
		6. Performing Organization Code
7. Author(s) C. Winkler, J. Bernard, P. Fancher, C. MacAdam, T. Post		8. Performing Organization Report No. UM-HSRI-76-26
9. Performing Organization Name and Address Highway Safety Research Institute The University of Michigan Huron Parkway & Baxter Road Ann Arbor, Michigan 48109		10. Work Unit No. (TRAIS) 360932
		11. Contract or Grant No.
12. Sponsoring Agency Name and Address Motor Vehicle Manufacturers Association 320 New Center Building Detroit, Michigan 48202		13. Type of Report and Period Covered
		14. Sponsoring Agency Code
15. Supplementary Notes		

16. Abstract

This report documents three digital computer programs for predicting the braking performance of commercial highway vehicles. The computer programs were developed by the Highway Safety Research Institute of The University of Michigan under the sponsorship of the Motor Vehicle Manufacturers Association. The three programs are applicable to straight trucks, tractor-semitrailers, and doubles combination vehicles. The programs model these vehicle types in detail and include the effects of tandem suspension dynamics, air brake system dynamics, brake fade, antilock system performance, and sprung mass dynamics.

The research studies leading to the development of the programs are discussed. The report concludes with a discussion of appropriate applications of these programs, and with a recommendation for further research into the areas of truck tire mechanics, the mechanical friction brake, and antilock systems.

17. Key Words commercial vehicles, truck, tractor-trailer, doubles, braking performance, tandem suspension, fade, antilock, simulation, tires, dynamics, brakes		18. Distribution Statement Unlimited	
19. Security Classif. (of this report) None	20. Security Classif. (of this page) None	21. No. of Pages 215	22. Price

Form DOT F 1700.7 (8-72) Reproduction of completed page authorized

☆ U. S. GOVERNMENT PRINTING OFFICE : 1973 725-504/328

UM-HSRI-76-26-1

PREDICTING THE BRAKING PERFORMANCE OF TRUCKS AND TRACTOR-TRAILERS

Phase III Technical Report

C. B. Winkler
J. E. Bernard
P. S. Fancher
C. C. MacAdam
T. M. Post

Project 360932

Truck and Tractor-Trailer Braking
and Handling Project

June 1976

Sponsored by

The Motor Vehicle Manufacturers Association

TABLE OF CONTENTS

FOREWORD

This report supersedes the material presented in an earlier report, "A Computer Based Mathematical Method for Predicting the Braking Performance of Trucks and Tractor-Trailers," by R. W. Murphy, J. E. Bernard, and C. B. Winkler, dated September 15, 1972. Also, the computer program described in this report supersedes the computer program associated with the earlier report.

1.0 INTRODUCTION

Since mid-1971, the Highway Safety Research Institute (HSRI) has been conducting research under the sponsorship of the Motor Vehicle Manufacturers Association (MVMA) to develop computer-based methods for analyzing and predicting the steering and braking performance of commercial motor vehicles. The initial achievements of this research work were presented in two major reports: (1) "A Computer Based Mathematical Method for Predicting the Braking Performance of Trucks and Tractor-Trailers," September 1972, and (2) "A Computer Based Mathematical Method for Predicting the Directional Response of Trucks and Tractor-Trailers," June 1973 (References [1]* and [2], respectively). The first report presented a comprehensive mathematical description (model) of the braking dynamics of commercial vehicles, including detailed representations of air system dynamics, braking systems, tandem suspensions, tire shear force performance, and wheel rotational dynamics. That report also included descriptions of methods for obtaining the vehicle parameters needed to use the simulation, and comparisons between vehicle test results and predicted results to validate the capabilities of the computer-based methods. The second report described a performance prediction method which contained all of the brake, suspension, and tire modeling features contained in the straight-line braking performance program, plus the possibility for lateral, roll, and yaw motions of the vehicle. As with the first program, this second program was validated against experimental test results on both straight trucks and articulated vehicles. The development of these computer programs constituted Phases I and II of the motor truck research study.

---

*Numbers in square brackets designate references given in Section 4.

During Phase III, the work of Phases I and II was extended significantly in the following studies:

1. Refinement of tandem-suspension models already developed, and the formulation of models for five additional suspension types.

2. Development of over-the-road equipment for measuring the longitudinal shear force characteristics of truck tires.

3. Development of models for typical truck anti-lock braking systems.

4. Extension of the straight-line braking program to include provision for simulating a doubles (tractor-semitrailer-trailer) combination.

5. Development of a brake temperature model to be used for simulating the decrease in brake effectiveness as a result of fade.

The results of these studies have been used to improve the existing computer programs by modifying and changing them appropriately as new models and component-representations have been formulated.

Detailed papers have been presented on the technical and scientific aspects of the work performed in Phases I, II, and III of this investigation. References 1 through 18 provide a bibliography of papers and reports related to the motor truck braking and handling project.

This report documents (under one title) the refined straight-line braking computer program which has been developed from the research activities conducted since the initial braking performance program was completed. These refinements are extremely important because, in response to FMVSS 121, all (or nearly all) new commercial vehicles will be equipped with antilock braking

systems. Thus, a useful simulation must be able to predict the interaction of antilock system performance with brake characteristics, tandem suspension dynamics, tire shear force properties, and wheel rotational dynamics during braking maneuvers. The simulation described in the next section is intended to provide this type of predictive capability.

In Section 2.0, the simulation methods are described from the user's point of view. The meaning of the input data is explained in the order that it is entered into the computer. Example results illustrating the important features of the simulation are presented. Due to the size and comprehensiveness of the mathematical model used to describe the motor truck, Section 2 is divided into the following subsections:

2.1 Suspension Options

2.2 Input Data for the Sprung Mass

2.3 The Brake Models

2.4 The Tire Models

2.5 The Antilock Models

2.6 Rough Road

The body of this report ends with a discussion of (1) the application of this simulation in predicting the braking performance of commercial vehicles, (2) other approaches to predicting braking performance, and (3) recommendations for research studies to attain an improved understanding of commercial vehicle braking.

The details of the computer subprograms are relegated to several appendices. The titles of these appendices are:

A - Program Flow Diagrams
B - The Suspension Models
C - The Sprung Mass Models
D - The Brake Models
E - The Antilock Model

2.0 DESCRIPTION OF THE SIMULATION MODEL

The Phase III simulation program actually consists of three individual digital computer program groups, one each for the simulation of the straight-line braking performance of straight trucks, tractor-semitrailers, and doubles combination vehicles. In addition, a single group of subprograms, which model elements common to each class of vehicle (viz., suspension, brake, and antilock systems plus road profile) is employed in the operation of each of the three main programs. Finally, the IBM system subroutine HPCG performs the digital integration of the state variables.

For purposes of identification, the following I.D. symbols are applied to the four program groups:

I.D.	Program Groups
PH3S	Phase III - Straight Truck
PH3A	Phase III - Articulated Vehicle (tractor-semitrailer)
PH3D	Phase III - Doubles
PH3	Phase III - Support Subprograms

This organization of programs has allowed for efficiency both in terms of program writing and use. The separation of vehicle types into individual programs simplified program writing and limits the volume of "excess baggage" carried by the program in actual use. The use of a group of supportive subprograms common to each of the vehicle programs alleviates the need for repetitive programming of sub-system operation and lowers the volume of computer memory needed to operate the programs.

Each of the three vehicle program groups consists of a MAIN program and INPUT, OUTPUT, and FCT1 subprograms. The simplified flow diagram of Figure 2.1 shows the relationships between all the individual elements of the simulation programs.* (This figure is applicable to each of the three vehicle programs.)

From the user's point of view, understanding the program implies, largely, understanding the input data. The remainder of Section 2.0 is intended to provide that understanding. As a preface to the detailed material which follows, a short overview of the organization of input flow will now be presented.

Although the volume of input data required is large, certain steps have been taken to ease the user's burden in dealing with the programs. First, the data has been grouped to correspond with certain physical sub-systems of the vehicle. (Table 2.1 indicates these groups and their order in the input flow.) Thus, user alterations to a basic vehicle (for example, a change of suspension type) are facilitated.

Second, a great number of options with regard to data entry are available to the user. For instance, in modeling the brakes, the user may choose to enter data in the form of "dynamometer curves" or design parameters of the brake itself, depending on what is available to him or on his choice of modeling technique. The various options available in the program may be included or excluded from the simulation (and from the input flow) by the entry of various "key" parameters located throughout the input flow.

The first data group to be entered in using any of the three Phase III programs is composed of a title followed by several of these "keys," specifically those which cue the program as to the use of the "Rough Road" option and the various suspension options to be used in computation.

---

*More detailed diagrams of the individual programs appear in Appendix A.

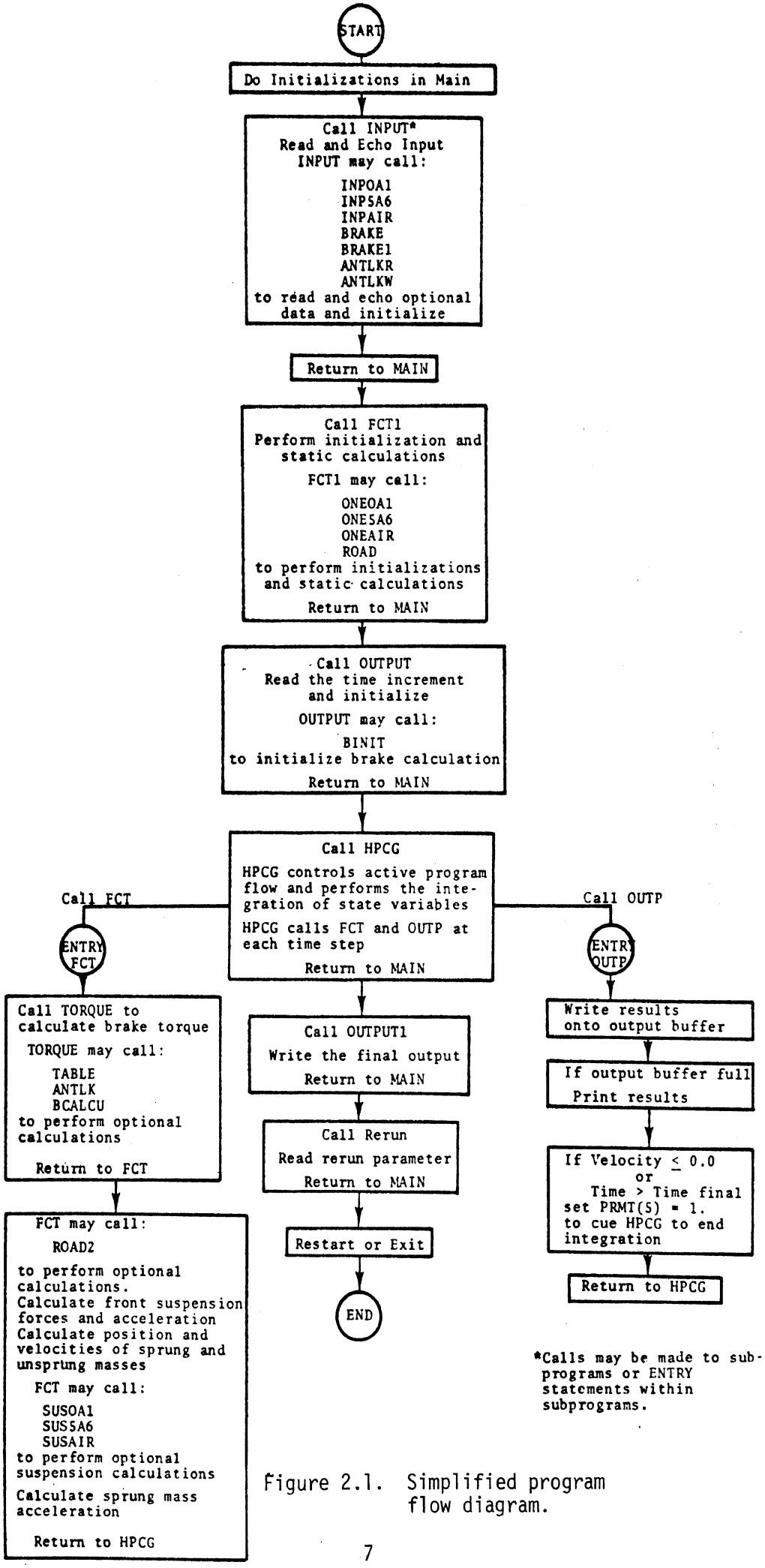

Figure 2.1. Simplified program flow diagram.

Table 2.1. General Input Flow

Data Group	Explanation
I. KEYS	Cues program as to the use of "Rough Road" and suspension options.
II. Suspensions	One suspension data group entered for each suspension on the vehicle starting from front and working rearward.
III. Sprung Mass	Data describing the vehicle's sprung masses.
IV. The Brakes	Includes options for analytical brake models or dynamometer curves plus imbalance, hysteresis, and fade.
V. Tires	Includes options for analytical tire model or entry of μ-slip curves.
VI. Antilock Systems	Optional data entry providing for the modeling of a wide variety of antilock systems.
VII. Other Options	"Rough Road"

An example for this group of input appears in Table 2.2. The data echo, output by the program, which would result from this input appears in Figure 2.2.

Table 2.2

Input	Comments
Key Section Input Example	Title: Format (20A4)
-1	Road Key: Format (I2); delete for smooth road
00	Rear Suspension Key: Format (I2)
03	Trailer Suspension Key: Format (I2); delete for straight truck program
01	Dolly Suspension Key: Format (I2); delete for straight truck or tractor-trailer programs
07	Second Trailer Suspension Key: Format (I2); delete for straight truck or tractor-trailer programs

The first line of input is a user-selected title which will be printed as a portion of the header on each output page.

The title is followed by a road key only if the user wishes to implement the "Road" option. If the user desires to simulate vehicle operation on any but a smooth road, a -1 integer must be entered here. This signals the program to call subroutine ROAD at the proper time and place. Subroutine ROAD is a user-supplied subprogram which describes the surface on which the vehicle is to operate. (Detailed requirements for this subprogram are given in Section 2.6.) If the vehicle is to operate on a smooth road, the road key is simply deleted.

```
KEYS:
   KROAD       ROAD KEY:  0 IMPLIES A SMOOTH ROAD
                         -1 IMPLIES A ROUGH ROAD                    -1

   KEY1        TRACTOR KEY                                            0
   KEY2        FIRST TRAILER KEY                                      3
   KEY3        DOLLY KEY                                              1
   KEY4        SECOND TRAILER KEY                                     7
               AXLE KEYS: SET TO 0  FOR SINGLE AXLE
                                 1  FOR WALKING BEAM
                                 2  FOR BASIC FOUR
                                    SPRING TANDEM
                                    SUSPENSION
                                 3  FOR FOUR SPRING
                                    TANDEM SUSPENSION
                                    WITH SPRING-TYPE
                                    TORQUE RODS
                                 4  FOR FOUR SPRING
                                    TANDEM SUSPENSION
                                    WITH LONG LOAD-LEVELER
                                 5  FOR MULTIPLE TORQUE
                                    ROD FOUR SPRING
                                    SUSPENSION
                                 6  FOR MULTIPLE TORQUE
                                    ROD FOUR SPRING
                                    SUSPENSION WITH SPRING-
                                    TYPE LOWER TORQUE ROD
                                 7  FOR AIR SUSPENSION
```

Figure 2.2. KEY Echo.

Following the road key, the suspension keys are entered. These keys indicate to the program the particular types of suspensions on the vehicle to be simulated (exclusive of the front suspension which must always be a single axle). Keys are entered in order for suspensions from fore to aft of the vehicle and are only entered for suspension positions appropriate for the vehicle being simulated. (See Table 2.2) The suspension key code appears in Figure 2.2.

The following sections detail, in their order of entry, the input parameter groups necessary to describe the vehicle being simulated.

2.1 Suspension Options

Following the "key" input group, parametric data describing each of the various suspensions used on the simulated vehicle are entered. These data are, of course, grouped by suspension and each suspension group is entered in order proceeding from front to rear of the vehicle.

Front suspension type is not optional and is always single axle. All other suspensions may be one of the eight options listed earlier in Figure 2.2.

In the Phase III programs, entered values of spring rates, coulomb friction, and viscous damping represent a total value for a given axle (with certain exceptions for the air suspension), i.e., the summation for both "sides." For example, entered spring rates represent the sum of the spring rates of the right and left springs on a particular axle.

Before discussing the individual suspension options, several points common to more than one option will be considered.

In the following sections, a "Suspension Reference Point" for each of the suspension types will be indicated in the several figures. For mathematical purposes, these points locate

the suspension relative to the sprung masses. Later, in Section 2.2, these reference points will be used to identify certain geometric parameters which describe the various sprung masses of a simulated vehicle.

Among the input parameters for the various suspensions are the effective viscous damping coefficients which model the effect of the shock absorbers. These coefficients are the slopes of the effective force-velocity curves for the shock absorber. The model is bilinear, as shown in Figure 2.3, thus allowing the user to select different damping coefficients for jounce and rebound. In all suspension models where viscous damping is present, the damping mechanism is assumed to have a vertical orientation. Thus, to determine the effective coefficient for use in the simulation, the geometry of the actual mounting configuration should be considered. For solid axle suspensions, the coefficient of the shock absorber itself should be multiplied by the square of the cosine of the angle between the shock absorber centerline and vertical.

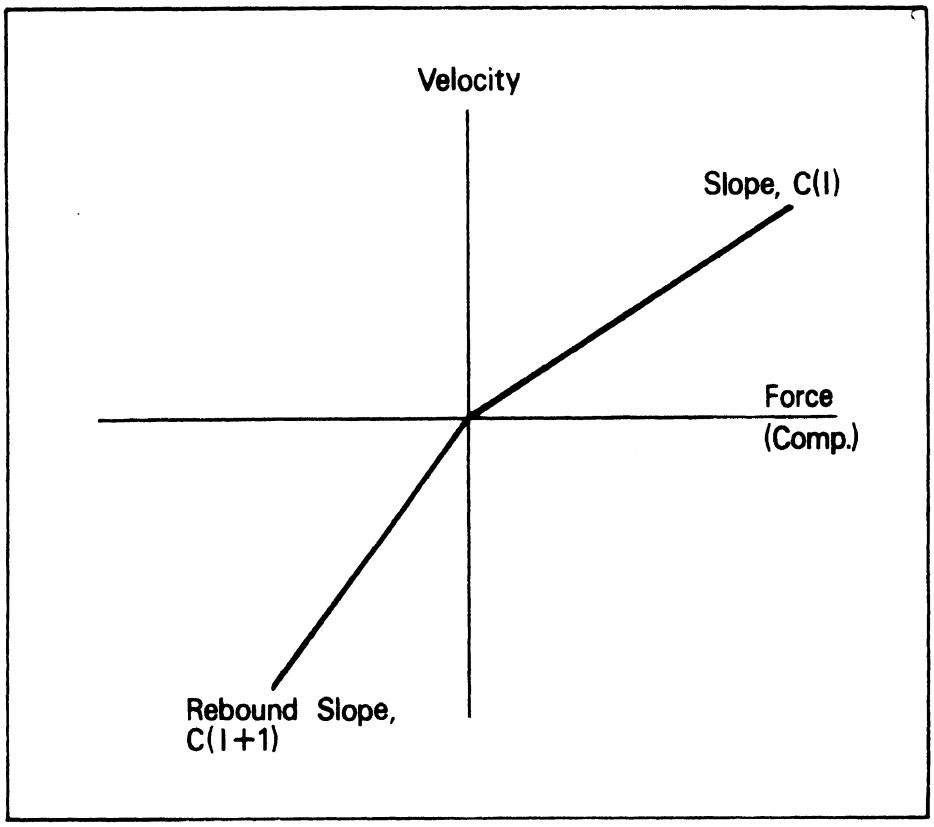

Figure 2.3. Characteristics of the shock absorber model.

Maximum coulomb friction is an input parameter for most of the suspension models. Typically, this number derives from the inter-leaf friction of the suspension. From the user's point of view, this value is one-half of the force hysteresis shown in the force deflection curves derived from laboratory experiment. For example, see Figure 2.4. Many truck suspensions have no shock absorbers, and so coulomb friction provides the only damping mechanisms in the suspension. In such cases, it is particularly important to enter realistic values of coulomb friction; if not, excessive suspension motions may result in the simulation.

The single axle and walking beam suspension models allow the option of nonlinear springs. To call forth this option, the user must enter a value of -1 for the spring constant (K) when entering suspension data. If K has been entered as -1, the final entries for the suspension constitute the spring tables; first the number of points in the table followed by the desired values of deflection versus force properties of the spring. Up to 25 points in the table are allowable. (An example of spring table use will be given in Section 2.1.1 - The Single Axle Suspension Option.)

Certain subtleties of the use of nonlinear spring tables should be addressed. First, the subroutine TABLE which handles a variety of table inputs to the simulation (including spring tables) is structured such that if parameter values outside the range of entered points are required, the tabulated function saturates in the y coordinate. For the spring table this results in a function of the form shown in Figure 2.5.

Thus to prevent spring saturation, the maximum and minimum points entered should be well beyond the expected range of operation. To be conservative, the minimum point should provide a tensile force several times the unsprung weight; the maximum point should provide a compressive force larger than the sprung

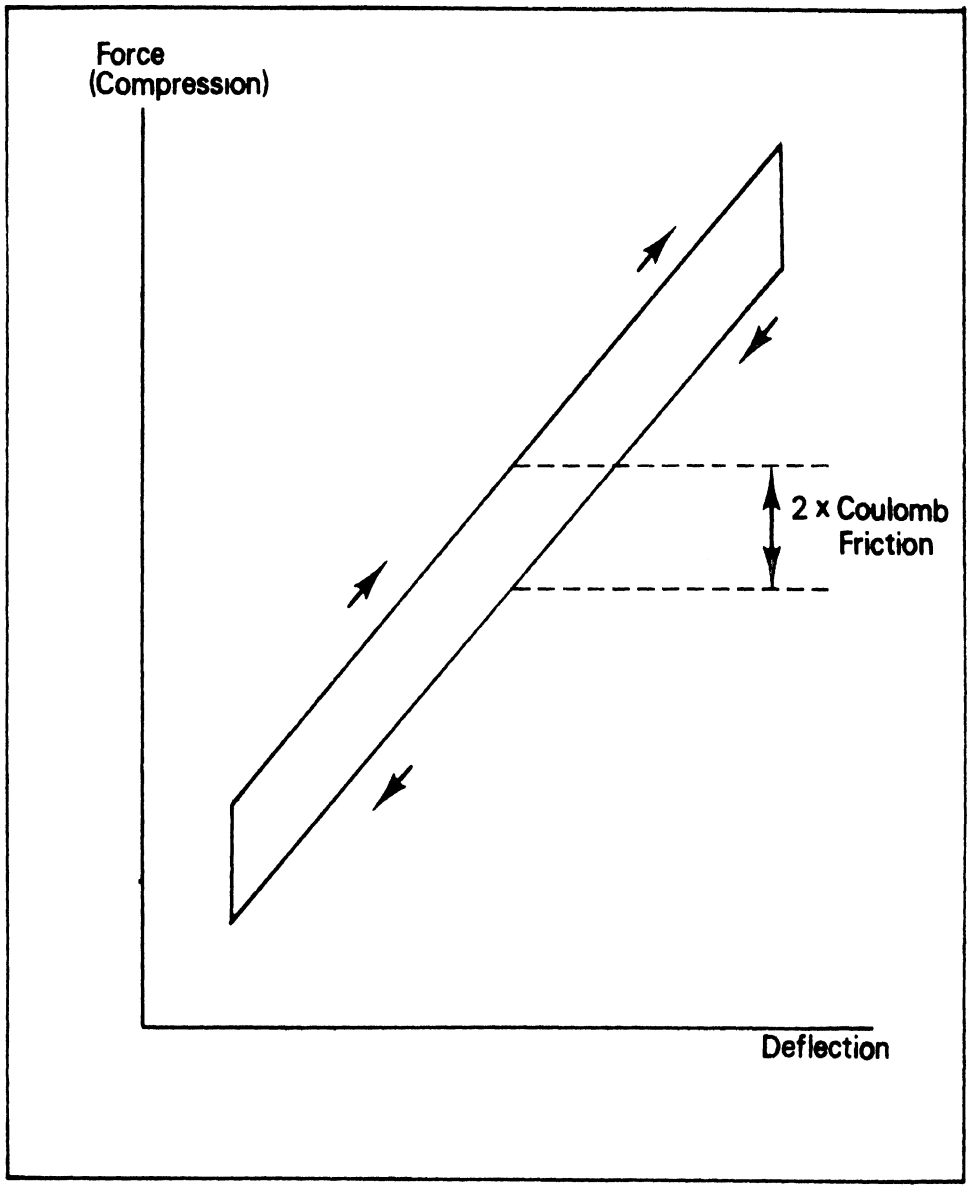

Figure 2.4. Determining coulomb friction from test data.

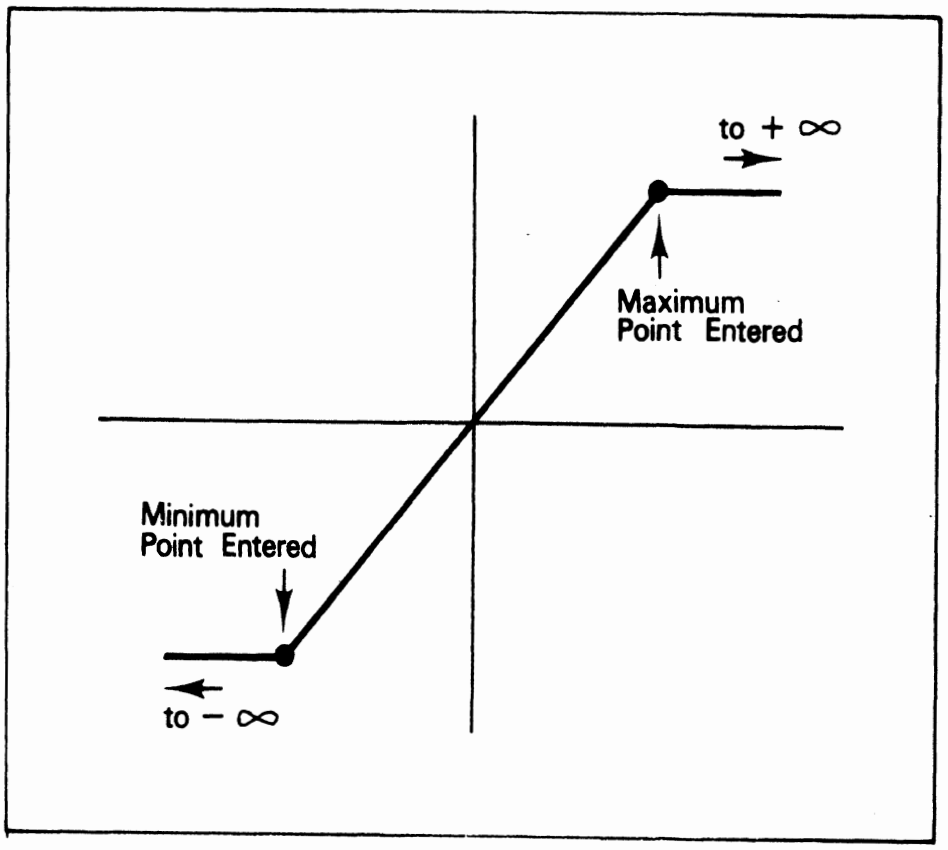

Figure 2.5. Subroutine TABLE saturation characteristics.

weight. In attaining these forces, excessive slopes must not be employed. That is, the very large force inputs should be accompanied by similarly large displacements. If excessive spring table slopes are input, the dynamic capability of the simulation's integration routine may be over-taxed causing the program to "blow up."

In entering nonlinear spring data, it is very important that the force data be accurate in both relative and absolute terms. However, because of the manner in which tabular data is handled, deflection data need be accurate in relative terms only. For example, spring tables A and B shown in Table 2.3 are equivalent while table C is quite different.

Table 2.3

Spring Table A		Spring Table B		Spring Table C	
04		04		04	
-6.0	-30000.	-10.	-30000.	-6.0	0.0
0.0	0.0	-4	0.0	0.0	30000.
8.0	20000.	4.	20000.	8.0	50000.
14.0	50000.	10.	50000.	14.0	80000.

The following sections describe the input data required for each of the suspension options. Front suspension data is, of course, identical to that of the single axle option. The mathematical models for the suspension options are reviewed in Appendix B.

2.1.1 The Single-Axle Suspension. A conceptual illustration showing each of the component parts of the single-axle suspension model appears in Figure 2.6. Table 2.4 gives an example of an input data set that might be used to implement this model in a simulation run. Note that the data is entered in alphabetic order. Figure 2.7 displays the resulting data echo which is output by the program.

Note that the example data set calls for the use of spring tables rather than the simple linear spring rate coefficient. To call forth this option, the spring rate (K) has been entered as -1. Then, following the entry of all other suspension data, the spring rate table was entered. The first line of the table indicates the number of points in the table. This is followed by the entry of the deflection versus force data. If a linear spring model was desired, the actual spring rate would have been entered for K and the spring table deleted.

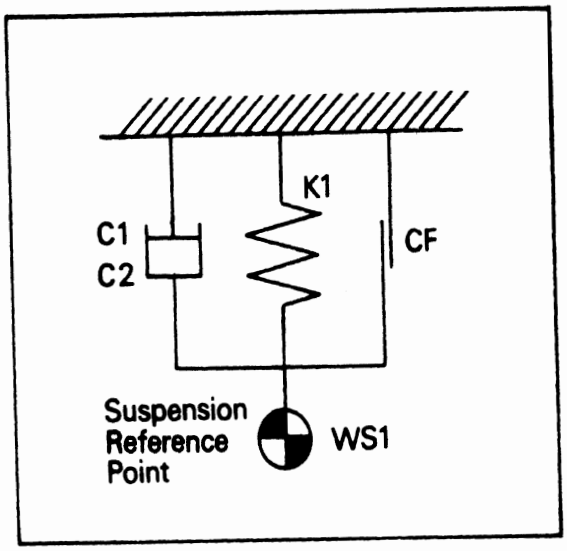

Figure 2.6. The single-axle suspension model.

```
REAR SUSPENSION INPUT PARAMETERS:

      SINGLE AXLE REAR SUSPENSION
   C1            VISCOUS DAMPING: JOUNCE (LB-SEC/IN)              8.33
   C2            VISCOUS DAMPING: REBOUND (LB-SEC/IN)            16.67
   CF            MAX. COULOMB FRICTION (LB)                    1800.00
   K             SPRING RATE (LB/IN)                             -1.00
   WS1           WEIGHT OF LEADING AXLE (IBS)                  1321.00

   SPRING DEFLECTION (IN) VS FORCE (LB)
            NO. OF POINTS:  4
        -6.0000    -30000.0000
         0.0            0.0
         8.0000     20000.0000
        14.0000     50000.0000
```

Figure 2.7. Single-axle suspension data echo.

Table 2.4. Single-Axle Suspension Input

Input		Comments
8.33		C1: Viscous damping coefficient in jounce (lb-sec/in); Format (F15.3)
16.67		C2: Viscous damping coefficient in rebound (lb-sec/in); Format (F15.3)
1800.		CF: Maximum coulomb friction (lb); Format (F15.3)
-1.		K: Spring rate (lb/in); -1. entry cues the spring table option; spring table deleted if K is positive; Format (F15.3)
1321.		WS: Unsprung weight (lb); Format (F15.3)
04		Number of entries in spring table; deleted if K has been entered as a positive number; Format (I2)
-6.0	-30000.	Spring deflection (inches) vs. force (lb); deleted if K has been entered as a positive number; Format (2F10.3)
0.0	0.0	
8.0	20000.	
14.0	50000.	

2.1.2 The Walking Beam Suspension. Figure 2.8 presents a conceptualization of the walking beam suspension model available as an option within the program. Table 2.5 presents an example of an input data set which might be used in implementing the model. The data echo program output which would result from the use of the data of Table 2.5 appears in Figure 2.9.

Compared to the single-axle suspension model discussed in Section 2.1.1, the walking beam model has additional parameters consisting of four geometric parameters plus PERCENT and, of course, a second unsprung weight. The definitions of the four geometric parameters (the AA's) should be made clear by Figure 2.8. Each of these parameters has a positive sense as shown in the figure.

The input parameter, PERCENT, describes the effectiveness of the torque rods in preventing inter-axle load transfer resulting from the application of brake torque. If PERCENT=100, the torque rods will be "perfect," i.e., there will be no inter-axle load transfer or, in other words, all brake torque will be reacted by the torque rod mechanism. If PERCENT=0, the torque rods will be completely ineffective, i.e., there will develop sufficient inter-axle load transfer to react the entire brake torque on the suspension. Intermediate values of PERCENT will result in the appropriate apportionment of the torque reaction effort between the load transfer and torque rod mechanisms. Determination of the appropriate value of PERCENT for a particular suspension may derive from baseline vehicle testing.

2.1.3 The Basic Four Spring Suspension. The Phase III computer programs include five suspension options, all of which are variations of the four spring tandem suspension. The basic four spring model discussed in this section is the four spring suspension with single torque rod and short load leveler.

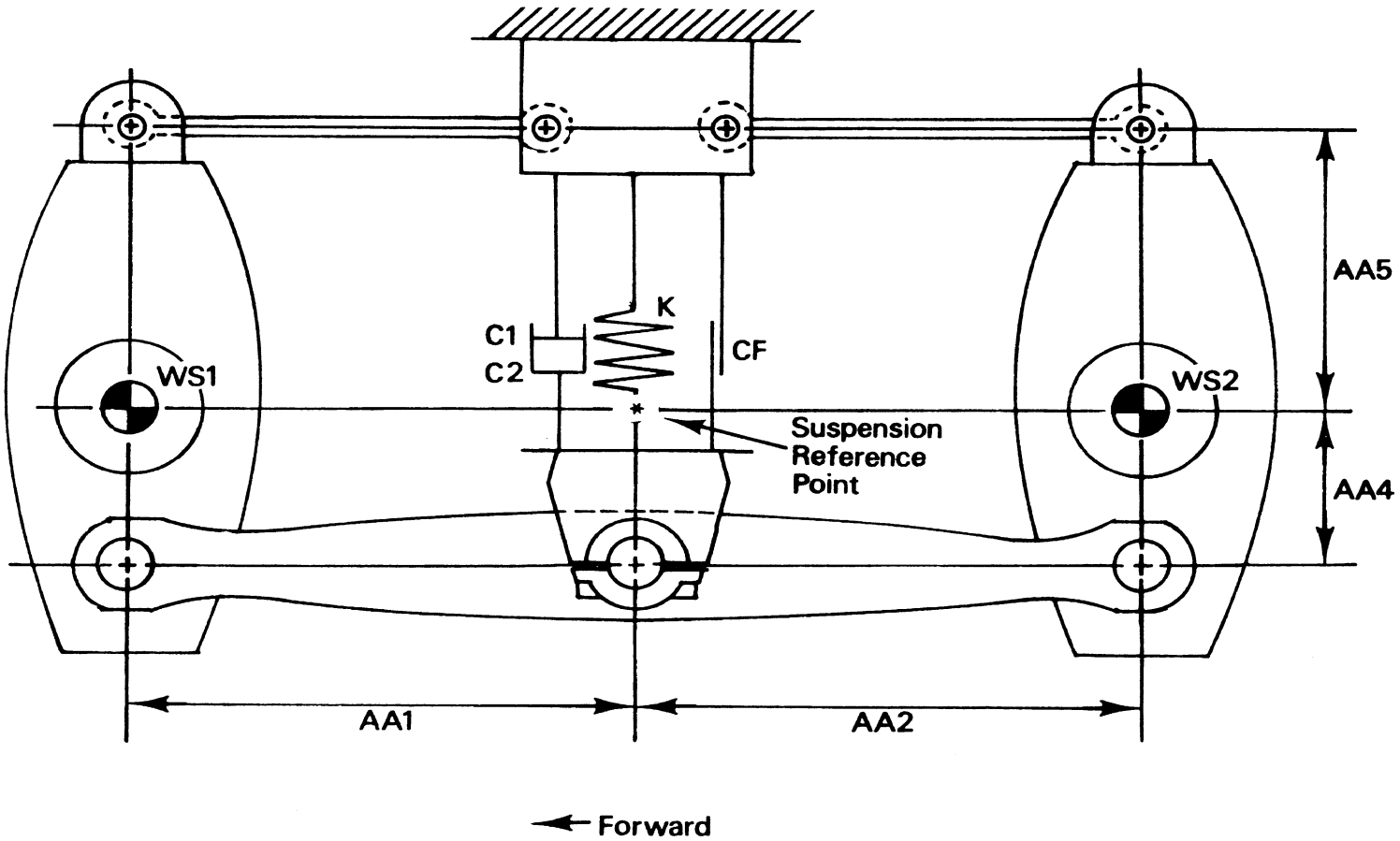

Figure 2.8. The walking beam suspension model.

Table 2.5. Walking Beam Suspension Input

Input	Comments
24.0	AA1: Horizontal distance from the walking beam pin to the leading axle center (in); Format (F15.3)
26.0	AA2: Horizontal distance from the walking beam pin to the trailing axle center (in); Format (F15.3)
8.0	AA4: Vertical distance from the axle centers down to the walking beam (in); Format (F15.3)
18.0	AA5: Vertical distance from the axle centers up to the torque rods (in); Format (F15.3)
0.0	C1: Viscous damping coefficient in jounce (lb-sec/in); Format (F15.3)
0.0	C2: Viscous damping coefficient in rebound (lb-sec/in); Format (F15.3)
4400.	CF: Maximum coulomb friction (lb); Format (F15.3)
30000.	K: Spring rate (lb/in); -1. entry cues the spring table option; spring table deleted if K is positive; Format (F15.3)
100.	PERCENT: Number between 0 and 100 indicating the effectiveness of the torque rods; Format (F15.3)
2078.	WS1: Unsprung weight of the leading axle (lb); Format (F15.3)
1972.	WS2: Unsprung weight of the trailing axle (lb); Format (F15.3)

WALKING BEAM TANDEM SUSPENSION

AA1	HORIZONTAL DIST. FROM WALKING BEAM PIN TO LEADING AXLE (IN)	24.00
AA2	HORIZONTAL DIST. FROM WALKING BEAM PIN TO TRAILING AXLE (IN)	26.00
AA4	VERTICAL DIST. FROM AXLE TO W.B. (IN)	8.00
AA5	VERTICAL DIST. FROM AXLE TO TORQUE ROD (IN)	18.00
C1	VISCOUS DAMPING: JOUNCE ON REAR AXLE(S) (LB-SEC/IN)	0.0
C2	VISCOUS DAMPING: REBOUND ON REAR AXLE(S) (LB-SEC/IN)	0.0
CF	MAX. COULOMB FRICTION, REAR SUSPENSION (LB)	4400.00
K	SPRING RATE, REAR SUSPENSION (LB/IN)	30000.00
PERCNT	PERCENT EFFECTIVENESS OF TORQUE RODS	100.00
WS1	WEIGHT OF FRONT TANDEM (LBS)	2078.00
WS2	WEIGHT OF REAR TANDEM (LBS)	1972.00

Figure 2.9. Walking beam data echo.

Figure 2.10 presents a sketch of the basic four spring suspension in which all the geometric parameters necessary as input are pictured. Note that all of the dimensions shown on this figure have a positive sense. Figure 2.11 shows the data echo computer output for this suspension and also serves as an example input listing.

Note that, in addition to the parameters which appear in Figure 2.10, both viscous and coulomb friction are available for input to the model. Also, different rates for leading and trailing axle springs may be entered, however, the model is only valid for small differences between these springs. The spring table option is not available for this or any other four spring suspension. Only linear springs are allowable.

The parameter MUS is the effective coefficient of friction acting at the contact interface of the leaf spring ends and the vehicle frame, or load leveler. This parameter is important in determining the inter-axle load transfer which occurs during braking. A laboratory method for determining this parameter is reviewed in Reference [8].

2.1.4 The Four Spring Tandem Suspension with Spring-Type Torque Rods. This suspension option is a modification of the basic four spring model which includes the use of spring-type torque rods. Figure 2.12 illustrates the suspension and shows all the necessary geometric parameters. All the dimensions shown in this figure are positive. Figure 2.13 shows the data echo which is output by the computer and also serves as an example input listing. Notice that in addition to the geometric data, the input list includes parameters for viscous and coulomb friction and for spring rates.

Most of the input parameters for this suspension are identical to those of the basic four spring suspension with a few notable exceptions. Referring to Figure 2.12, notice that the

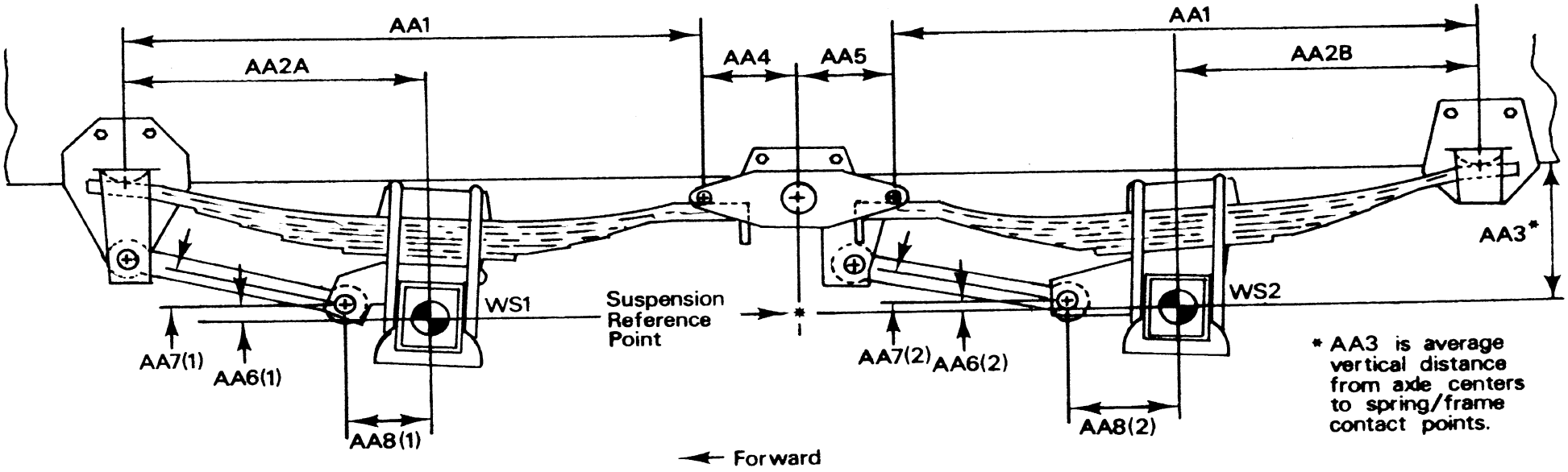

Figure 2.10. The basic four spring suspension model.

BASIC FOUR SPRING TANDEM SUSPENSION

AA1	AVERAGE LEAF SPRING LENGTH: HORIZONTAL DISTANCE FROM FRONT TO REAR LEAF/FRAME CONTACT POINT(IN)	40.85
AA2A	HORIZONTAL DISTANCE FROM FOREMOST LEAF/ FRAME CONTACT TO AXLE CENTER: LEADING AXLE (IN)	21.60
AA2B	HORIZONTAL DISTANCE FROM FOREMOST LEAF/ FRAME CONTACT TO AXLE CENTER: TRAILING AXLE (IN)	19.25
AA3	AVERAGE VERTICAL DIST.FROM LEAF/FRAME CONTACT TO AXLE CENTER (IN)	10.00
AA4	DIST. FROM FRONT LEAF/LOAD LEVELER CONTACT TO LOAD LEVELER PIN (IN)	6.75
AA5	DIST. FROM REAR LEAF/LOAD LEVELER CONTACT TO LOAD LEVELER PIN(IN)	6.75
AA6(1)	VERTICAL DISTANCE FROM AXLE CENTER UP TO TORQUE ROD: LEADING AXLE (IN)	7.00
AA6(2)	VERTICAL DISTANCE FROM AXLE CENTER UP TO TORQUE ROD: TRAILING AXLE(IN)	7.00
AA7(1)	AVERAGE ANGLE BETWEEN TORQUE RODS AND HORIZONTAL: LEADING AXLE (DEG)	13.00
AA7(2)	AVERAGE ANGLE BETWEEN TORQUE RODS AND HORIZONTAL: TRAILING AXLE(DEG)	13.00
AA8(1)	HORIZONTAL DISTANCE FROM AXLE CENTER FORWARD TO TORQUE ROD COMPLIANCE CENTER: LEADING AXLE (IN)	-1.00
AA8(2)	HORIZONTAL DISTANCE FROM AXLE CENTER FORWARD TO TORQUE ROD COMPLIANCE CENTER: TRAILING AXLE (IN)	-1.00
C1	VISCOUS DAMPING: JOUNCE ON LEADING AXLE (LB-SEC/IN)	0.0
C2	VISCOUS DAMPING: REBOUND ON LEADING AXLE (LB-SEC/IN)	0.0
C3	VISCOUS DAMPING: JOUNCE ON TRAILING AXLE (LB-SEC/IN)	0.0
C4	VISCOUS DAMPING: REBOUND ON TRAILING AXLE (LB-SEC/IN)	0.0
CF1	MAX. COULOMB FRICTION, LEADING AXLE (LB)	4400.00
CF2	MAX. COULOMB FRICTION, TRAILING AXLE (LB)	4400.00
K1	SPRING RATE OF LEAF SPRING: LEADING AXLE (LB/IN)	10400.00
K2	SPRING RATE OR LEAF SPRING: TRAILING AXLE (LB/IN)	10400.00
MUS	COEFFICIENT OF FRICTION,LEAF-FRAME CONTACT POINT	0.320
WS1	UNSPRUNG WEIGHT:LEADING AXLE (LB)	2330.00
WS2	UNSPRUNG WEIGHT:TRAILING AXLE (LB)	2074.00

Figure 2.11. Basic four spring suspension data echo.

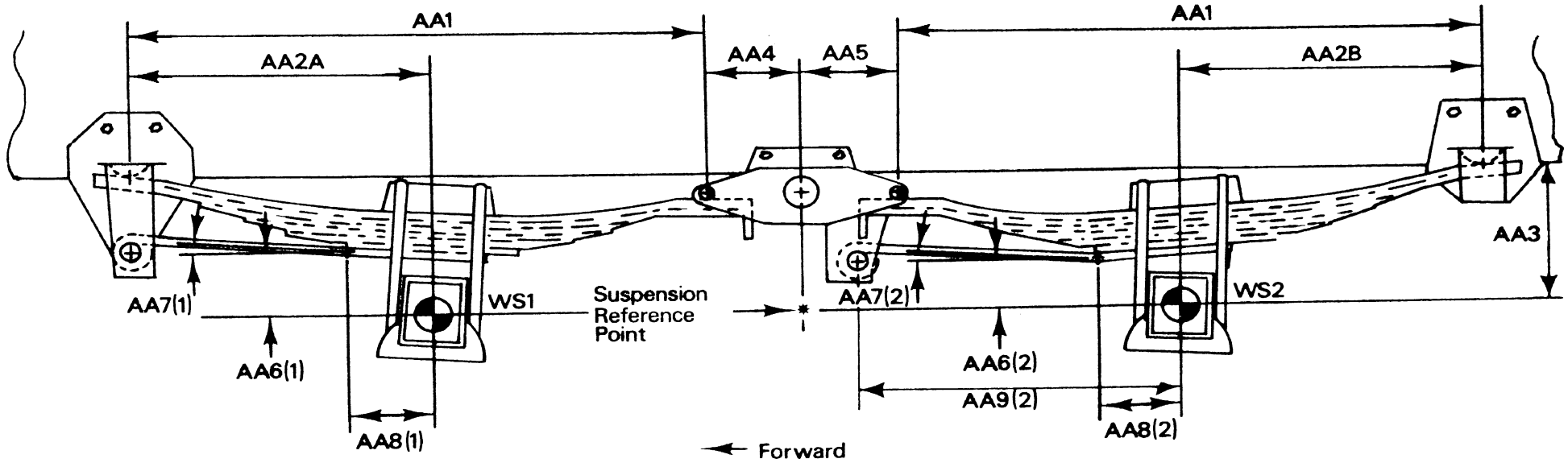

Figure 2.12. The four spring suspension with spring-type torque rods.

FOUR SPRING TANDEM SUSPENSION WITH
SPRING TYPE TORQUE RODS

AA1	AVERAGE LEAF SPRING LENGTH: HORIZONTAL DISTANCE FROM FRONT TO REAR LEAF/FRAME CONTACT POINT(IN)	40.85
AA2A	HORIZONTAL DISTANCE FROM FOREMOST LEAF/ FRAME CONTACT TO AXLE CENTER: LEADING AXLE (IN)	21.60
AA2B	HORIZONTAL DISTANCE FROM REARMOST LEAF/ FRAME CONTACT TO AXLE CENTER: TRAILING AXLE (IN)	19.25
AA3	AVERAGE VERTICAL DIST.FROM LEAF/FRAME CONTACT TO AXLE CENTER (IN)	10.00
AA4	DIST. FROM FRONT LEAF/LOAD LEVELER CONTACT TO LOAD LEVELER PIN (IN)	6.75
AA5	DIST. FROM REAR LEAF/LOAD LEVELER CONTACT TO LOAD LEVELER PIN(IN)	6.75
AA6(1)	VERTICAL DISTANCE FROM AXLE CENTER UP TO TORQUE ROD: LEADING AXLE (IN)	7.00
AA6(2)	VERTICAL DISTANCE FROM AXLE CENTER UP TO TORQUE ROD: TRAILING AXLE(IN)	7.00
AA7(1)	AVERAGE ANGLE BETWEEN TORQUE RODS AND HORIZONTAL: LEADING AXLE (DEG)	13.00
AA7(2)	AVERAGE ANGLE BETWEEN TORQUE RODS AND HORIZONTAL: TRAILING AXLE(DEG)	13.00
AA8(1)	HORIZONTAL DISTANCE FROM AXLE CENTER FORWARD TO TORQUE ROD: LEADING AXLE(IN)	1.00
AA8(2)	HORIZONTAL DISTANCE FROM AXLE CENTER FORWARD TO TORQUE ROD: TRAILING AXLE(IN)	1.00
AA9(1)	HORIZONTAL DISTANCE FROM AXLE CENTER FORWARD TO LOWER TORQUE ROD FRAME PIN: LEADING AXLE (IN)	20.00
AA9(2)	HORIZONTAL DISTANCE FROM AXLE CENTER FORWARD TO LOWER TORQUE ROD FRAME PIN: TRAILING AXLE (IN)	19.00
C1	VISCOUS DAMPING: JOUNCE ON LEADING AXLE (LB-SEC/IN)	0.0
C2	VISCOUS DAMPING: REBOUND ON LEADING AXLE (LB-SEC/IN)	0.0
C3	VISCOUS DAMPING: JOUNCE ON TRAILING AXLE (LB-SEC/IN)	0.0
C4	VISCOUS DAMPING: REBOUND ON TRAILING AXLE (LB-SEC/IN)	0.0
CF1	MAX. COULOMB FRICTION, LEADING AXLE (LB)	4400.00
CF2	MAX. COULOMB FRICTION, TRAILING AXLE (LB)	4400.00
K1	SPRING RATE OF LEAF SPRING: LEADING AXLE (LB/IN)	10400.00
K2	SPRING RATE OR LEAF SPRING: TRAILING AXLE (LB/IN)	10400.00
KTR1	SPRING RATE OF LOWER TORQUE ROD: LEADING AXLE (LB/IN)	1250.00
KTR2	SPRING RATE OF LOWER TORQUE ROD: TRAILING AXLE (LB/IN)	1250.00
MUS	COEFFICIENT OF FRICTION,LEAF-FRAME CONTACT POINT	0.250
WS1	UNSPRUNG WEIGHT:LEADING AXLE (LB)	2330.00
WS2	UNSPRUNG WEIGHT:TRAILING AXLE (LB)	2074.00

Figure 2.13. Four spring suspension with spring-type torque rods data echo.

parameters AA6 and AA8 locate the first "free point" of the torque rod member (i.e., the point where this member separates from the leaf spring stack) with respect to the axle center. The parameter AA9 indicates the horizontal distance from the axle center forward to the point where the torque rod attaches to the vehicle frame.

The torque rod spring rates (KTR1 and KTR2) are linear spring rates (lb/in) as would derive from the experiment indicated in Figure 2.14.

2.1.5 The Four Spring Tandem Suspension with Long Load Leveler. The parametric data necessary for the use of the four spring tandem suspension with long load leveler (FSS-LLL) is very much similar to that of the preceding four spring suspensions. Figure 2.15 illustrates the suspension and indicates all the needed geometric parameters. All dimensions shown in this figure have a positive sense. Figure 2.16 contains a program-produced data echo and also serves as an example listing of the required input. Notice that in addition to the parameters shown in Figure 2.15, this list also includes viscous and coulomb friction, and spring rate entries.

There are some four spring suspensions in use whose operation is similar to the FSS-LLL shown in Figure 2.15 (i.e., load leveling takes place between the rear contact points of the leading and trailing springs), but which use a different load leveling mechanism, possibly as shown in Figure 2.17. Such a suspension may be simulated by using the values of AA4 and AA5 such that (1) their sum indicates the proper span from spring contact point to spring contact point, and (2) their ratio indicates the appropriate lever ratio. For example, using the notation of Figure 2.17:

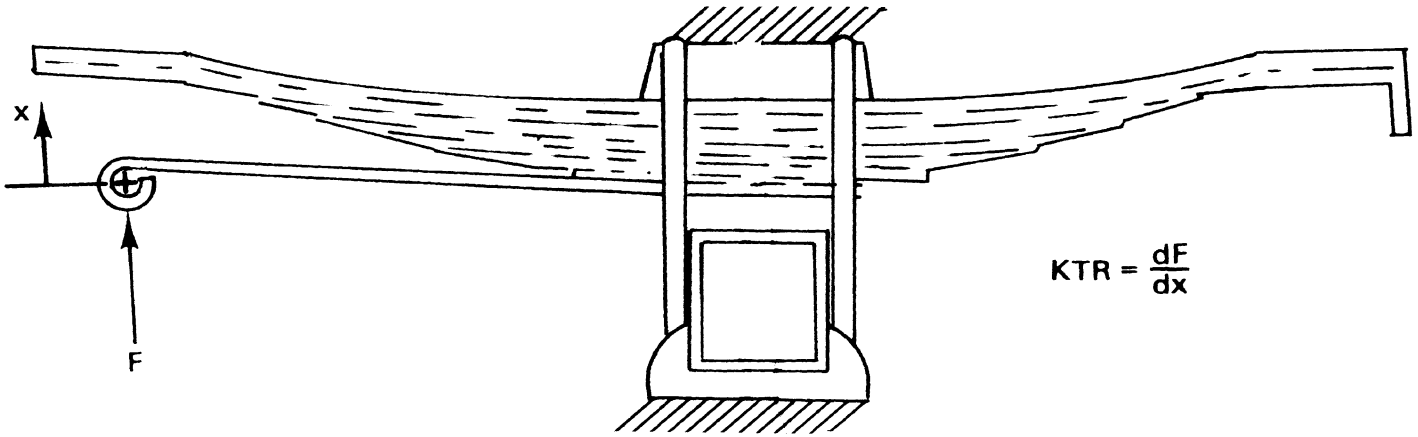

Figure 2.14. Determining the torque rod spring constant.

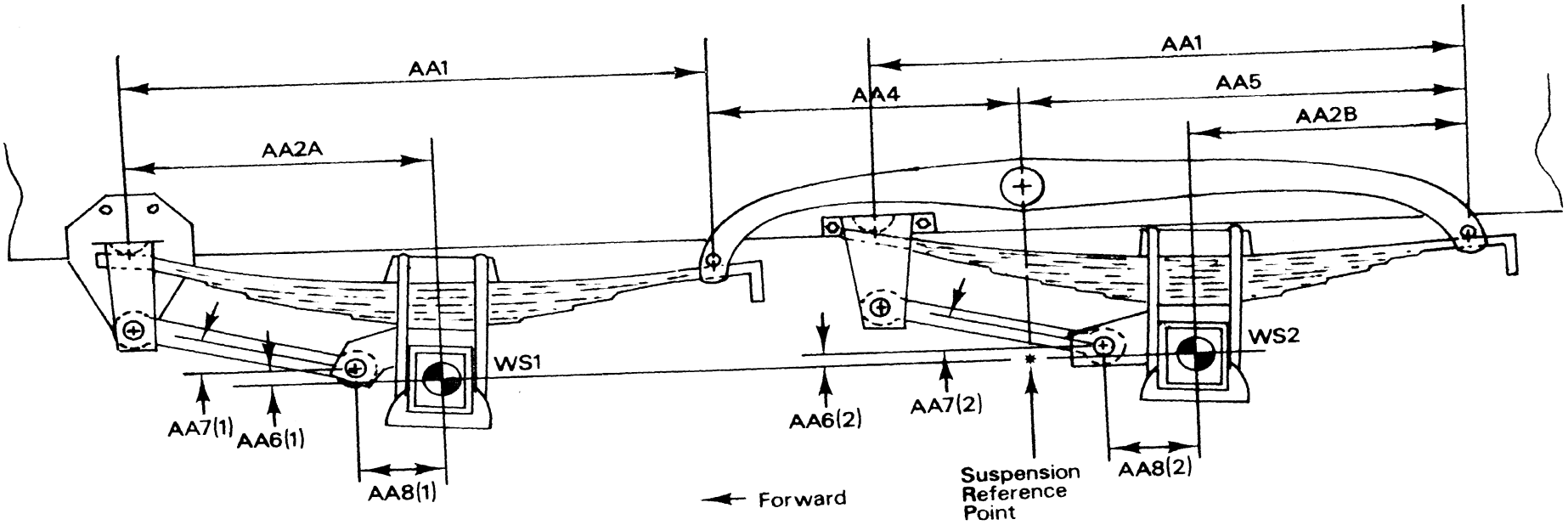

Figure 2.15. The four spring suspension with long load leveler.

FOURSPRING TANDEM SUSPENSION WITH
LONG LOAD LEVELERS

AA1	AVERAGE LEAF SPRING LENGTH: HORIZONTAL DISTANCE FROM FRONT TO REAR LEAF/FRAME CONTACT POINT(IN)	40.00
AA2A	HORIZONTAL DISTANCE FROM FOREMOST LEAF/ FRAME CONTACT TO AXLE CENTER: LEADING AXLE (IN)	19.00
AA2B	HORIZONTAL DISTANCE FROM REARMOST LEAF/ FRAME CONTACT TO AXLE CENTER: TRAILING AXLE (IN)	21.00
AA3	AVERAGE VERTICAL DIST.FROM LEAF/FRAME CONTACT TO AXLE CENTER (IN)	9.50
AA4	DIST. FROM FRONT LEAF/LOAD LEVELER CONTACT TO LOAD LEVELER PIN (IN)	26.75
AA5	DIST. FROM REAR LEAF/LOAD LEVELER CONTACT TO LOAD LEVELER PIN(IN)	26.75
AA6(1)	VERTICAL DISTANCE FROM AXLE CENTER UP TO TORQUE ROD: LEADING AXLE (IN)	6.50
AA6(2)	VERTICAL DISTANCE FROM AXLE CENTER UP TO TORQUE ROD: TRAILING AXLE(IN)	6.50
AA7(1)	AVERAGE ANGLE BETWEEN TORQUE RODS AND HORIZONTAL: LEADING AXLE (DEG)	13.00
AA7(2)	AVERAGE ANGLE BETWEEN TORQUE RODS AND HORIZONTAL: TRAILING AXLE(DEG)	13.00
AA8(1)	HORIZONTAL DISTANCE FROM AXLE CENTER FORWARD TO TORQUE ROD: LEADING AXLE(IN)	3.75
AA8(2)	HORIZONTAL DISTANCE FROM AXLE CENTER FORWARD TO TORQUE ROD: TRAILING AXLE(IN)	3.75
C1	VISCOUS DAMPING: JOUNCE ON LEADING AXLE (LB-SEC/IN)	0.0
C2	VISCOUS DAMPING: REBOUND ON LEADING AXLE (LB-SEC/IN)	0.0
C3	VISCOUS DAMPING: JOUNCE ON TRAILING AXLE (LB-SEC/IN)	0.0
C4	VISCOUS DAMPING: REBOUND ON TRAILING AXLE (LB-SEC/IN)	0.0
CF1	MAX. COULOMB FRICTION, LEADING AXLE (LB)	4400.00
CF2	MAX. COULOMB FRICTION, TRAILING AXLE (LB)	4400.00
K1	SPRING RATE OF LEAF SPRING: LEADING AXLE (LB/IN)	10000.00
K2	SPRING RATE OR LEAF SPRING: TRAILING AXLE (LB/IN)	10000.00
WS1	UNSPRUNG WEIGHT:LEADING AXLE (LB)	2330.00
WS2	UNSPRUNG WEIGHT:TRAILING AXLE (LB)	2074.00

Figure 2.16. Four spring suspension with long load leveler data echo.

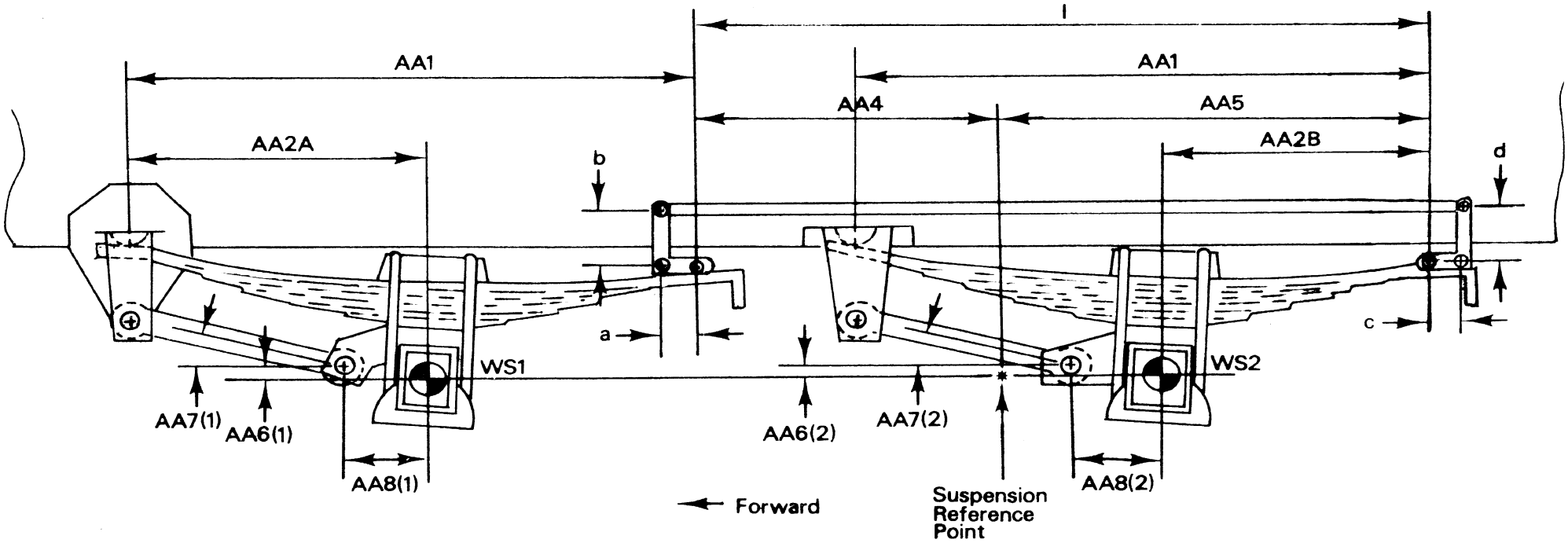

Figure 2.17. Alternate four spring suspension with long load leveler.

$$AA4 + AA5 = \ell \tag{2.1}$$

$$\frac{AA4}{AA5} = \frac{a\ d}{b\ c} \tag{2.2}$$

from which

$$AA4 = \frac{\ell}{1 + \frac{b\ c}{a\ d}} \tag{2.3}$$

and

$$AA5 = \frac{\ell}{1 + \frac{a\ d}{b\ c}} \tag{2.4}$$

obtains.

2.1.6 The Multiple Torque Rod Four Spring Suspension. Although much of the parametric data required for use in the multiple torque rod four spring suspension (MTRFSS) is similar to that required by the preceding four spring suspensions, there are several significant differences. These differences result from the differing mechanisms by which this suspension reacts brake torque.* A sketch of the MTRFSS showing many of the required input parameters appears in Figure 2.18. Figure 2.19 shows a conceptualization of the suspension reflecting the manner in which it is modeled in the simulation. Figure 2.20 presents an example set of input for the MTRFSS by displaying the input data echo which is output by the computer program.

The three figures should adequately describe to the reader all the necessary input parameters with the following exceptions:** AA6 and AA8, the parameters which locate the "center of torsional compliance" of the torque rod mechanism; KTQ, the torsional or

---

*Details of the modeling of this mechanism are given in Appendix B.

**Parameter subscripts are dropped since the following comments are applicable to either leading or trailing axles.

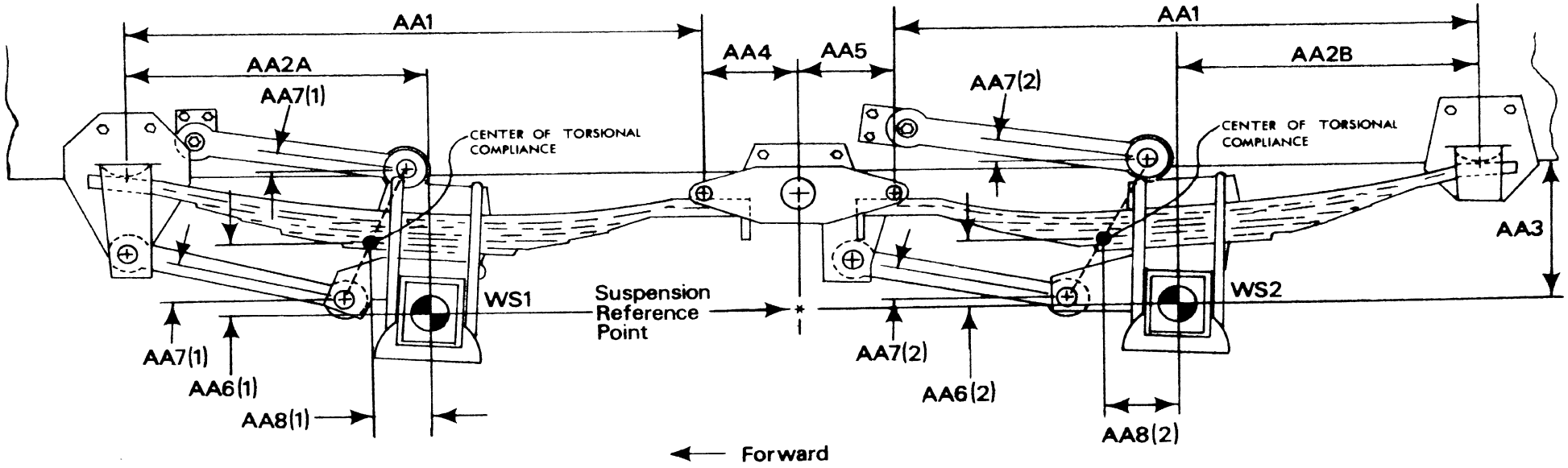

Figure 2.18. The multiple torque rod four spring suspension.

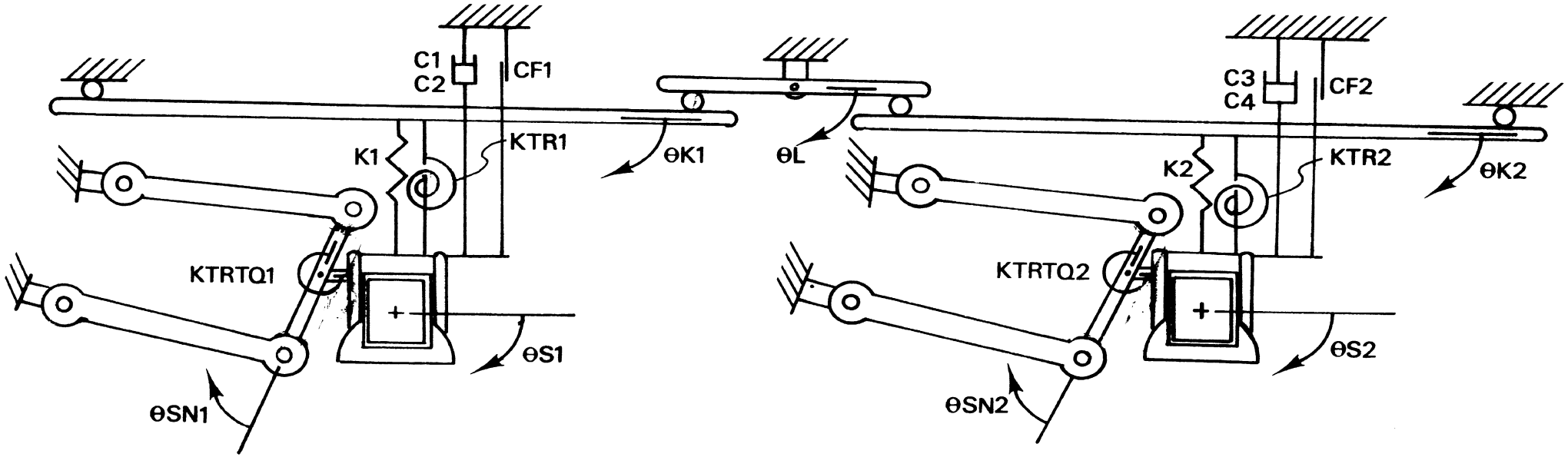

Figure 2.19. The MTRFSS model concept.

MULTIPLE TORQUE ROD FOUR SPRING
TANDEM SUSPENSION

AA1	AVERAGE LEAF SPRING LENGTH: HORIZONTAL DISTANCE FROM FRONT TO REAR LEAF/FRAME CONTACT POINT(IN)	40.00
AA2A	HORIZONTAL DISTANCE FROM FOREMOST LEAF/ FRAME CONTACT TO AXLE CENTER: LEADING AXLE (IN)	19.00
AA2B	HORIZONTAL DISTANCE FROM REARMOST LEAF/ FRAME CONTACT TO AXLE CENTER: TRAILING AXLE (IN)	21.00
AA3	AVERAGE VERTICAL DIST.FROM LEAF/FRAME CONTACT TO AXLE CENTER (IN)	9.50
AA4	DIST. FROM FRONT LEAF/LOAD LEVELER CONTACT TO LOAD LEVELER PIN (IN)	6.75
AA5	DIST. FROM REAR LEAF/LOAD LEVELER CONTACT TO LOAD LEVELER PIN(IN)	6.75
AA6(1)	VERTICAL DISTANCE FROM AXLE CENTER UP TO TORQUE ROD COMPLIANCE CENTER: LEADING AXLE (IN)	6.50
AA6(2)	VERTICAL DISTANCE FROM AXLE CENTER UP TO TORQUE ROD COMPLIANCE CENTER: TRAILING AXLE (IN)	6.50
AA7(1)	AVERAGE ANGLE BETWEEN TORQUE RODS AND HORIZONTAL: LEADING AXLE (DEG)	13.00
AA7(2)	AVERAGE ANGLE BETWEEN TORQUE RODS AND HORIZONTAL: TRAILING AXLE(DEG)	13.00
AA8(1)	HORIZONTAL DISTANCE FROM AXLE CENTER FORWARD TO TORQUE ROD COMPLIANCE CENTER: LEADING AXLE (IN)	3.75
AA8(2)	HORIZONTAL DISTANCE FROM AXLE CENTER FORWARD TO TORQUE ROD COMPLIANCE CENTER: TRAILING AXLE (IN)	3.75
C1	VISCOUS DAMPING: JOUNCE ON LEADING AXLE (LB-SEC/IN)	0.0
C2	VISCOUS DAMPING: REBOUND ON LEADING AXLE (LB-SEC/IN)	0.0
C3	VISCOUS DAMPING: JOUNCE ON TRAILING AXLE (LB-SEC/IN)	0.0
C4	VISCOUS DAMPING: REBOUND ON TRAILING AXLE (LB-SEC/IN)	0.0
CF1	MAX. COULOMB FRICTION, LEADING AXLE (LB)	4400.00
CF2	MAX. COULOMB FRICTION, TRAILING AXLE (LB)	4400.00
K1	SPRING RATE OF LEAF SPRING: LEADING AXLE (LB/IN)	10000.00
K2	SPRING RATE OR LEAF SPRING: TRAILING AXLE (LB/IN)	10000.00
KTQ1	TORSIONAL SPRING RATE OF LEAF SPRING: LEADING AXLE (IN-LB/DEG)	70000.00
KTQ2	TORSIONAL SPRING RATE OF LEAF SPRING: TRAILING AXLE (IN-LB/DEG)	70000.00
KTRTQ1	TORSIONAL SPRING RATE OF TORQUE ROD ASSEMBLY: LEADING AXLE (IN-LB/DEG)	70000.00
KTRTQ2	TORSIONAL SPRING RATE OF TORQUE ROD ASSEMBLY: TRAILING AXLE (IN-LB/DEG	70000.00
NACOEF1	NOMINAL AXLE ANGULAR POSITION COEFFICIENT: LEADING AXLE (DEG/IN)	0.00
NACOEF2	NOMINAL AXLE ANGULAR POSITION COEFFICIENT: TRAILING AXLE (DEG/IN)	0.00
PRCTN1	STATIC NORMAL LOAD PERCENTAGE: LEADING AXLE	50.00
WS1	UNSPRUNG WEIGHT:LEADING AXLE (LB)	2330.00
WS2	UNSPRUNG WEIGHT:TRAILING AXLE (LB)	2074.00

Figure 2.20. MTRFSS data echo.

"wrap-up" spring rate of the leaf spring; KTRTQ, the torsional spring rate of the torque rod mechanism; NACOEF, the nominal axle angular coefficient; and PRCTN1, the percentage of total static normal tire load carried by the leading axle. To clarify the meaning of these parameters, first consider the model of Figure 2.19. Brake torques which are applied to either of the sprung masses will be reacted by two mechanisms—one, the "wrap-up" reaction of the leaf spring conceptualized by the torsional spring KTQ, and two, the torsional reaction of the torque rod assembly embodied in the conceptual element KTRTQ. The distribution of the brake torque reaction between these two mechanisms is dependent on the relative rates of the torsional springs and on various positions assumed by elements throughout the suspension. (The distribution of brake torque reaction is most important in determining inter-axle load transfer.)

KTRTQ, then, is the effective torsional spring rate of the torque rod assembly, or, using the notation of Figure 2.21:

$$\text{KTRTQ} = \left.\frac{dT}{d\theta S}\right|_{T=0} \tag{2.5}$$

As shown in Figure 2.19, this spring produces a moment reaction between the torque rod assembly and the sprung mass at their conceptual attachment point which is the center of torsional compliance of the torque rod assembly. In a physical sense, this point is the center of rotation of the sprung mass which results from the application of a torque as shown in Figure 2.21. (In the program input, this point is located by AA6 and AA8.)

KTQ is the torsional spring rate of the suspension's leaf spring. This parameter may be determined experimentally or may be estimated by the equation:

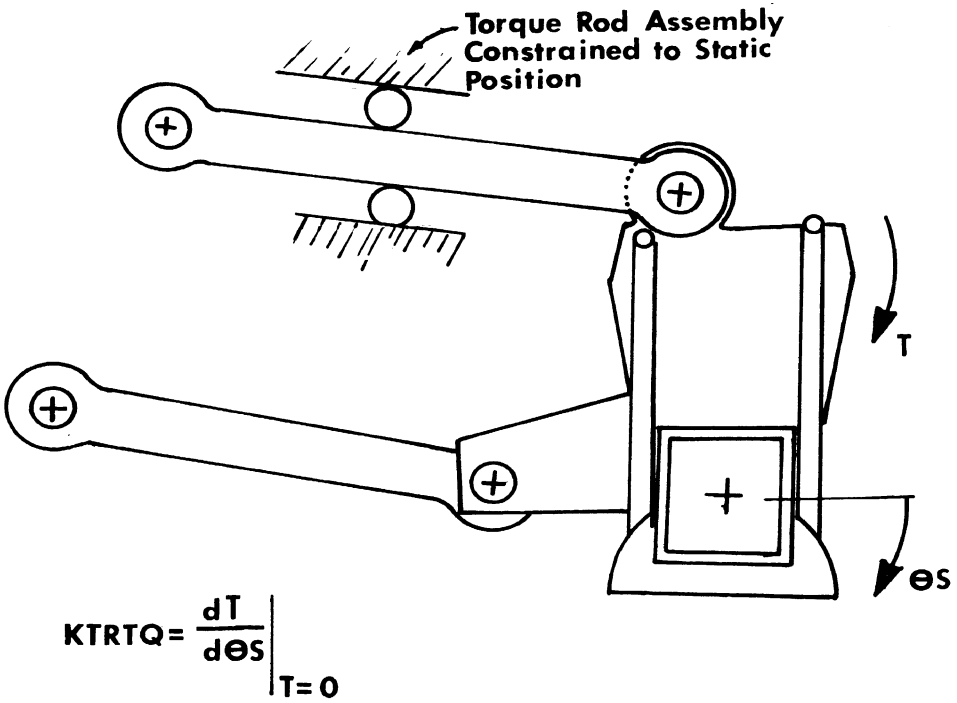

Figure 2.21. Direct measurement of KTRTQ.

$$KTQ = \frac{K \cdot AA1^2}{4 \cdot 57.3} \tag{2.6}$$

where K is the vertical spring rate of the leaf spring in lb/in, AA1 is the length of the spring in inches and KTQ is in in-lb/deg.

The nominal axle angular position coefficient is used by the model to determine the angle θSN of Figure 2.19. For the user's purposes, it is defined as

$$NACOEF \equiv \left.\frac{d\theta SN}{dZSP}\right|_{ZSP=0} \tag{2.7}$$

as illustrated in Figure 2.22. (The motions indicated in the figure should be determined under zero load condition.)

Finally, the parameter PRCTN1, the percentage of the total static normal load carried at the front axle, may be considered. The MTRFSS model, as shown in Figure 2.19, is indeterminate with respect to static tire normal loads unless information describing the "preset" of the various torsional springs is known. PRCTN1 provides this information. In entering this parameter, two options are available to the user. First, he may enter a value between (0) and (100) and the static normal tire loads will be distributed between the two axles according to this entered value. Second, the user may enter any value outside this (0) to (100) percent range, and the program will assume that the "preset" of the KTRTQ springs is zero. In this case, the static tire normal loads will be calculated in a manner which is identical to that which would be used for the basic four spring suspension.

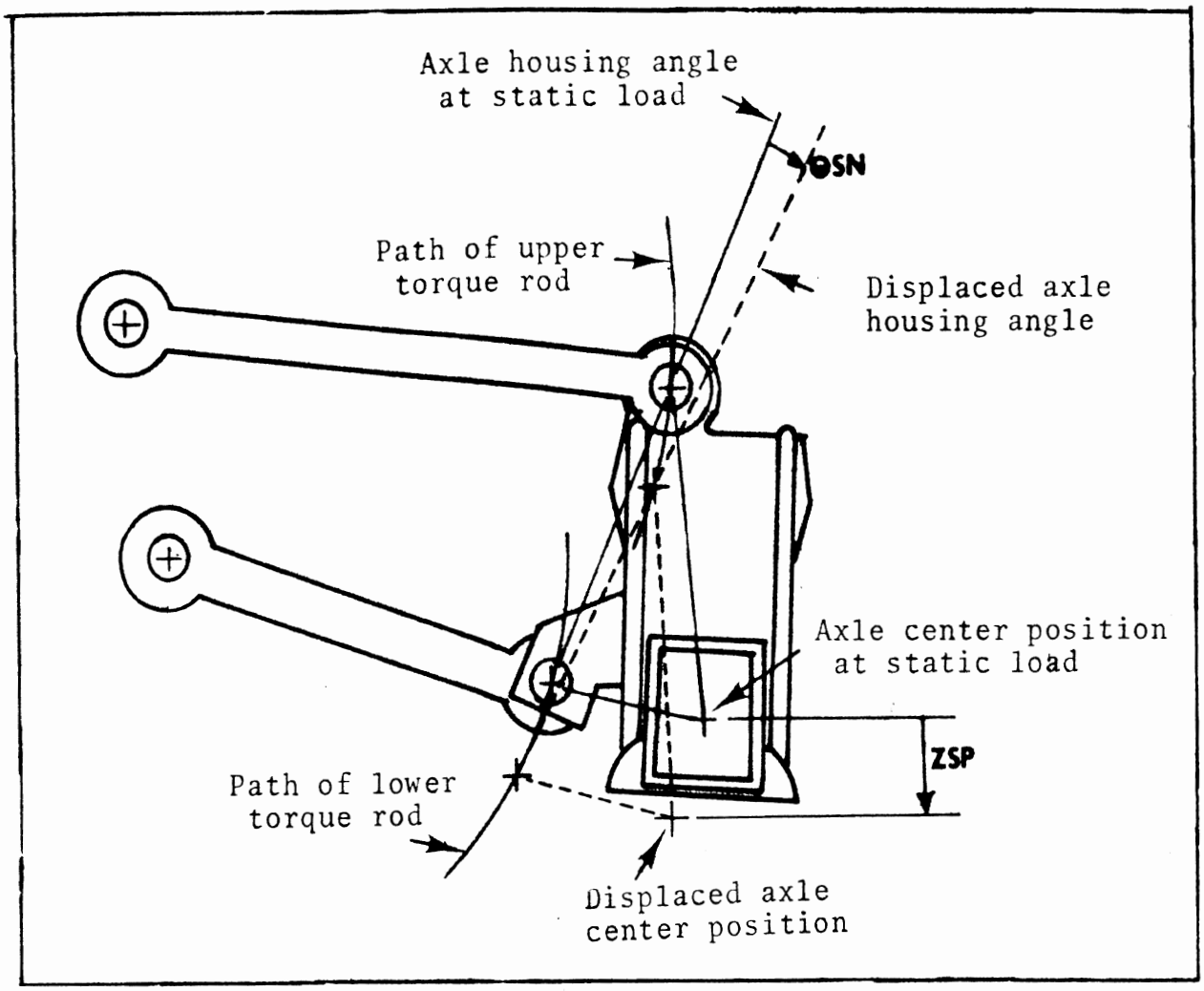

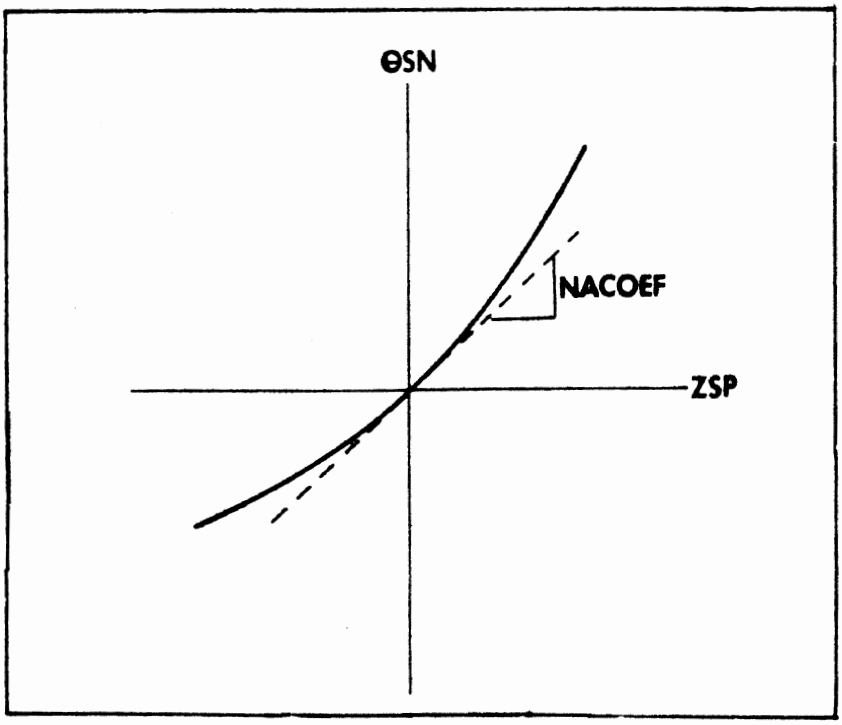

Figure 2.22. Determining NACOEF.

2.1.7 The Multiple Torque Rod Four Spring Suspension with Spring-Type Lower Torque Rod. This suspension option is a modification of the MTRFSS option (described in the previous section), which includes the use of spring-type lower torque rods. Figure 2.23 illustrates the suspension and Figure 2.24 presents an example of the required input by showing the input data echo which is output by the computer program.

All parametric data required is virtually identical to that of the MTRFSS with the addition of the geometric parameters AA9(1) and AA9(2) (see Figure 2.23) and the torque rod spring rates, KTR1 and KTR2. These KTR parameters are the linear spring rates of the leading and trailing axle lower torque rods, as would be determined by the method illustrated previously in Figure 2.14.

2.1.8 The Air Suspension. From the user's point of view, the air suspension option is more complex than the other suspensions. In addition to the parameters needed to describe the mechanical system (similar to the parameters needed for other suspensions), several other parameters are required to describe the pneumatic system, including the air spring and the air delivery network. Also, a variety of sub-options allow selection of single-axle or tandem suspensions and four-bar or trailing-arm suspension linkages.

Starting with a description of the mechanical system parameters, let us consider first a tandem suspension composed of two, four-bar linkage-type axles, as shown in Figure 2.25. The figure illustrates all the geometric parameters required by the model to describe this type of suspension. Note that all the dimensions are shown in this figure with a positive sense.

Using this suspension as a baseline, let us now consider possible variations.

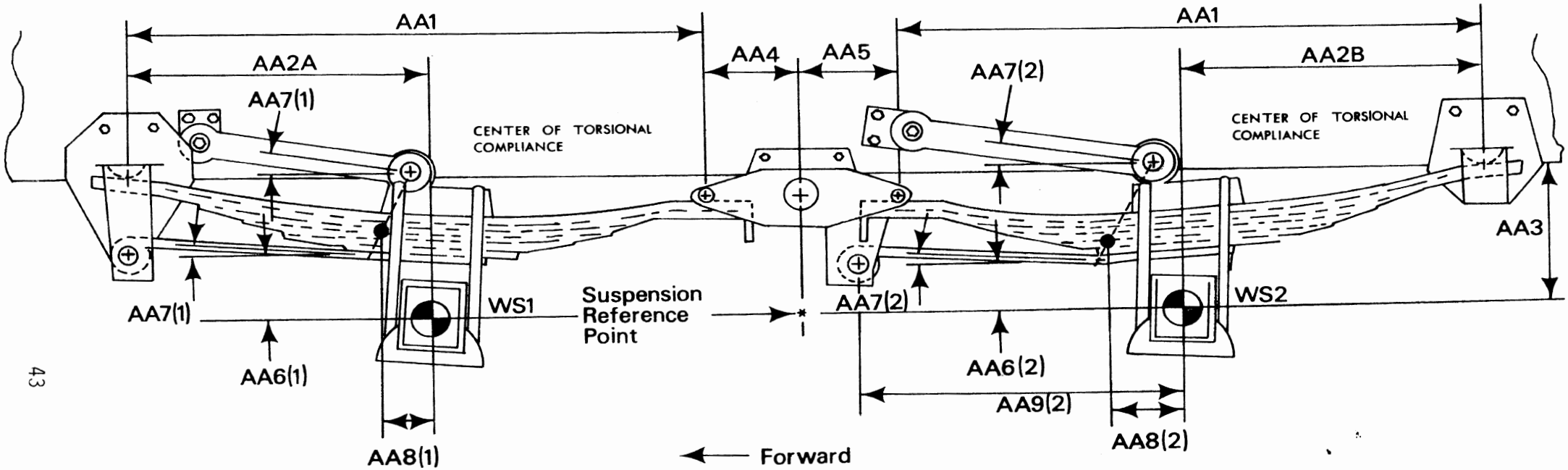

Figure 2.23. The MTRFSS with spring-type lower torque rods.

```
MULTIPLE TORQUE ROD FOUR SPRING
TANDEM SUSPENSION WITH SPRING-TYPE
LOWER TORQUE ROD

AA1        AVERAGE LEAF SPRING LENGTH:
           HORIZONTAL DISTANCE FROM FRONT TO REAR
           LEAF/FRAME CONTACT POINT(IN)                    40.00
AA2A       HORIZONTAL DISTANCE FROM FOREMOST LEAF/
           FRAME CONTACT TO AXLE CENTER:
           LEADING AXLE (IN)                               19.00
AA2B       HORIZONTAL DISTANCE FROM REARMOST LEAF/
           FRAME CONTACT TO AXLE CENTER:
           TRAILING AXLE (IN)                              21.00
AA3        AVERAGE VERTICAL DIST.FROM LEAF/FRAME
           CONTACT TO AXLE CENTER (IN)                      9.50
AA4        DIST. FROM FRONT LEAF/LOAD LEVELER
           CONTACT TO LOAD LEVELER PIN (IN)                 6.75
AA5        DIST. FROM REAR LEAF/LOAD LEVELER
           CONTACT TO LOAD LEVELER PIN(IN)                  6.75
AA6(1)     VERTICAL DISTANCE FROM AXLE CENTER
           UP TO TORQUE ROD COMPLIANCE CENTER:
           LEADING AXLE (IN)                                6.50
AA6(2)     VERTICAL DISTANCE FROM AXLE CENTER
           UP TO TORQUE ROD COMPLIANCE CENTER:
           TRAILING AXLE (IN)                               6.50
AA7(1)     AVERAGE ANGLE BETWEEN TORQUE RODS
           AND HORIZONTAL:  LEADING AXLE (DEG)             13.00
AA7(2)     AVERAGE ANGLE BETWEEN TORQUE RODS
           AND HORIZONTAL:  TRAILING AXLE(DEG)             13.00
AA8(1)     HORIZONTAL DISTANCE FROM AXLE CENTER
           FORWARD TO TORQUE ROD COMPLIANCE
           CENTER:  LEADING AXLE (IN)                       3.75
AA8(2)     HORIZONTAL DISTANCE FROM AXLE CENTER
           FORWARD TO TORQUE ROD COMPLIANCE
           CENTER:  TRAILING AXLE (IN)                      3.75
AA9(1)     HORIZONTAL DISTANCE FROM AXLE CENTER
           FORWARD TO LOWER TORQUE ROD FRAME PIN:
           LEADING AXLE (IN)                               12.00
AA9(2)     HORIZONTAL DISTANCE FROM AXLE CENTER
           FORWARD TO LOWER TORQUE ROD FRAME PIN:
           TRAILING AXLE (IN)                              12.00
C1         VISCOUS DAMPING: JOUNCE ON LEADING AXLE
           (LB-SEC/IN)                                      0.0
C2         VISCOUS DAMPING: REBOUND ON LEADING AXLE
           (LB-SEC/IN)                                      0.0
C3         VISCOUS DAMPING: JOUNCE ON TRAILING AXLE
           (LB-SEC/IN)                                      0.0
C4         VISCOUS DAMPING: REBOUND ON TRAILING AXLE
           (LB-SEC/IN)                                      0.0
CF1        MAX. COULOMB FRICTION, LEADING AXLE (LB)      4400.00
CF2        MAX. COULOMB FRICTION, TRAILING AXLE (LB)     4400.00
K1         SPRING RATE OF LEAF SPRING:
           LEADING AXLE (LB/IN)                         10000.00
K2         SPRING RATE OR LEAF SPRING:
           TRAILING AXLE (LB/IN)                        10000.00
KTQ1       TORSIONAL SPRING RATE OF LEAF SPRING:
           LEADING AXLE (IN-LB/DEG)                     70000.00
KTQ2       TORSIONAL SPRING RATE OF LEAF SPRING:
           TRAILING AXLE (IN-LB/DEG)                    70000.00
KTR1       SPRING RATE OF LOWER TORQUE ROD:
           LEADING AXLE (LB/IN)                          1000.00
KTR2       SPRING RATE OF LOWER TORQUE ROD:
           TRAILING AXLE (LB/IN)                         1000.00
KTRTQ1     TORSIONAL SPRING RATE OF TORQUE
           ROD ASSEMBLY: LEADING AXLE (IN-LB/DEG)       70000.00
KTRTQ2     TORSIONAL SPRING RATE OF TORQUE
           ROD ASSEMBLY: TRAILING AXLE (IN-LB/DEG       70000.00
NACOEF1    NOMINAL AXLE ANGULAR POSITION
           COEFFICIENT:  LEADING AXLE (DEG/IN)              0.00
NACOEF2    NOMINAL AXLE ANGULAR POSITION
           COEFFICIENT:  TRAILING AXLE (DEG/IN)             0.00
PRCTN1     STATIC NORMAL LOAD PERCENTAGE:
           LEADING AXLE                                    50.00
WS1        UNSPRUNG WEIGHT:LEADING AXLE (LB)             2330.00
WS2        UNSPRUNG WEIGHT:TRAILING AXLE (LB)            2074.00
```

Figure 2.24. MTRFSS with spring-type torque rods data echo.

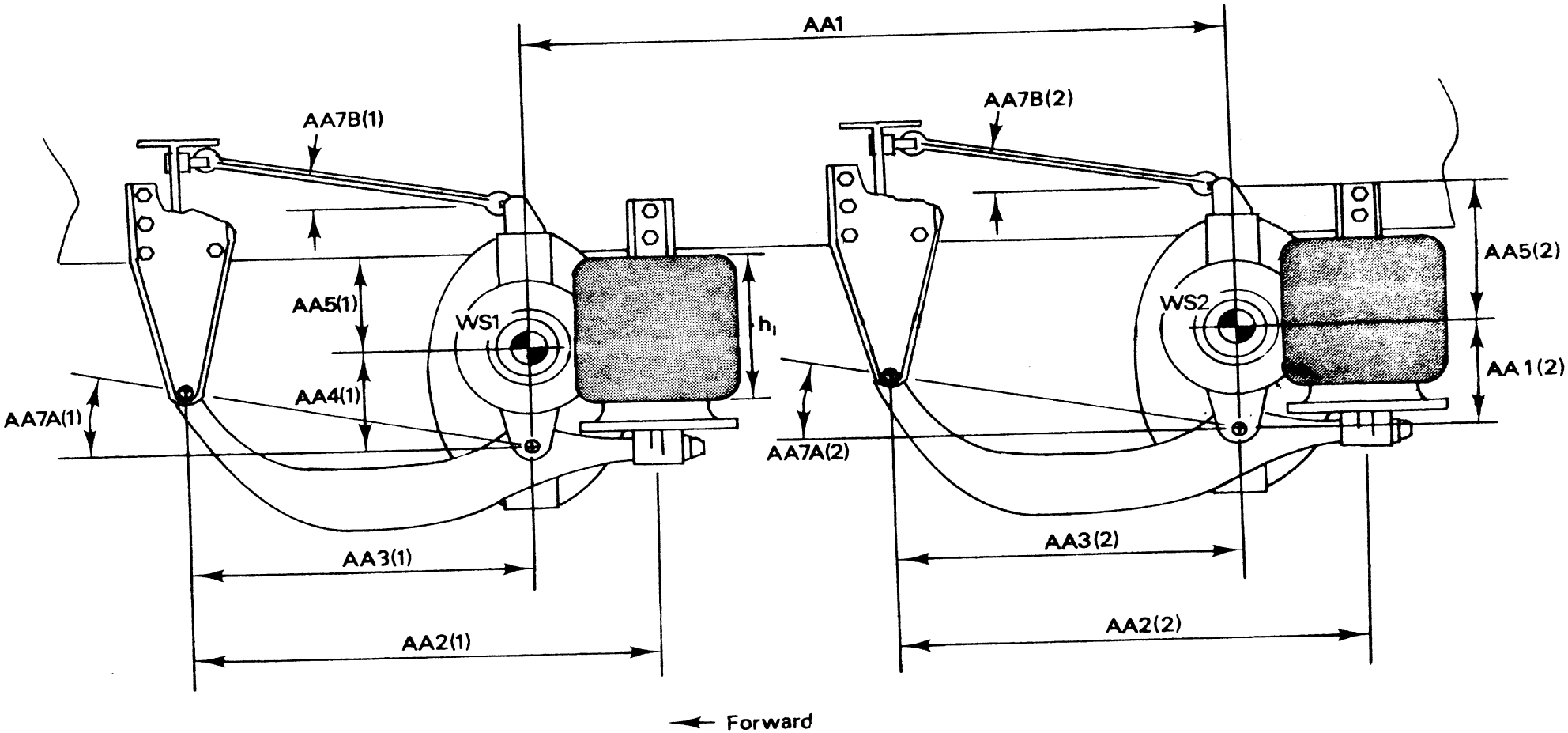

Figure 2.25. The air suspension model with four-bar linkage suspensions.

Either or both of the axles of the suspension may be converted from the four-bar type to the trailing-arm type. The geometry of the trailing-arm axle is shown in Figure 2.26. (The subscripts (1) and (2) have been deleted from this figure since it is applicable to either leading or trailing axles.) Note that the definitions of AA2 and AA3 remain unchanged, the definition of AA4 has been altered, and the parameters AA5, AA7A and AA7B are no longer needed. In order to cue the computer program that a particular axle is to be of the trailing-arm type, the parameter AA5 for that axle is entered as 0.0. When this is done, the program will delete from the input flow the AA7A and AA7B parameters for that same axle. For example, if AA5(1) is entered as 0.0, AA7A(1) and AA7B(1) will not be read, and the leading axle will be treated as a trailing-arm type. If, in the unlikely event that the user wishes to enter a true value of zero for the parameter AA5 on a four-bar type axle, a very small non-zero number should be entered instead.

The baseline suspension may also be converted to a single-axle suspension. This is accomplished simply by entering a value of 0.0 for the parameter AA1. Thereafter, all mechanical and pneumatic parameters pertaining to the second axle will automatically be deleted from the input flow. The pneumatic system parameter, CINTR (to be discussed later), will also be deleted. A single-axle suspension may be of either the four-bar or trailing-arm type.

In addition to the geometric parameters, the mechanical system parameters also include the unsprung weights of the leading and trailing axles (WS1 and WS2, respectively) and the viscous damping coefficients, C1, C2, C3, and C4. As in other suspensions, C1 and C2 apply to the leading axle, C3 and C4 to the trailing axle; C1 and C3 are for jounce and C2 and C4 are for rebound. Coulomb friction is not included in the air suspension.

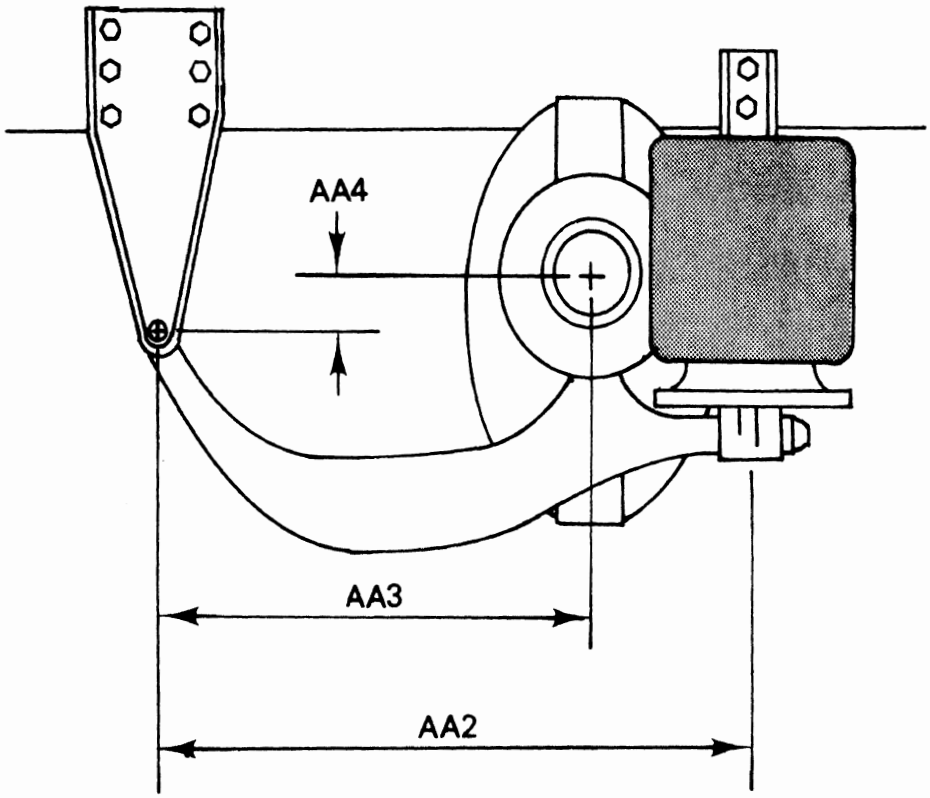

Figure 2.26. The trailing-arm air suspension.

We will now consider the pneumatic elements of the air suspension model. Each axle of the air suspension requires five parameters to describe its air spring. Unlike the case for other suspensions, these parameters are for one spring only, not the sum of both springs on the axle. The five parameters are:

1. A_L: the effective air spring area with respect to load at the nominal operating height

$$A_L \equiv \left.\frac{\partial L}{\partial P}\right|_{h=h_o} \tag{2.8}$$

2. A_V: the effective air spring area with respect to volume at the nominal operating height

$$A_V = \left.\frac{\partial V}{\partial h}\right|_{h=h_o} \tag{2.9}$$

3. h_o: the nominal operating height of the air spring

4. K_p: the air spring constant pressure spring rate at the nominal operating pressure

$$K_p \equiv - \left.\frac{\partial L}{\partial h}\right|_{P=P_o} \tag{2.10}$$

5. L_o: the nominal operating air spring load

6. P_o: the nominal operating air spring (gauge) pressure

7. V_o: the nominal operating air spring volume

where in these definitions

h is the height of the air spring

L is the load on the air spring

P is the gauge air pressure of the air spring

V is the internal volume of the air spring

These seven parameters may be determined from manufacturers' published data. Consider Figure 2.27. This figure contains a plot of an example air spring characteristic [19] as published by the manufacturer.

To determine the necessary input parameters for the air spring, first determine the nominal operating point of the air spring. It is most convenient for the user to designate the static air spring condition as the nominal condition, although somewhat better results may be obtained if the nominal condition is defined as a "midpoint" in the operating range which the spring will experience in a simulation run.* Either way, the user must determine the nominal height, h_0, and nominal load, L_0. (Note that L_0 is the air spring load, not the axle load.) Then from data such as given in Figure 2.27, nominal pressure, P_0, and volume, V_0, may be determined to complete the definition of the nominal operating point. The parameter A_V is the slope of the "Vol" plot (Figure 2.27) at h_0. The constant pressure spring rate, K_p, is the negative of the slope of the constant pressure plot for $P=P_0$ at the operating point, (h_0, L_0). The effective area with respect to load, A_L, is the rate of change of load with respect to pressure at the operating point and along a line of constant height (see Figure 2.27).

Besides the air spring, the air suspension model includes accommodation for an air delivery system. The model allows the inclusion of a height control valve to service either or both axles and inter-axle air flow path. A schematic of the modeled air delivery system is given in Figure 2.28.

---

*Further discussion is given in Appendix B, Section B.9.3.

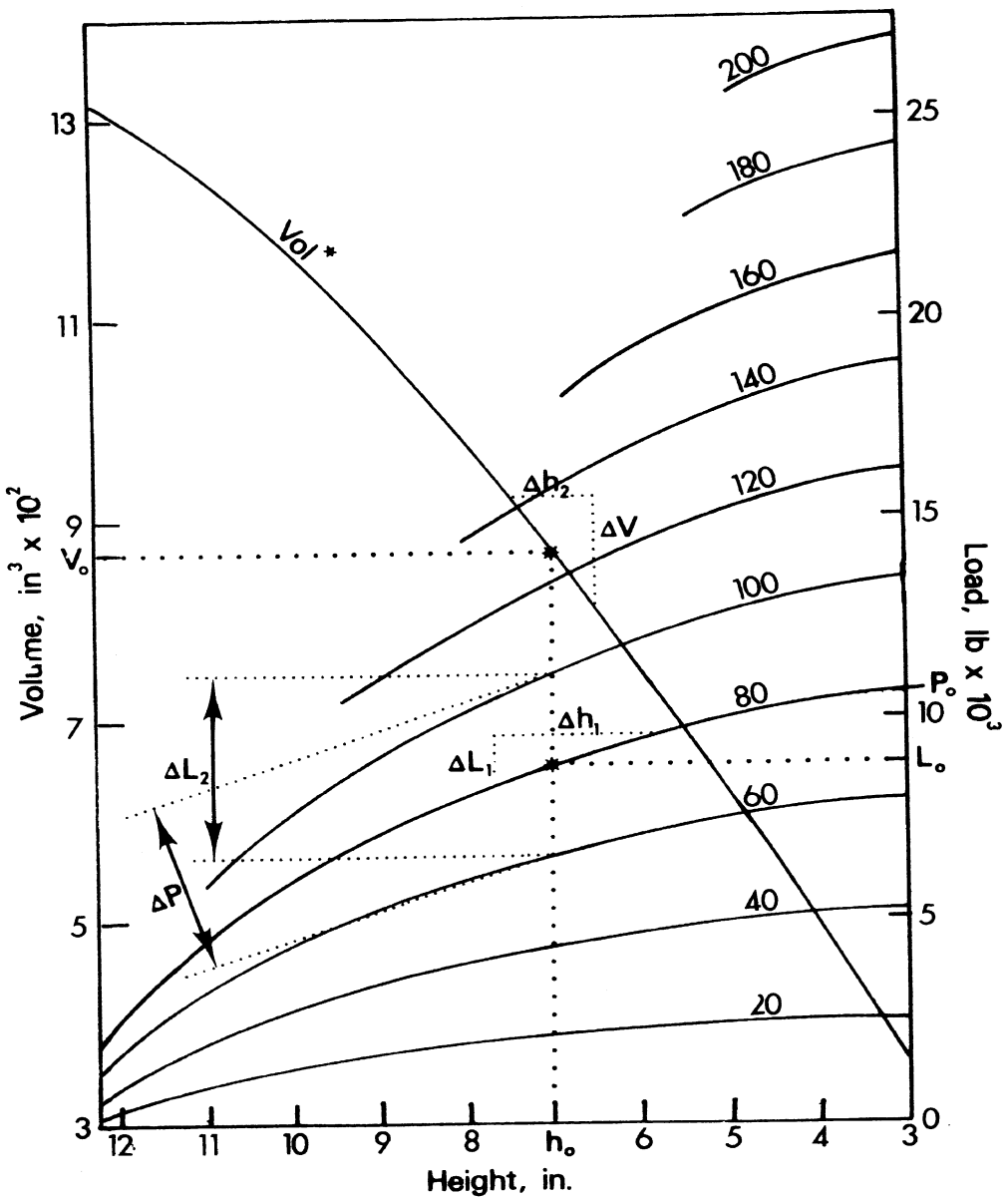

The Operating Point is defined by:

Nominal Volume ; $V_o = 870\ in^3$
Nominal Height ; $h_o = 7.0$ in
Nominal Load ; $L_o = 8800$ lb
Nominal Press ; $P_o = 80$ psig

The Dynamic Characteristics are:

Effective Area, Volume:

$$A_V \equiv \left.\frac{dV}{dh}\right|_{h_o} = \frac{\Delta V}{\Delta h_2} = 120\ in^2$$

Effective Area, Load;

$$A_L \equiv \left.\frac{\partial L}{\partial P}\right|_{h_o} \approx \frac{\Delta L_2}{\Delta P} = 112\ in^2$$

Constant Pressure Spring Rate;

$$K_P \equiv -\left.\frac{\partial L}{\partial h}\right|_{P_o} = -\frac{\Delta L_1}{\Delta h_1} = 667\ \frac{lb}{in}$$

*This plot applies to volume vs. height axes only. All other plots apply to the load vs. height axes only.

Figure 2.27. Example air spring data and model characteristics.

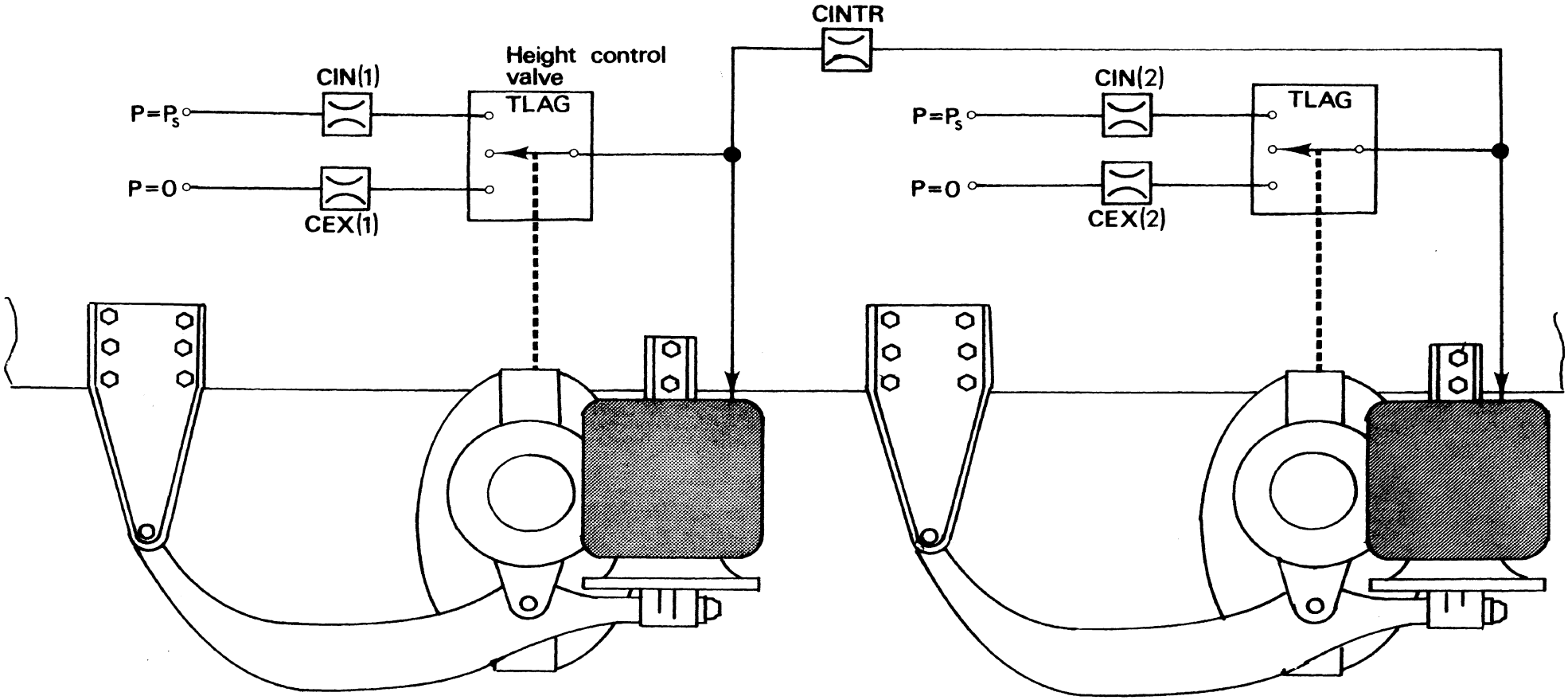

Figure 2.28. The air delivery system model.

Notice that each of the several air flow paths are characterized as a "lumped" restriction, each with a characteristic flow coefficient. Flow paths through the height control valves are characterized by an exhaust flow coefficnet (CEX) and an input flow coefficient (CIN). An additional flow coefficient (CINTR) describes the air line interconnecting the two springs.*

The height regulator valves also possess a time lag function (TLAG). That is, the valve will exhaust (or fill) the air spring only if the spring height has been greater (or less) than h_o for TLAG seconds. On the other hand, the valve will return to its closed position immediately when spring height equals h_o.

Each of the flow coefficients may be determined by experiment. Either a "constant pressure" or "constant volume" experiment might be used.

Figure 2.29 illustrates, in concept, an appropriate constant volume experimental setup.

The equation:

$$C = \frac{V}{P_e - P} \frac{dP}{dt} \tag{2.11}$$

where

V is the enclosed volume

P is the gauge pressure within the volume

P_e is the constant exhaust (supply) gauge

C is the flow coefficient of the network exhausting (supplying) the volume

t is time

---

*Like the air spring parameters, all of the flow coefficients are for one side of the vehicle, not the sum of both sides.

C: flow coefficient

P_e: constant exhaust pressure

V : constant volume

P : pressure

$P=P_1$ at time t_o

$P=P_2$ at time $t_o+\Delta t$

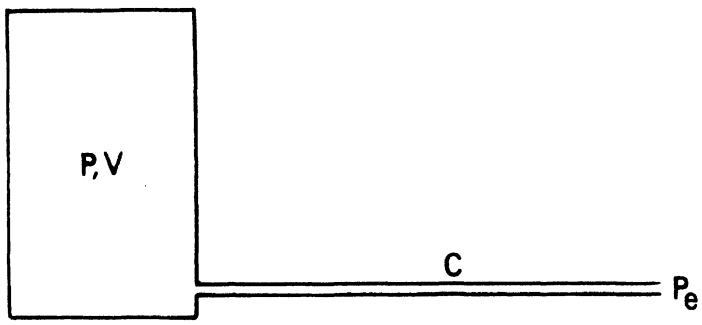

Figure 2.29. Determining flow coefficient with a constant volume experiment.

applies to this arrangement of apparatus, and may be used, with experimental data, to calculate the flow coefficient. Equation (2.11) may also be used in its integrated form:

$$C = \frac{V}{\Delta t} \ \ell n \ \frac{P_e - P_2}{P_e - P_1} \tag{2.12}$$

where $P_1 \equiv P$ at time t_o

$P_2 = P$ at time $t_o + \Delta t$

A similar expression which may serve as the basis for a constant pressure experiment is

$$C = \frac{P + P_{at}}{P_e - P} \ \frac{dV}{dt} \tag{2.13}$$

or in its integrated form

$$C = \frac{P + P_{at}}{P_e - P} \ \frac{V_2 - V_1}{\Delta t} \tag{2.14}$$

where the new symbol, P_{at}, is atmospheric pressure and

$V_1 = V$ at time t_o

$V_2 = V$ at time $t_o + \Delta t$

A conceptualization of an appropriate constant pressure experimental arrangement appears in Figure 2.30.

The air delivery system described in the preceding paragraphs may be much more complex than is generally needed. Often the characteristic time lag of real height control valves will be longer than the total time of a simulated stop. In such cases, it behooves the user to simply enter a large value for TLAG (and

C : flow coefficient

P : constant pressure

P_e : constant exhaust pressure

V : enclosed volume

$V = V_1$ at time t_o

$V = V_2$ at time $t_o + \Delta t$

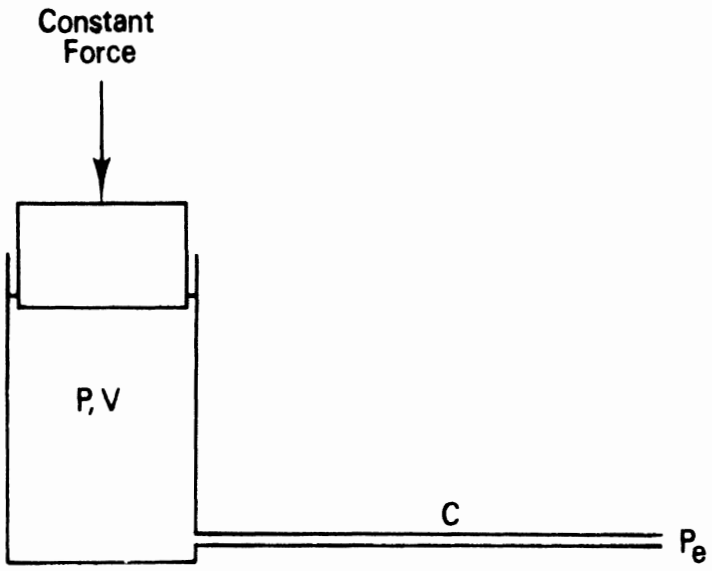

Figure 2.30. Determining flow coefficient with constant pressure experiment.

any value for the valve flow coefficients) or zero values for the valve flow coefficients, thus effectively eliminating the valves from the simulation.* Air flow between the axles of a tandem suspension may, however, perform an important load-leveling function and may, therefore, require accurate determination of CINTR.

In addition to the parameters discussed above, one other input parameter may be required for the air suspension. If a tandem suspension is to be used, and there is no inter-connecting air line between the two axles (i.e., CINTR=0), then the static distribution of load between the two axles is indeterminate. In this case, the input parameter PRCTN1 must be entered. The value of PRCTN1 is the percentage of the total suspension static load which is carried by the leading axle. PRCTN1 is omitted from the input flow if a single-axle suspension is employed or if CINTR $\neq$ 0.

Figures 2.31 through 2.33 present examples of required input flow for three variations of the air suspension option. The first example is of our selected baseline suspension, i.e., a tandem suspension composed of two four-bar type axles. Notice that CINTR $\neq$ 0 and, therefore, PRCTN1 does not appear. In the second example, another tandem suspension, the leading axle is of the trailing-arm type. AA5(1) has been entered as 0.0 to indicate to the program the use of a trailing-arm axle and the parameters AA7A(1) and AA7B(1) have consequently been deleted from the input flow. In this example, CINTR = 0.0 has also been entered, requiring the entry of the parameter PRCTN1. The final example is of a single-axle, four-bar type suspension. The parameter AA1 has been given the value 0.0 to indicate a single-axle suspension, and all parameters associated with the second axle have been deleted.

---

*The use of zero valve flow coefficient is also the appropriate method for removing one of the two height control valves from the network, if desired.

AIR SUSPENSION: TANDEM AXLE

AA1	HORIZONTAL DISTANCE FROM AXLE CENTER TO AXLE CENTER (IN)	57.00
AA2(1)	HORIZONTAL DISTANCE FROM MAIN ARM/ BODY CONNECTION PIN REARWARD TO AIR SPRING CENTER LINE (IN):LEADING AXLE	39.00
AA2(2)	HORIZONTAL DISTANCE FROM MAIN ARM/ BODY CONNECTION PIN REARWARD TO AIR SPRING CENTER LINE (IN):TRAILING AXLE	39.00
AA3(1)	HORIZONTAL DISTANCE FROM MAIN ARM/ BODY CONNECTION PIN REARWARD TO AXLE CENTER (IN):LEADING AXLE	29.50
AA3(2)	HORIZONTAL DISTANCE FROM MAIN ARM/ BODY CONNECTION PIN REARWARD TO AXLE CENTER (IN):TRAILING AXLE	29.50
AA4(1)	VERTICAL DISTANCE FROM AXLE CENTER DOWN TO MAIN ARM/AXLE CONNECTION PIN (IN): LEADING AXLE	3.00
AA4(2)	VERTICAL DISTANCE FROM AXLE CENTER DOWN TO MAIN ARM/AXLE CONNECTION PIN (IN): TRAILING AXLE	9.00
AA5(1)	VERTICAL DISTANCE FROM A POINT DIRECTLY ABOVE THE AXLE CENTER ON THE LINE OF ACTION OF THE TORQUE ROD,DOWN TO THE AXLE CENTER (IN):LEADING AXLE	12.00
AA5(2)	VERTICAL DISTANCE FROM A POINT DIRECTLY ABOVE THE AXLE CENTER ON THE LINE OF ACTION OF THE TORQUE ROD,DOWN TO THE AXLE CENTER (IN):TRAILING AXLE	12.00
AA7A(1)	ANGLE BETWEEN THE HORIZONTAL AND A LINE THROUGH THE TWO MAIN ARM CONNECTION PINS (DEG):LEADING AXLE	12.00
AA7A(2)	ANGLE BETWEEN THE HORIZONTAL AND A LINE THROUGH THE TWO MAIN ARM CONNECTION PINS (DEG):TRAILING AXLE	12.00
AA7B(1)	ANGLE BETWEEN THE TORQUE ROD AND THE HORIZONTAL (DEG):LEADING AXLE	12.00
AA7B(2)	ANGLE BETWEEN THE TORQUE ROD AND THE HORIZONTAL (DEG):TRAILING AXLE	12.00
AL1	EFFECTIVE AIR SPRING AREA WITH RESPECT TO LOAD (IN**2):LEADING AXLE	112.00
AL2	EFFECTIVE AIR SPRING AREA WITH RESPECT TO LOAD (IN**2):TRAILING AXLE	112.00
AV1	EFFECTIVE AIR SPRING AREA WITH RESPECT TO VOLUME (IN**2):LEADING AXLE	120.00
AV2	EFFECTIVE AIR SPRING AREA WITH RESPECT TO VOLUME (IN**2):TRAILING AXLE	120.00
C1	VISCOUS DAMPING: JOUNCE ON LEADING AXLE (LB-SEC/IN)	8.33
C2	VISCOUS DAMPING: REBOUND ON LEADING AXLE (LB-SEC/IN)	16.67
C3	VISCOUS DAMPING: JOUNCE ON TRAILING AXLE (LB-SEC/IN)	8.33
C4	VISCOUS DAMPING: REBOUND ON TRAILING AXLE (LB-SEC/IN)	16.67
CEX1	HEIGHT REGULATOR EXHAUST FLOW COEFFICIENT (IN**3/SEC): LEADING AXLE	0.0
CEX2	HEIGHT REGULATOR EXHAUST FLOW COEFFICIENT (IN**3/SEC): TRAILING AXLE	0.0
CIN1	HEIGHT REGULATOR INPUT FLOW COEFFICIENT (IN**3/SEC): LEADING AXLE	0.0
CIN2	HEIGHT REGULATOR INPUT FLOW COEFFICIENT (IN**3/SEC): TRAILING AXLE	0.0
CINTR	INTERSPRING FLOW COEFFICIENT (IN**3/SEC)	3000.00
H01	NOMINAL AIR SPRING HEIGHT (IN): LEADING AXLE	7.00
H02	NOMINAL AIR SPRING HEIGHT (IN): TRAILING AXLE	7.00
KP1	CONSTANT PRESSURE AIR SPRING RATE (LB/IN):LEADING AXLE	667.00
KP2	CONSTANT PRESSURE AIR SPRING RATE (LB/IN):TRAILING AXLE	667.00
LO1	NOMINAL AIR SPRING LOAD (LB): LEADING AXLE	8800.00
LO2	NOMINAL AIR SPRING LOAD (LB): TRAILING AXLE	8800.00
PO1	NOMINAL AIR SPRING PRESSURE (PSI): LEADING AXLE	80.00
PO2	NOMINAL AIR SPRING PRESSURE (PSI): TRAILING AXLE	80.00
PS	AIR SUSPENSION SUPPLY PRESSURE (PSIG):	100.00
TLAG	HEIGHT REGULATOR TIME LAG	3.00
V01	NOMINAL AIR SPRING VOLUME (IN): LEADING AXLE	870.00
V02	NOMINAL AIR SPRING VOLUME (IN): TRAILING AXLE	870.00
WS1	UNSPRUNG WEIGHT (LB):LEADING AXLE	2078.00
WS2	UNSPRUNG WEIGHT (LB):TRAILING AXLE	1972.00

Figure 2.31. Tandem four-bar/four-bar air suspension data echo.

AIR SUSPENSION: TANDEM AXLE

AA1	HORIZONTAL DISTANCE FROM AXLE CENTER TO AXLE CENTER (IN)	57.00
AA2(1)	HORIZONTAL DISTANCE FROM MAIN ARM/ BODY CONNECTION PIN REARWARD TO AIR SPRING CENTER LINE (IN):LEADING AXLE	39.00
AA2(2)	HORIZONTAL DISTANCE FROM MAIN ARM/ BODY CONNECTION PIN REARWARD TO AIR SPRING CENTER LINE (IN):TRAILING AXLE	39.00
AA3(1)	HORIZONTAL DISTANCE FROM MAIN ARM/ BODY CONNECTION PIN REARWARD TO AXLE CENTER (IN):LEADING AXLE	29.50
AA3(2)	HORIZONTAL DISTANCE FROM MAIN ARM/ BODY CONNECTION PIN REARWARD TO AXLE CENTER (IN):TRAILING AXLE	29.50
AA4(1)	VERTICAL DISTANCE FROM AXLE CENTER DOWN TO MAIN ARM/FRAME CONNECTION PIN (IN): LEADING AXLE	9.00
AA4(2)	VERTICAL DISTANCE FROM AXLE CENTER DOWN TO MAIN ARM/AXLE CONNECTION PIN (IN): TRAILING AXLE	9.00
AA5(2)	VERTICAL DISTANCE FROM A POINT DIRECTLY ABOVE THE AXLE CENTER ON THE LINE OF ACTION OF THE TORQUE ROD,DOWN TO THE AXLE CENTER (IN):TRAILING AXLE	12.00
AA7A(2)	ANGLE BETWEEN THE HORIZONTAL AND A LINE THROUGH THE TWO MAIN ARM CONNECTION PINS (DEG):TRAILING AXLE	12.00
AA7B(2)	ANGLE BETWEEN THE TORQUE ROD AND THE HORIZONTAL (DEG):TRAILING AXLE	12.00
AL1	EFFECTIVE AIR SPRING AREA WITH RESPECT TO LOAD (IN**2):LEADING AXLE	112.00
AL2	EFFECTIVE AIR SPRING AREA WITH RESPECT TO LOAD (IN**2):TRAILING AXLE	112.00
AV1	EFFECTIVE AIR SPRING AREA WITH RESPECT TO VOLUME (IN**2):LEADING AXLE	120.00
AV2	EFFECTIVE AIR SPRING AREA WITH RESPECT TO VOLUME (IN**2):TRAILING AXLE	120.00

C1	VISCOUS DAMPING: JOUNCE ON LEADING AXLE (LB-SEC/IN)	8.33
C2	VISCOUS DAMPING: REBOUND ON LEADING AXLE (LB-SEC/IN)	16.67
C3	VISCOUS DAMPING: JOUNCE ON TRAILING AXLE (LB-SEC/IN)	8.33
C4	VISCOUS DAMPING: REBOUND ON TRAILING AXLE (LB-SEC/IN)	16.67
CEX1	HEIGHT REGULATOR EXHAUST FLOW COEFFICIENT (IN**3/SEC): LEADING AXLE	0.0
CEX2	HEIGHT REGULATOR EXHAUST FLOW COEFFICIENT (IN**3/SEC): TRAILING AXLE	0.0
CIN1	HEIGHT REGULATOR INPUT FLOW COEFFICIENT (IN**3/SEC): LEADING AXLE	0.0
CIN2	HEIGHT REGULATOR INPUT FLOW COEFFICIENT (IN**3/SEC): TRAILING AXLE	0.0
CINTR	INTERSPRING FLOW COEFFICIENT (IN**3/SEC)	0.0
H01	NOMINAL AIR SPRING HEIGHT (IN): LEADING AXLE	7.00
H02	NOMINAL AIR SPRING HEIGHT (IN): TRAILING AXLE	7.00
KP1	CONSTANT PRESSURE AIR SPRING RATE (LB/IN):LEADING AXLE	667.00
KP2	CONSTANT PRESSURE AIR SPRING RATE (LB/IN):TRAILING AXLE	667.00
LO1	NOMINAL AIR SPRING LOAD (LB): LEADING AXLE	8800.00
LO2	NOMINAL AIR SPRING LOAD (LB): TRAILING AXLE	8800.00
PO1	NOMINAL AIR SPRING PRESSURE (PSI): LEADING AXLE	80.00
PO2	NOMINAL AIR SPRING PRESSURE (PSI): TRAILING AXLE	80.00
PRCTN1	STATIC NORMAL LOAD PERCENTAGE: LEADING AXLE	50.00
PS	AIR SUSPENSION SUPPLY PRESSURE (PSIG):	100.00
TLAG	HEIGHT REGULATOR TIME LAG	3.00
V01	NOMINAL AIR SPRING VOLUME (IN): LEADING AXLE	870.00
V02	NOMINAL AIR SPRING VOLUME (IN): TRAILING AXLE	870.00
WS1	UNSPRUNG WEIGHT (LB):LEADING AXLE	2078.00
WS2	UNSPRUNG WEIGHT (LB):TRAILING AXLE	1972.00

Figure 2.32. Tandem trailing-arm/four-bar air suspension data echo.

AIR SUSPENSION: SINGLE AXLE

AA1	HORIZONTAL DISTANCE FROM AXLE CENTER TO AXLE CENTER (IN)	0.0
AA2(1)	HORIZONTAL DISTANCE FROM MAIN ARM/ BODY CONNECTION PIN REARWARD TO AIR SPRING CENTER LINE (IN):LEADING AXLE	39.00
AA3(1)	HORIZONTAL DISTANCE FROM MAIN ARM/ BODY CONNECTION PIN REARWARD TO AXLE CENTER (IN):LEADING AXLE	29.50
AA4(1)	VERTICAL DISTANCE FROM AXLE CENTER DOWN TO MAIN ARM/AXLE CONNECTION PIN (IN): LEADING AXLE	9.00
AA5(1)	VERTICAL DISTANCE FROM A POINT DIRECTLY ABOVE THE AXLE CENTER ON THE LINE OF ACTION OF THE TORQUE ROD,DOWN TO THE AXLE CENTER (IN):LEADING AXLE	12.00
AA7A(1)	ANGLE BETWEEN THE HORIZONTAL AND A LINE THROUGH THE TWO MAIN ARM CONNECTION PINS (DEG):LEADING AXLE	12.00
AA7B(1)	ANGLE BETWEEN THE TORQUE ROD AND THE HORIZONTAL (DEG):LEADING AXLE	12.00
AL1	EFFECTIVE AIR SPRING AREA WITH RESPECT TO LOAD (IN**2):LEADING AXLE	112.00
AV1	EFFECTIVE AIR SPRING AREA WITH RESPECT TO VOLUME (IN**2):LEADING AXLE	120.00
C1	VISCOUS DAMPING: JOUNCE ON LEADING AXLE (LB-SEC/IN)	8.33
C2	VISCOUS DAMPING: REBOUND ON LEADING AXLE (LB-SEC/IN)	16.67
CEX1	HEIGHT REGULATOR EXHAUST FLOW COEFFICIENT (IN**3/SEC): LEADING AXLE	0.0
CIN1	HEIGHT REGULATOR INPUT FLOW COEFFICIENT (IN**3/SEC): LEADING AXLE	0.0
H01	NOMINAL AIR SPRING HEIGHT (IN): LEADING AXLE	7.00
KP1	CONSTANT PRESSURE AIR SPRING RATE (LB/IN):LEADING AXLE	667.00
LO1	NOMINAL AIR SPRING LOAD (LB): LEADING AXLE	8800.00
PO1	NOMINAL AIR SPRING PRESSURE (PSI): LEADING AXLE	80.00
PS	AIR SUSPENSION SUPPLY PRESSURE (PSIG):	100.00
TLAG	HEIGHT REGULATOR TIME LAG	3.00
V01	NOMINAL AIR SPRING VOLUME (IN): LEADING AXLE	870.00
WS1	UNSPRUNG WEIGHT (LB):LEADING AXLE	2078.00

Figure 2.33. Single four-bar air suspension data echo.

2.2 The Sprung Masses

The third grouping of data in the input flow of the Phase III program describes the sprung masses of the vehicle to be simulated. This is true for both the straight truck, tractor-trailer, and doubles combination programs. In the following sections, the appropriate input flow for the sprung mass data group for each of these programs will be described. The mathematical models of the sprung masses are described in Appendix C.

2.2.1 The Straight Truck Sprung Mass. Figure 2.34 illustrates all of the input parameters required by the straight truck program to describe the vehicle's sprung mass. Figure 2.35 gives an example of the sprung mass section of the input data echo which is output by the program. Note that the order of the data is identical to the required order for input of this data group. In addition to the sprung mass parametric data, three other variables, GRADE, TIMF, and VEL, are included in the data. GRADE is the slope (in percent) of the roadway with a positive entry implying "uphill" and negative, "downhill." The variable TIMF is the maximum real time that the simulation will be allowed to run. In a braking simulation run, the program will be halted whenever the vehicle comes to a stop or when the time reaches TIMF seconds, whichever occurs first. The parameter VEL indicates (in ft/sec) the initial velocity of the vehicle.

Most of the sprung mass parameters are self-explanatory from the information provided by Figures 2.34 and 2.35. Recall that the "Suspension Reference Points" referred to in these figures have been defined earlier for each of the suspension options available.

Notice that the weight, pitch moment of inertia, and center of gravity position of the vehicle's own sprung mass and of the payload mass are described separately in the input data. This allows the user to change payloads on the vehicle more easily. If the user wishes to simulate an empty vehicle, the payload

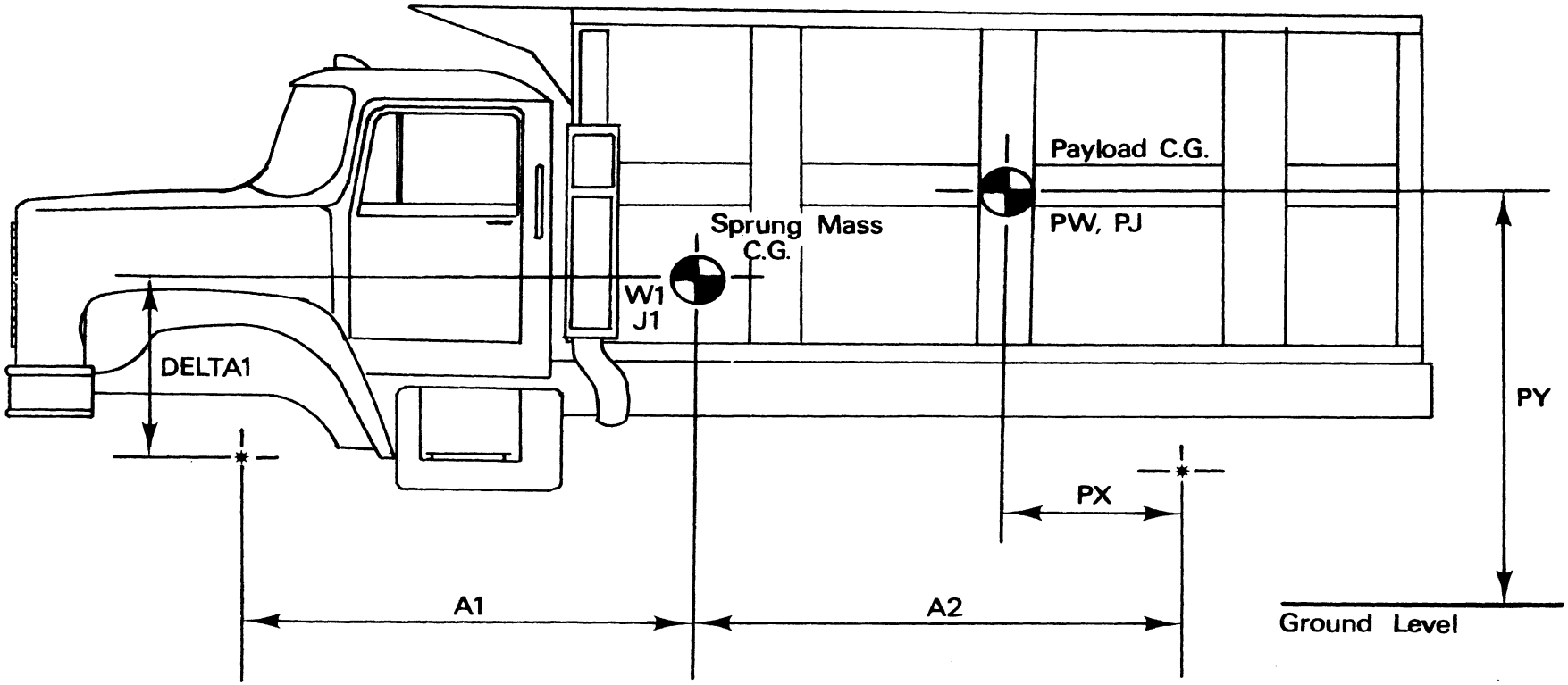

* Suspension Reference Points

Figure 2.34. The sprung mass of the straight truck.

SPRUNG MASS :

A1	REFERENCE POINT OF FRONT SPRUNG MASS CG TO SUSPENSION (IN)	105.00
A2	HORIZONTAL DISTANCE FROM SPRUNG MASS CG TO REFERENCE POINT OF REAR SUSPENSION (IN)	60.00
DELTA1	STATIC VERTICAL DISTANCE, FRONT AXLE TO SPRUNG MASS CG (IN)	27.67
GRADE	PERCENT GRADE (POSITIVE IS UPHILL)	5.00
J1	SPRUNG MASS POLAR MOMENT OF INERTIA (IN-LB-SEC**2)	103492.00
PW	WEIGHT OF PAYLOAD (LBS)	24000.00
PJ	POLAR MOMENT OF PAYLOAD (IN-LB-SEC**2)	100000.00
PX	HORIZONTAL DISTANCE FROM CENTER OF REAR SUSPENSION TO MASS CENTER (IN)	30.00
PZ	VERTICAL DISTANCE FROM GROUND TO PAYLOAD CENTER OF MASS (IN)	72.00
TIME	MAX. REAL TIME FOR SIMULATION	1.00
VEL	INITIAL VELOCITY (FPS)	88.00
W1	SPRUNG WEIGHT OF TRUCK (LBS)	16033.00

Figure 2.35. Straight truck sprung mass data echo.

weight (PW) is simply entered as 0.0. When this is done, the other parameters describing the payload (PJ, PX, and PY) will be omitted from the input flow.

2.2.2 The Tractor-Trailer Sprung Masses. The parameters required by the program to describe the two sprung masses of a tractor-trailer are illustrated in Figure 2.36. In Figure 2.37, an example of the input data flow is given by showing the input echo output of the computer program. As was described in Section 2.2.1, the parameters GRADE, TIMF, and VEL are also included in this input group.

Several of the geometric parameters referred to in the figures locate the various centers of gravity relative to the "Suspension Reference Points." These points have been defined earlier in Section 2.1 for each of the various suspension options.

Data describing the vehicle's payload (PW, PJ, PX, and PY) are entered separately from similar parameters which describe the inertial properties of the trailer itself. Thus the user may easily change vehicle loading from run to run. If an empty vehicle is desired, the user enters a payload weight of zero (PW = 0.0) and the remaining payload parameters (PJ, PX, and PY) are omitted from the input flow.

2.2.3 The Doubles Combination Sprung Masses. The input required to describe the sprung masses of the doubles combination is similar to, but, of course, more extensive than that required for the straight truck and tractor-trailer simulations. The doubles input data are described in Figures 2.38 and 2.39. The inertial properties of the payloads for both trailers are again entered as separate values from those of the trailers themselves. Either or both trailers may be run "empty" by setting the appropriate payload weight(s) to zero and omitting the remaining parameters describing the payload(s).

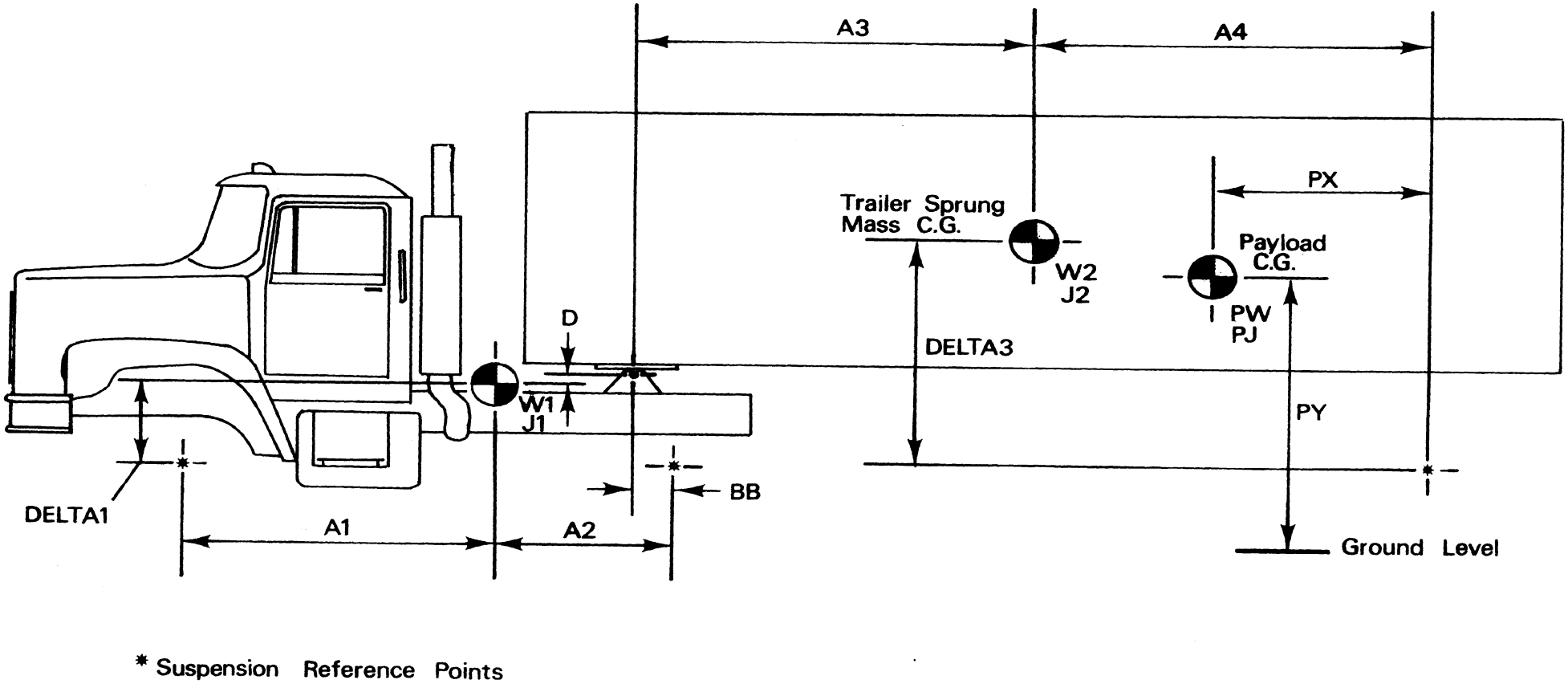

Figure 2.36. The sprung masses of the tractor-trailer.

SPRUNG MASS :

A1	HORIZONTAL DISTANCE FROM TRACTOR CG TO REFERENCE POINT OF TRACTOR FRONT SUSPENSION (IN)	35.90
A2	HORIZONTAL DISTANCE FROM TRACTOR CG TO REFERENCE POINT OF TRACTOR REAR SUSPENSION (IN)	106.10
A3	HORIZONTAL DISTANCE FROM TRAILER CG TO 5TH WHEEL (IN)	222.00
A4	HORIZONTAL DISTANCE FROM TRAILER CG TO REFERENCE POINT OF TRAILER SUSPENSION (IN)	144.00
BR	HORIZONTAL DISTANCE FROM 5TH WHEEL TO REFERENCE POINT OF TRACTOR REAR SUSPENSION (IN)	0.0
D	VERTICAL DISTANCE FROM 5TH WHEEL CONNECTION DOWN TO TRACTOR CG (IN)	-4.50
DELTA1	STATIC VERTICAL DISTANCE, TRACTOR CG TO TRACTOR FRONT AXLE (IN)	33.30
DELTA3	STATIC VERTICAL DISTANCE, TRAILER CG TO TRAILER AXLE(S) (IN)	49.50
GRADE	PERCENT GRADE (POSITIVE IS UPHILL)	5.00
J1	TRACTOR POLAR MOMENT (IN-LB-SEC**2)	53374.00
J2	TRAILER POLAR MOMENT OF INERTIA (IN-LB-SEC**2)	607200.00
PW	WEIGHT OF PAYLOAD (LBS)	0.0
TIME	MAXIMUM TRAL TIME FOR SIMULATION (SEC)	1.00
VEL	INITIAL VELOCITY (FT/SEC)	44.00
W1	SPRUNG WEIGHT OF TRACTOR (LBS)	9245.00
W2	SPRUNG WEIGHT OF TRAILER (LBS)	8120.00

Figure 2.37. Tractor-trailer sprung mass data echo.

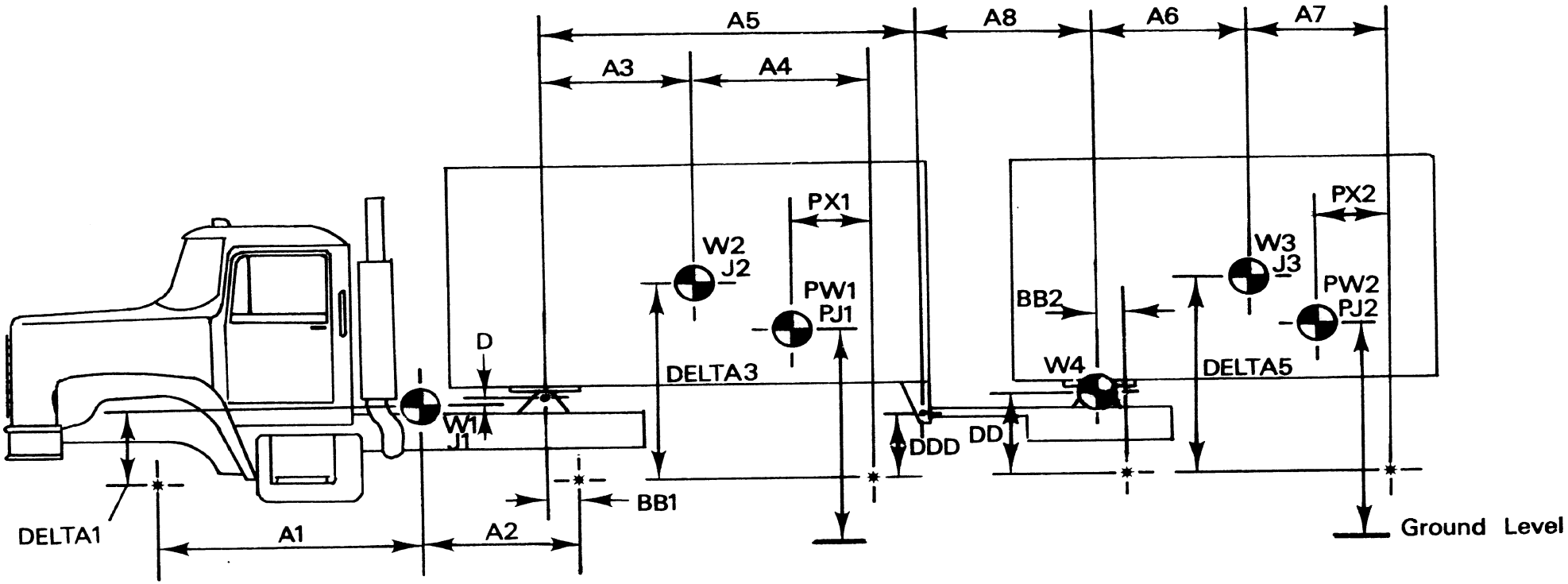

* Suspension Reference Points

Figure 2.38. Sprung masses of the doubles combination.

SPRUNG MASS :

A1	HORIZONTAL DISTANCE FROM TRACTOR CG TO REFERENCE POINT OF TRACTOR FRONT SUSPENSION (IN)	35.90
A2	HORIZONTAL DISTANCE FROM TRACTOR CG TO REFERENCE POINT OF TRACTOR REAR SUSPENSION (IN)	106.10
A3	HORIZONTAL DISTANCE FROM FIRST TRAILER CG TO FIRST TRAILER KING PIN (IN)	222.00
A4	HORIZONTAL DISTANCE FROM FIRST TRAILER CG TO REFERENCE POINT OF FIRST TRAILER SUSPENSION (IN)	144.00
A5	HORIZONTAL DISTANCE FROM FIRST TRAILER KING PIN TO DOLLY TONGUE HITCH (IN)	376.00
A6	HORIZONTAL DISTANCE FROM SECOND TRAILER CG TO SECOND TRAILER KING PIN (IN)	222.00
A7	HORIZONTAL DISTANCE FROM SECOND TRAILER CG TO REFERENCE POINT OF SECOND TRAILER SUSPENSION (IN)	144.00
A8	HORIZONTAL DISTANCE FROM DOLLY TONGUE HITCH TO DOLLY 5TH WHEEL (IN)	72.00
BB1	HORIZONTAL DISTANCE FROM TRACTOR 5TH WHEEL REARWARD TO REFERENCE POINT OF TRACTOR REAR SUSPENSION (IN)	0.0
BB2	HORIZONTAL DISTANCE FROM DOLLY 5TH WHEEL REARWARD TO DOLLY SUSPENSION REFERENCE POINT (IN)	6.00
D	VERTICAL DISTANCE DOWNWARD FROM TRACTOR 5TH WHEEL TO TRACTOR CG (IN)	-4.50
DD	VERTICAL DISTANCE DOWNWARD FROM DOLLY FIFTH WHEEL TO DOLLY SUSPENSION REFERENCE POINT(IN)	29.50
DDD	VERTICAL DISTANCE DOWNWARD FROM DOLLY TONGUE HITCH TO FIRST TRAILER SUSPENSION REFERENCE POINT (IN)	26.00
DELTA1	STATIC VERTICAL DISTANCE, TRACTOR CG TO TRACTOR FRONT AXLE (IN)	33.30
DELTA3	STATIC VERTICAL DISTANCE, FIRST TRAILER CG TO FIRST TRAILER AXLE(S) (IN)	49.50
DELTA5	STATIC VERTICAL DISTANCE, SECOND TRAILER CG TO SECOND TRAILER AXLE(S) (IN)	49.50
GRADE	PERCENT GRADE (POSITIVE IS UPHILL)	5.00
J1	TRACTOR POLAR MOMENT (IN-LB-SEC**2)	53374.00
J2	FIRST TRAILER POLAR MOMENT OF INERTIA (IN-LB-SEC**2)	706200.00
J3	SECOND TRAILER POLAR MOMENT OF INERTIA (IN-LB-SEC**2)	706200.00
PW1	WEIGHT OF FIRST TRAILER PAYLOAD (LBS)	0.0
PW2	WEIGHT OF SECOND TRAILER PAYLOAD (LB)	35000.00
PJ2	POLAR MOMENT OF SECOND TRAILER PAYLOAD (IN-LB-SEC**2)	75000.00
PX2	HORIZONTAL DISTANCE FROM REFERENCE POINT OF SECOND TRAILER SUSPENSION TO SECOND TRAILER PAYLOAD MASS CENTER (IN)	144.00
PZ2	VERTICAL DISTANCE FROM GROUND TO SECOND TRAILER PAYLOAD MASS CENTER (IN)	75.00
TIMF	MAXIMUM REAL TIME FOR SIMULATION (SEC)	2.00
VEL	INITIAL VELOCITY (FT/SEC)	44.00
W1	SPRUNG WEIGHT OF TRACTOR (LB)	9245.00
W2	SPRUNG WEIGHT OF FIRST TRAILER (LB)	8120.00
W3	SPRUNG WEIGHT OF SECOND TRAILER (LB)	8120.00
W4	SPRUNG WEIGHT OF DOLLY (LB)	1.00

Figure 2.39. Double combinations sprung mass data echo.

The dolly requires only one inertial parameter--its weight. The simulation assumes the dolly to have zero moment of inertia and to have its center of gravity located at the fifth wheel.

As in the truck and tractor-trailer programs, the parameters GRADE, TIMF, and VEL are also included in the sprung mass data group.

2.3 The Brake Models

The stopping distance capability of any commercial vehicle has first-order dependence on the brake torque. Unfortunately, the relationship between brake line pressure and brake torque is extremely difficult to quantify. There are two factors underlying this difficulty, namely, (1) the characteristics of the brakes often change with time, and (2) appropriate brake torque versus line pressure data is often difficult to procure.

In spite of these obstacles, reasonable calculations can and have been made. For example, time averaged torque values, from spin-down dynamometer data or from the deceleration history measured during vehicle testing, may be used to predict braking performance. Although fluctuations in deceleration due to fade are ignored in this procedure, reasonable predictions of stopping distance may well result. Consider, for example, Figure 2.40 in which simulated and measured deceleration time histories are presented for a straight truck.* Note that although the simulation ignores brake fade, the time average deceleration, and thus stopping distance, is quite accurate.

The first two braking subsections of this report will concern the simulation of time average brake torque. This may be done using brake modules or tabular "dynamometer curves," as discussed in Subsection 2.3.1. The next two subsections discuss the simulation of brake imbalance and hysteresis, both of major

---

*A more detailed description of this test is given in Reference 3.

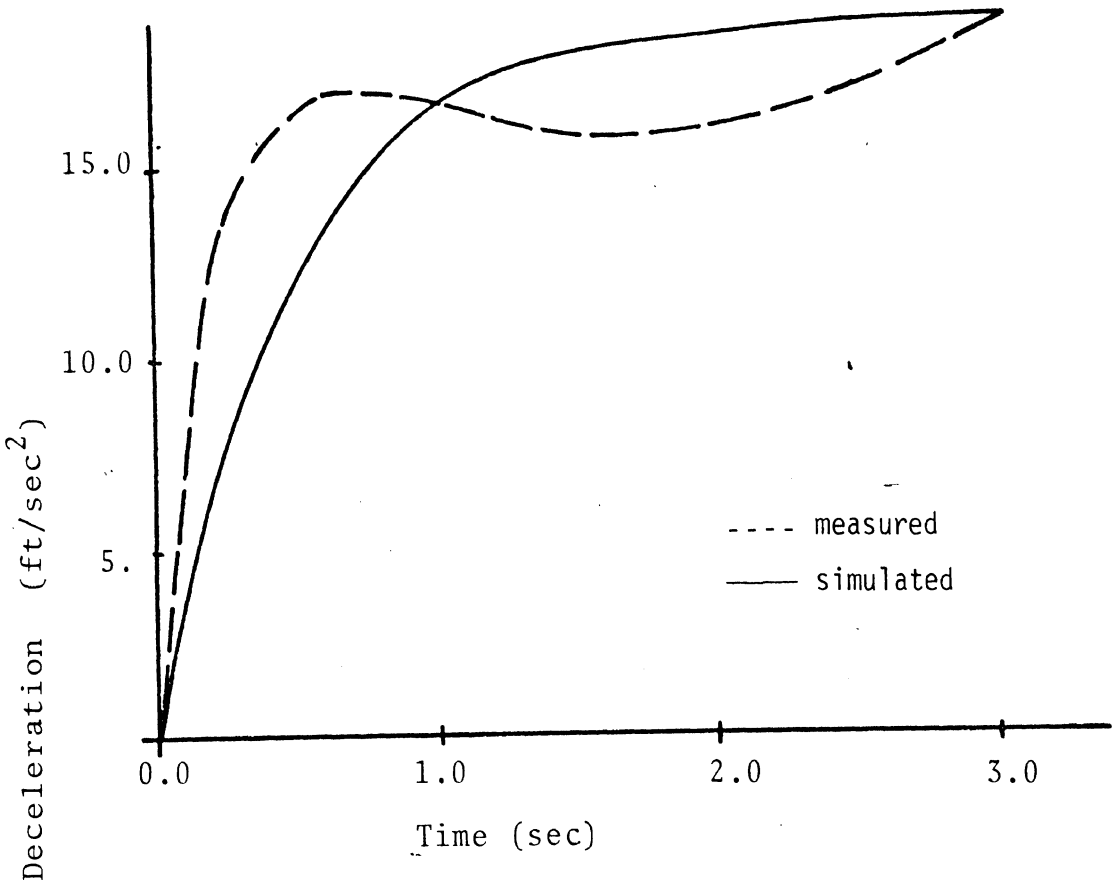

Figure 2.40. Simulated and measured deceleration time histories.

interest in antilock system modeling. Finally, a methodology for the prediction of brake fade will be discussed in subsection 2.3.4. It will be shown that the newly developed fade algorithm will allow calculations very much similar in character to the TEST curve presented in Figure 2.40.

2.3.1 Time-Averaged Brake Torque. The time-averaged brake torque is assumed to be a unique* function of the line pressure at that brake. In the absence of the intervention of an antilock system, the line pressure at each brake is a function of the time history of the treadle valve pressure and the time delays inherent in the air system. In the next subsection the computation of the line pressure without an antilock system is discussed. The antilock brake algorithm is explained in Section 2.5.

Brake Timing.

In the absence of intervening antilock logic, the response of the brake system to control inputs applied at the treadle valve is characterized by two parameters (per axle): the time delay, and the rise time. The time delay is defined as the time elapsed from the instant that the pressure starts to rise at the output of the treadle valve to the instant that pressure starts to rise in a given brake actuator. For the purposes of this program, rise time of the brake is defined as the time elapsed from the instant that pressure starts to increase in the brake chamber to the instant that the pressure reaches 63% of the commanded value, as a result of a step application of pressure at the treadle valve. The simulated pressure response at any given axle is given by the equation

$$\frac{dP(I)}{dt} + \frac{(P-P(I))}{TQ(I,2)} = 0 \qquad (2.15)$$

*With one possible exception—line pressure/torque hysteresis as explained in Section 2.3.3.

where

P is the treadle valve pressure at time t

P(I) is the pressure at the Ith axle

$$\bar{t} = t - TQ(I,1) \tag{2.16}$$

TQ(I,1) is the time delay

TQ(I,2) is the rise time.

Equation (2.15) can be solved for a step application of treadle pressure P_0 at time t_0. The pressure response at the Ith axle is

$$P(I) = 0, \bar{t} \leq 0 \tag{2.17}$$

$$P(I) = P_0\left(1-\exp\left(\frac{t-\bar{t}}{TQ(I,2)}\right)\right), \bar{t} > 0 \tag{2.18}$$

where

$$\bar{t} = t-t_0 - TQ(I,1) \tag{2.19}$$

The response at the Ith axle to a step pressure at the treadle valve is delayed by time delay TQ(I,1). The pressure will then rise toward P_0, reaching $.63P_0$ approximately TQ(I,1) + TQ(I,2) seconds after the step application at the treadle valve. Thus, the time delay is TQ(I,1) and the rise time is characterized by TQ(I,2).

In general, the pressure at the treadle valve varies with time. Thus, provision is made in the program for the user to specify a table of values for pressure versus time.

An example is given for illustration. Typical brake pressure response curves are given in Figure 2.41. The curves calculated using Equation (2.15) above are given in Figure 2.42.

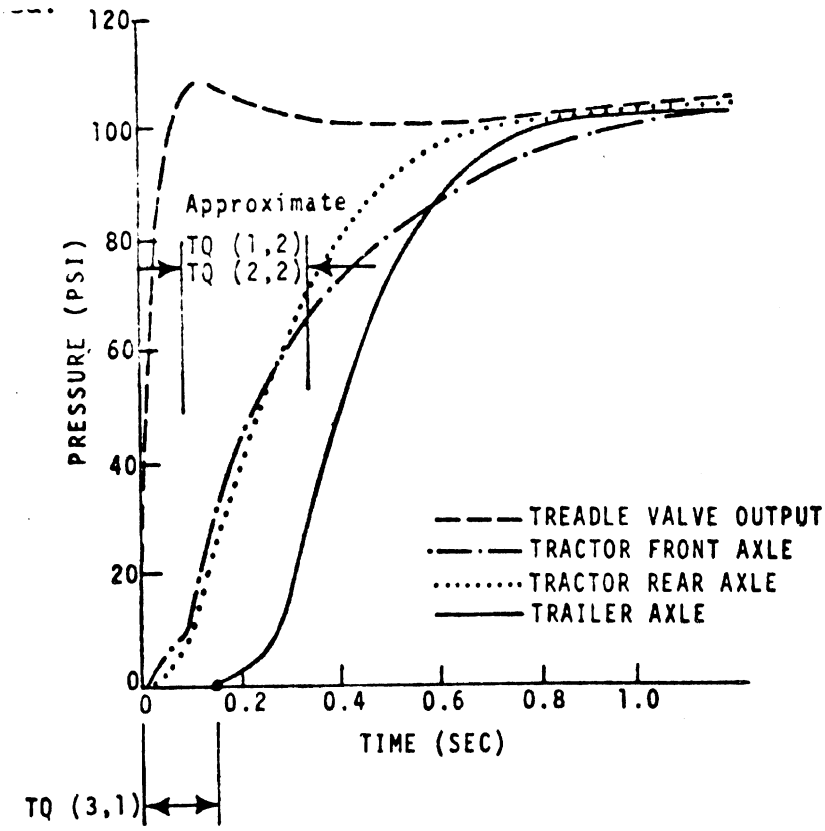

Figure 2.41. Typical empirical brake pressure application response curves.

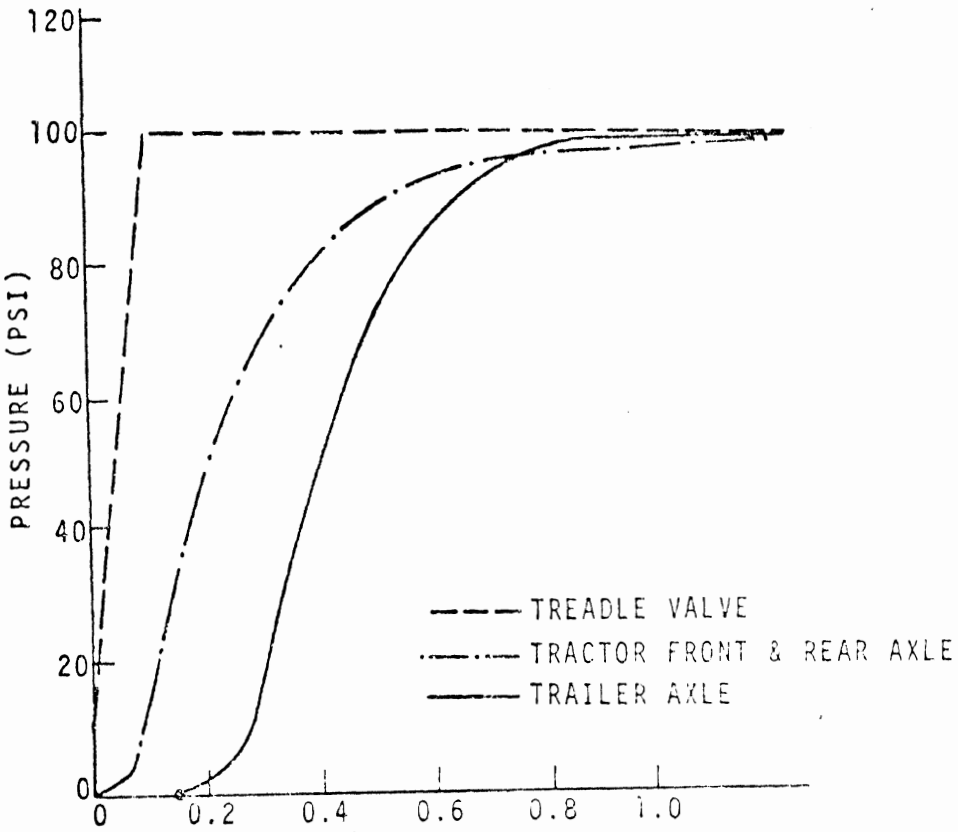

Figure 2.41. Typical empirical brake pressure application response curves.

The time-pressure points used to produce the treadle valve curve in Figure 2.42 were:

Time, sec	Pressure, psi
0.0	0
0.1	100

The brake time response parameters used were:

TQ(1,1) = TQ(2,1) = 0

TQ(3,1) = 0.15

TQ(1,2) = TQ(2,2) = TQ(3,2) = 0.23

The TQ's are entered following the sprung mass data group. The entries are two per record in 2F10.4 format. One set of TQ must be entered for each axle. For example, for a three-axle vehicle:

TQ(1,1)	TQ(1,2)
TQ(2,1)	TQ(2,2)
TQ(3,1)	TQ(3,2)

Note that the number of TQ data pairs <u>must</u> equal the number of axles on the vehicle.

The last TQ entry is followed by tabular entries of time versus treadle valve pressure. The initial entry for the table is the number of points in the table in I2 format. This should be followed by paired (pressure, torque) values, two per record. in 2F10.4 format. The line pressure histories shown in Figure 2.42 were generated using the input data presented in Table 2.6.

Table 2.6. Input Data Used to Generate Figure 2.42.

Data	Explanation
0., .23	
0., .23	TQ values
.15, .23	
03	Number of pairs in table
0., 0.	
.1, 100.	Table of treadle valve pressure vs. time in the format time, pressure
1., 100.	

Calculation of Brake Torque

Brake torque may be generated by means of torque-line pressure curves, such as would be obtained from a brake dynamometer, or by means of brake modules in which detailed design parameters for the brakes on each axle must be specified. In either case, the input data follows the treadle valve pressure versus time table.

If dynamometer curves are used, one table of values of line pressure versus torque must be supplied for each axle. Then, in the course of the integration process during the simulation, a linear interpolation is made to produce the value of brake torque for the given instantaneous value of brake line pressure at each axle.

If, on the other hand, brake modules are specified, the brake torque is calculated using the brake system parameters specified by the user. Brakes must be specified on an axle-by-axle basis. Options include: no brakes, S-cam, dual or single wedge, duo-servo self-actuating, duplex, and disc.

The data should be input as follows:

If tables are to be used, the data for each brake should be entered starting with the front brakes. This data should immediately follow the time versus treadle valve pressure table. Each table should be headed by an integer in I2 format indicating the number of tabular entries for that axle in 2F10.4 format. Up to 25 pairs per axle may be input. The data listed in Table 2.7 indicate dynamometer curves for a three-axle straight truck.

Table 2.7. Line Pressure Versus Brake Torque for a Three-Axle Truck

Data	Explanation
03	Follows the last treadle valve vs. time entry
0., 0.	
15., 0.	
100., 150000.	
03	Start of data for axle 2
0., 0.	
15., 0.	
100., 250000	
03	Start of data for axle 3
15., 0.	
100., 25000	

Note that the torque values are the total for one side of the vehicle in in-lbs. The above table indicates a pushout pressure of 15 psi at each axle, with a maximum of 150,000 in-lbs front and 250,000 in-lbs on each rear axle.

If modules are to be used, the integer -1 should be entered immediately following the treadle valve pressure versus time table.

Then the parameters describing the brake are entered. A list of the brake options and the input variables for each option are presented in Appendix C. (These modules are the same as those presented in the Phase I report [1].)

2.3.2 Brake Imbalance. Brake imbalance is not usually considered in straight-line braking simulations, since the model is a "bicycle," and yaw moments are not calculated. The normal course of action is to calculate the brake forces and normal forces for only one wheel per axle, and then multiply by two to find the forces to use in the differential equations describing the vehicle motion. There are cases, however, when it is useful to perform calculations separately for each side, as will be shown below.

The present simulation is intended to be useful both for the study of brake fade and the study of antilock systems. Brake imbalance interacts with brake fade by causing a different heat flux to be applied to the brakes on the left and right side. More important, brake imbalance directly affects antilock operation since the input signal to the antilock logic is dependent on the spin rate of each wheel on the axle.

Side-to-side imbalance may be simulated in the following way. The user should enter, immediately following the last entry of the dynamometer tables or brake modules, the parameters XMAC(I), one for each axle.

The brake torque, T, which has been calculated from the dynamometer tables or modules, will then be entered in the following way:

$$TL = T(1 + \frac{XMAC}{100})$$

$$TR = T(1 - \frac{XMAC}{100})$$

where TL and TR will be assumed to be left and right side values, respectively. Note that XMAC = 10 will result in a left side torque about twenty percent higher than the right side torque.

Since the brake torque is different from side to side, separate wheel spin calculations and brake force calculations must be performed. This will be reflected in the output by an additional page of information for each axle. In this case, one page for each axle will be labeled right side and one page will be labeled left side, and the normal loads and brake forces printed on those pages will be one side values rather than the sum of the left side and right side values normally printed.

The XMAC parameters are entered one to a record in F10.4 format. Note if XMAC(1) is entered as a negative number, XMAC(2) through XMAC(N), where N is the number of axles on the vehicle, are not to be entered, and imbalance will be ignored.

2.3.3 Hysteresis. Although hysteretic effects are found in many mechanical systems, it is only recently that hysteresis of commercial vehicle brakes has been a subject of considerable interest. This interest is a by-product of the intense study now being applied to antilock braking systems.

Some data illustrating hysteresis in commercial vehicle brakes has been presented in Reference 10. It is shown that hysteresis may be more pronounced if the wheel spins down to a locked condition and back up again, rather than cycling from low to high slip values without wheel lockup. This is illustrated in Figures 2.43 and 2.44 which are reproduced from Reference 10.

In Figure 2.43, measured brake torque versus line pressure data are shown for an S-cam brake subject to slowly varying brake line pressure. These data were measured at constant spin rate on the HSRI mobile brake dynamometer. In Figure 2.44, further measured data are given for the same brake. In this case, however,

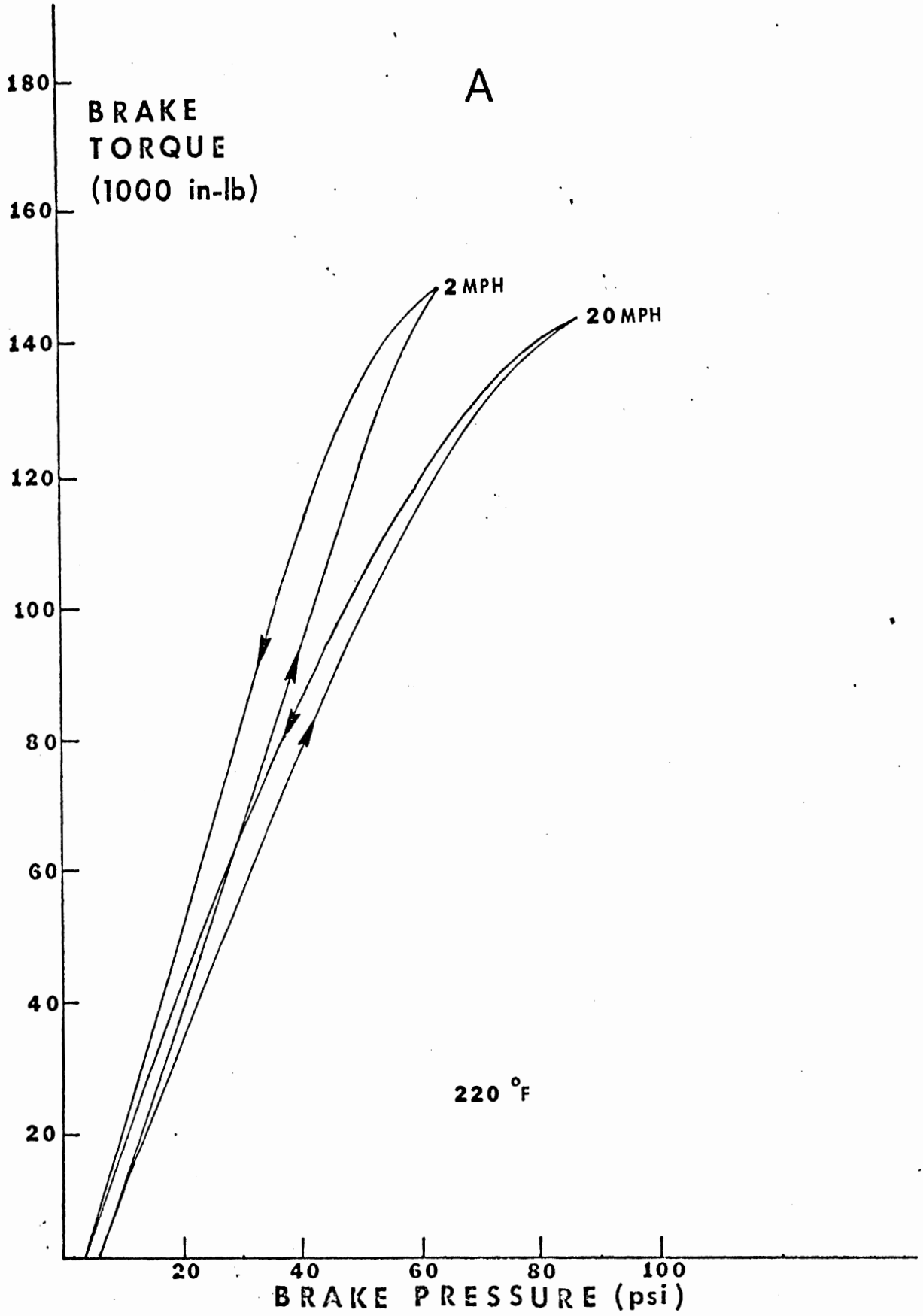

Figure 2.43. Measured brake torque vs. line pressure for an S-cam brake. No wheel lockup.

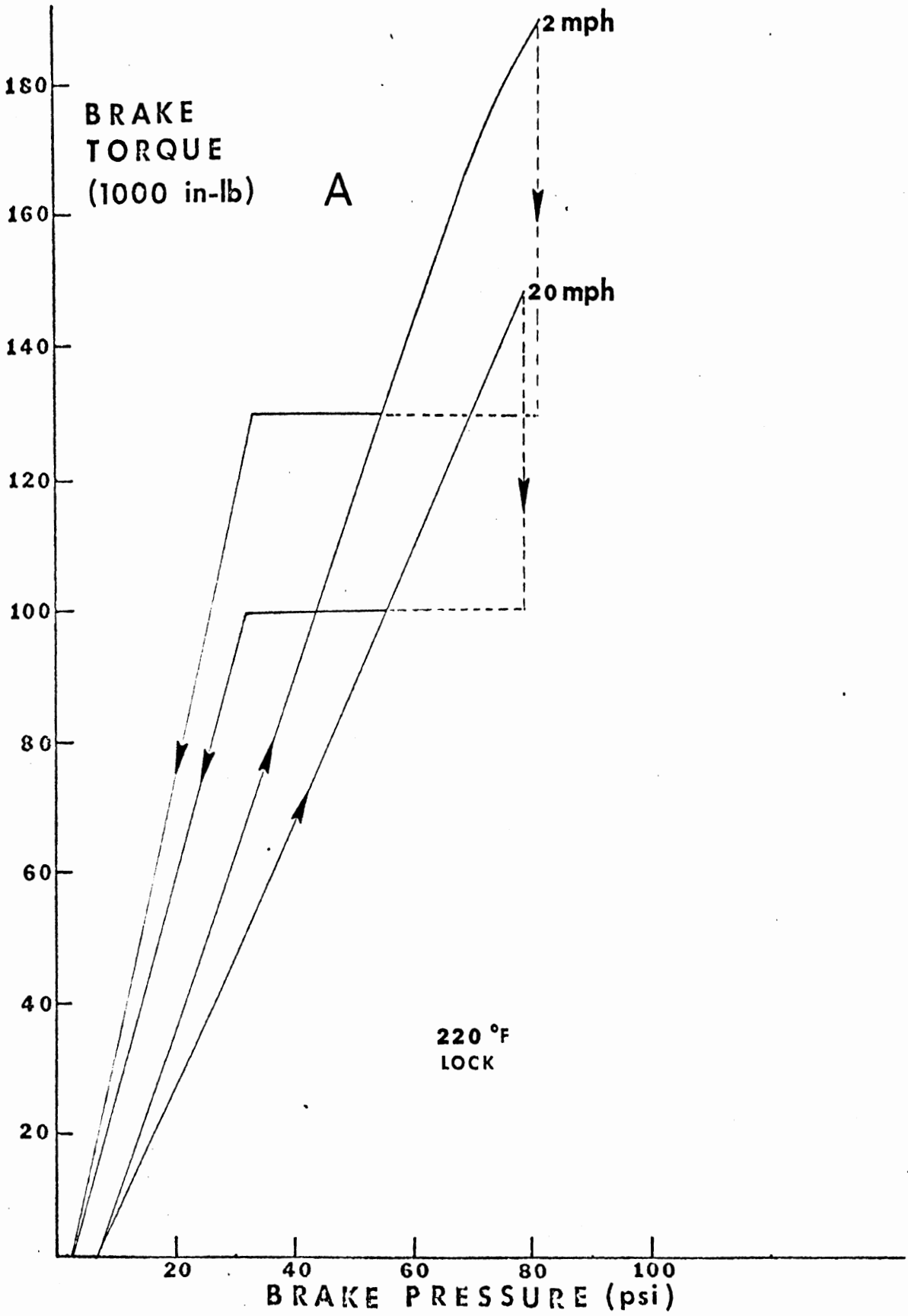

Figure 2.44. Measured brake torque vs. line pressure for an S-cam brake, with wheel lockup.

sufficient line pressure was supplied to lock the wheel, resulting in the increased hysteresis indicated by the horizontal solid lines in the figure.

Provision has been made to simulate hysteresis in the brake torque/line pressure relationship. For each brake the user may enter the parameters HY and HYL. The brake torque will then cycle over the loop shown in Figure 2.45a if wheel lock does not occur and over the loop shown in Figure 2.45b is wheel lock does occur. Note that the lower torque values in these figures derive from user input data, either in tabular form or from the brake modules, and the upper torque values in the figures are linearly related to the lower values by a factor of HY and HYL, respectively.

A flow chart for the hysteresis algorithm, which is in subroutine OUTPUT, is presented in Figure 2.46. The HY and HYL values are entered on separate records in F15.5 format as shown in Table 2.8. Note that the HY and HYL entries follow the XMAC imbalance input. Further, note that if HY(1) is set to zero, the remaining HY and HYL will not be read, and hysteresis will be neglected.

Table 2.8. Entry of the Hysteresis Data.

Data	Explanation
XMAC	Torque imbalance coefficient
HY(1)...	If (HY(1).EQ.0) don't enter any more HY or HYL
HYL(1) HY(2) HYL(2)	Additional entries for up to nine axles (doubles). Enter only sufficient data for number of axles on simulated vehicle.
Input data to the brake fade algorithm	
ILOCK	

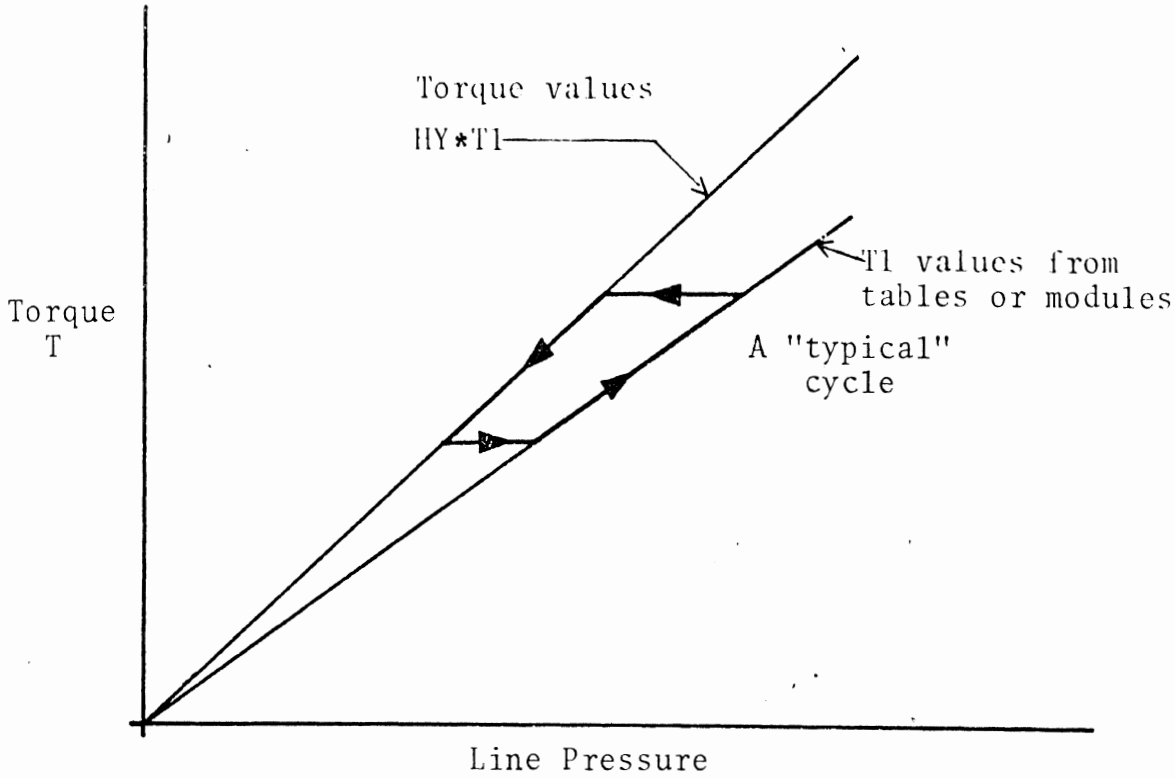

Figure 2.45a. Brake torque cycle, no lockup.

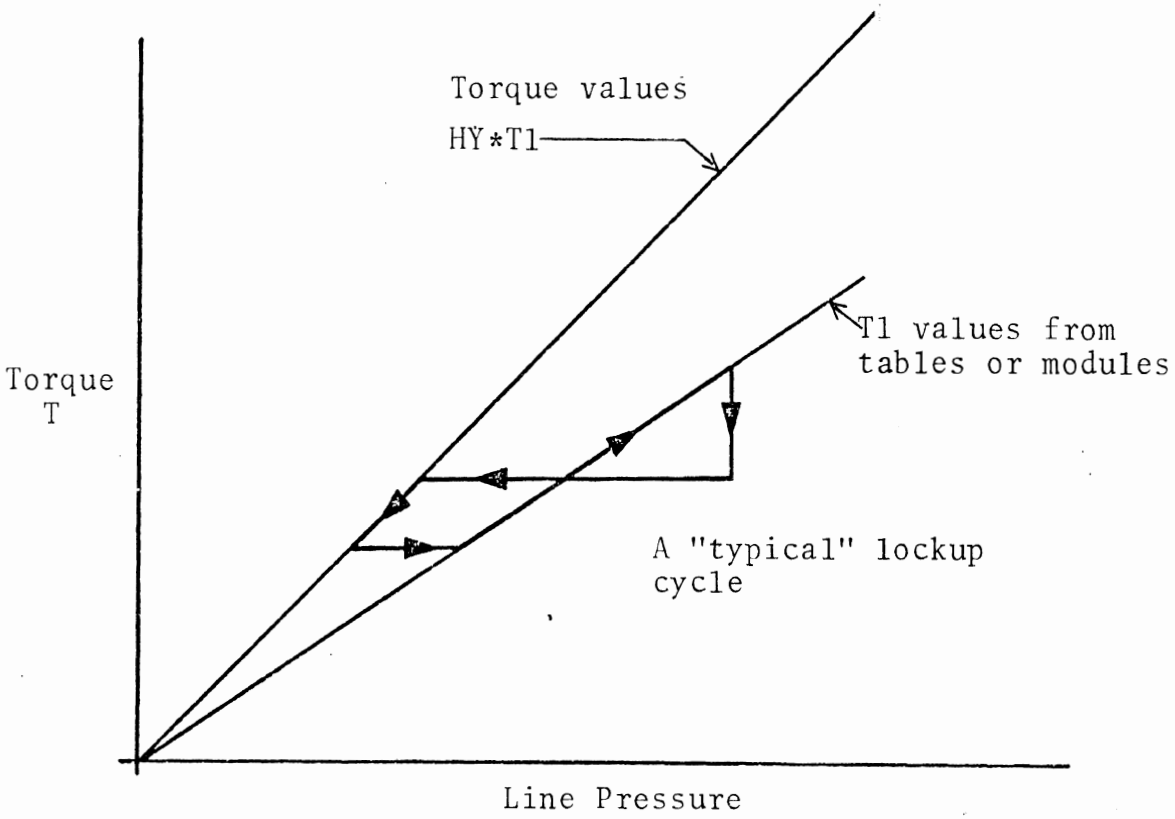

Figure 2.45b. Brake torque cycle with lockup.

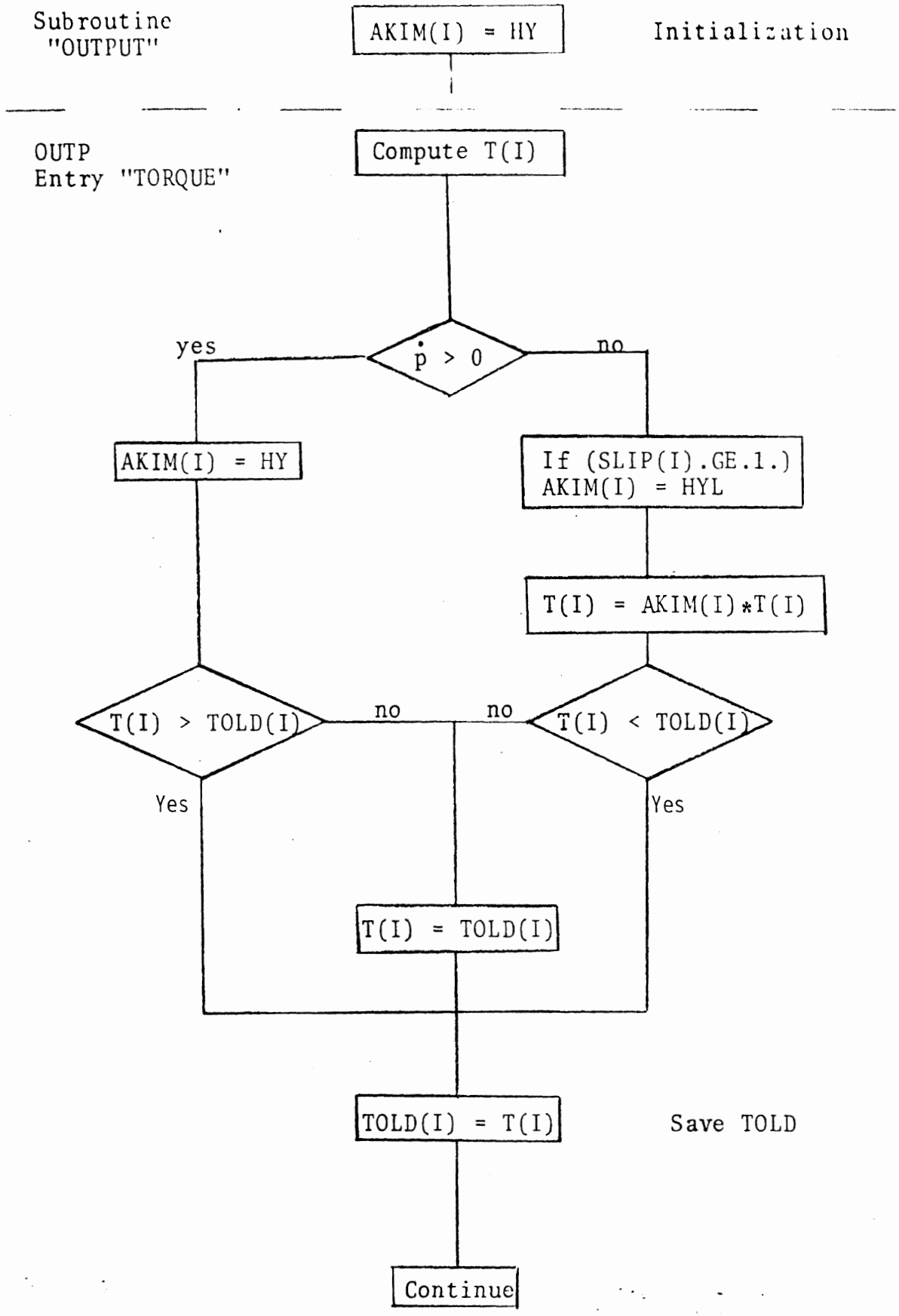

Figure 2.46. A flow chart of the hysteresis algorithm.

2.3.4 Brake Fade. A survey of the literature or a cursory examination of germane empirical data will indicate that the frictional forces generated at the lining-drum interface should be expected to be a function of brake geometry. The choice of leading and/or trailing shoes, for example, affects the pressure distribution between lining and drum, and results in various levels of so-called "self-actuation" [1]. This information is input to the simulation through the modules or tables of dynamometer data, as discussed in Section 2.3.1.

Other, more subtle, interactions between the geometry and the friction forces, such as changes in linings and drums due to temperature, are also important [20]. These latter interactions give rise to time-dependent torque changes at a constant line pressure which have come to be called "brake fade."

To date, it is not within the state of the art to accurately predict brake fade under all conditions. Nevertheless, useful estimations of brake fade are feasible using the existing technology. These estimations will be based on computed temperatures of the lining-drum interface coupled with routinely available "average" torque-line pressure information.

Accordingly, in the following subsection, the method of temperature calculation as a function of an arbitrarily varying wheel spin rate and brake torque will be explained. It will then be shown how a reasonable estimation of brake torque and brake fade may be modeled on the basis of calculated temperature and conventional dynamometer data.

Brake Temperature Calculations

This subsection contains a detailed analysis including the physical assumptions and the mathematical considerations leading to a means of calculating drum surface temperature. The resulting computational scheme can be programmed concisely for incorporation in simulations of vehicle braking performance.

The description of temperature within a body with no heat source is given by the heat flow or diffusion equation

$$k \nabla^2 u = \frac{\partial u}{\partial t} \tag{2.20}$$

subject to the boundary condition

$$- \alpha \nabla u = \bar{q}$$

where

u = temperature within the body

k = diffusivity of the body

α = conductivity of the body

$\bar{q}$ = heat flux at the body surface.

To facilitate the calculations of the temperature at the lining-drum interface, Equation (2.20) may be simplified according to the following assumptions (see Figure 2.47):

(1) Since brake drums have radii which are large compared with the drum thickness, the drum may be modeled as a flat strip.

(2) Since, in the course of one braking maneuver, we expect no appreciable heat loss through the drum during the braking application, the outer drum surface is assumed to be insulated.

(3) The rate of energy input per unit area at the drum-lining interface is constant over the rubbing area of the drum.

(4) A constant proportion of the heat generated at the drum lining interface is assumed to flow into the drum.

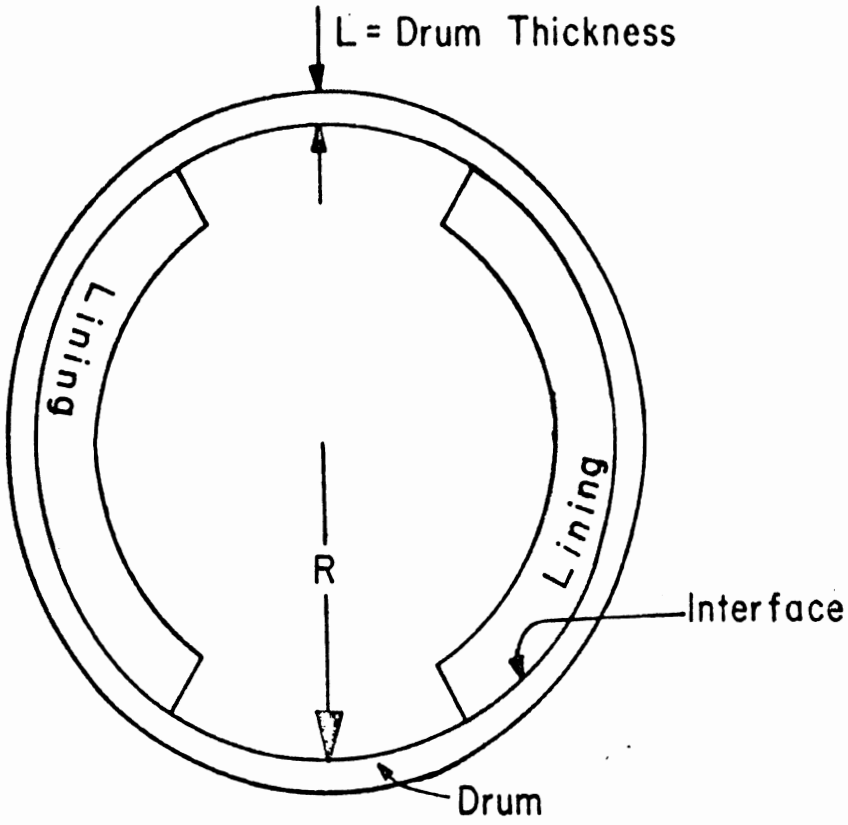

$R \gg L$

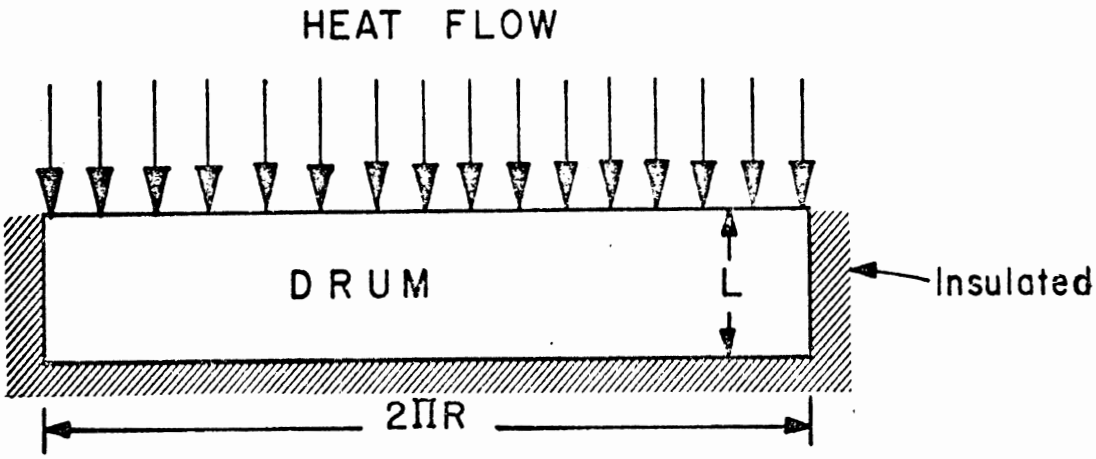

Figure 2.47. Schematic diagram, brake drum and lining.

Under these four assumptions, which have been previously used in the analysis of the temperature in brake drums [21], Equation (2.20) may be significantly simplified, viz:

$$\frac{\partial u}{\partial t}(x, t) = k \frac{\partial^2 u}{\partial x^2}(x, t) \qquad 0 \leq x \leq L \qquad t > 0 \tag{2.21}$$

under the boundary conditions

$$\frac{\partial u}{\partial x}(0, t) = -\frac{\beta T \Omega}{\alpha \Lambda} \tag{2.22a}$$

$$\frac{\partial u}{\partial x}(L, t) = 0 \tag{2.22b}$$

and with the initial temperature profile

$$u(x, 0) = u_0(x) \tag{2.22c}$$

where

u = drum temperature

t = time

x = spacial coordinate, x=0 at the drum-lining interface, x=L at the outside of the drum

α = drum material conductivity

k = diffusivity of drum material

Λ = total drum area which contacts the lining during a wheel rotation

L = drum thickness

β = proportion of the heat generated which enters the drum

T = brake torque

Ω = wheel spin rate

A good approximation for β (see [21]) is given by

$$\beta = \frac{1}{1 + \frac{A_L \alpha_L \rho_L \; C_{\rho L}}{A \; \alpha\rho \; C_\rho}}$$

where

C_ρ = specific heat of the drum

ρ = conductivity of the drum

and the quantities subscripted with L are the corresponding properties for the lining. For most drum-shoe combinations, the value of β is about .95.

A solution to Equation (2.21) may be found in the form

$$u(x, t) = X(x) \; A(t) \tag{2.23}$$

where X satisfies the homogenous boundary conditions

$$X'(0) = X'(L) = 0 \tag{2.24}$$

where the prime indicates differentiation with respect to x. Substitution into Equation (2.21) yields

$$\frac{1}{k} \frac{\dot{A}}{A} = \frac{X''}{X} = -\lambda^2 \tag{2.25}$$

where the dot indicates differentiation with respect to time. Thus

$$X'' + \lambda^2 X = 0 \tag{2.26}$$

The solution to (2.26) is

$$X = C \cos \lambda x + D \sin \lambda x, \quad \lambda \neq 0 \tag{2.27a}$$

$$X = \overline{C} + \overline{D}x \qquad \lambda = 0 \tag{2.27b}$$

Application of boundary conditions (2.24) to Equations (2.27) yields

$$D = \overline{D} = 0 \tag{2.28a}$$

and $$\lambda_n = \frac{n\pi}{L} \quad n = 0,1,2,\ldots \tag{2.28b}$$

Thus

$$u(x, t) = \sum_{n=0}^{\infty} A_n(t) \cos \lambda_n x \tag{2.29}$$

where the summation is a Fourier series solution for u valid over the interval [0, L]. The Fourier coefficients $A_n(t)$ are given by

$$A_n(t) = \frac{2}{L} \int_0^L u(x, t) \cos \lambda_n x \, dx \tag{2.30a}$$

$$A_0(t) = \frac{1}{L} \int_0^L u(x, t) dx \tag{2.30b}$$

Differentiating A_n with respect to time yields

$$\dot{A}_n(t) = \frac{2}{L} \int_0^L \frac{\partial u}{\partial t}(x, t) \cos \lambda_n x \, dx \tag{2.31a}$$

$$\dot{A}_0(t) = \frac{1}{L} \int_0^L \frac{\partial u}{\partial t}(x, t) dx \tag{2.31b}$$

But

$$\frac{\partial u}{\partial t}(x, t) = k \frac{\partial^2 u}{\partial x^2}(x, t) \tag{2.32}$$

thus

$$\dot{A}_n(t) = \frac{2k}{L} \int_0^L \frac{\partial^2 u}{\partial x^2}(x, t) \cos \lambda_n x \, dx \tag{2.33a}$$

$$\dot{A}_0(t) = \frac{k}{L} \int_0^L \frac{\partial^2 u}{\partial x^2} dx \tag{2.33b}$$

Integrating by parts twice gives

$$A_n(t) = \frac{2k}{L} \left[\frac{\partial u}{\partial x} \cos \lambda_n x + \lambda_n u \sin \lambda_n x \right]_0^L - \frac{2k\lambda_n^2}{L} \int_0^L u(x, t) \cos \lambda_n x \, dx \tag{2.34a}$$

$$\dot{A}_0(t) = \frac{k}{L} \left[\frac{\partial u}{\partial x}(x, t) \right]_0^L \tag{2.34b}$$

Noting that

$$\alpha \frac{\partial u}{\partial x}(0, t) = - f(t) = - \frac{\beta T \omega}{A} \tag{2.35a}$$

$$\frac{\partial u}{\partial x}(L, t) = - \tag{2.35b}$$

and

$$\frac{2}{L} \int_0^L u(x, t) \cos \lambda_n x \, dx = A_n(t) \tag{2.36}$$

the following ordinary differential equations are generated:

$$\dot{A}_n(t) + k\lambda_n^2 A_n(t) = \frac{2k}{\alpha L} f(t) \tag{2.37a}$$

$$\dot{A}_o(t) = \frac{k}{\alpha L} f(t) \tag{2.37b}$$

with initial conditions from Equation (2.30)

$$A_n(0) = \frac{2}{L}\int_0^L u(x, 0) \cos \lambda_n x \, dx \tag{2.38a}$$

$$A_o(0) = \frac{1}{L}\int_0^L u(x, 0)dx \tag{2.38b}$$

The solution of Equations (2.37) for the A_n may be handled numerically for arbitrary f(t). Further, it should be noted that the coefficient of the A_n term increases with n^2, an indication that the A_n will rapidly approach zero with increasing n.

The numerical solution of Equation (2.37a) may be facilitated by consideration of a constant forcing function $f(t_o)$ for $t \geq t_o$. In that case

$$A_n(t) = \frac{2f(t_o)L}{\alpha\pi^2 n^2} + \left(A_n(t_o) - \frac{2f(t_o)L}{\alpha\pi^2 n^2}\right) e^{-k\lambda_n^2(t-t_o)} \tag{2.39}$$

Substituting into Equation (2.29) and noting that

$$\sum_1^\infty \frac{1}{n^2} \cos \frac{n \pi x}{L} = \frac{\pi^2}{12} \left(2 - \frac{6x}{L} + \frac{3x^2}{L^2}\right) \tag{2.40}$$

yields

$$u(x, t) = A_0(t) + \frac{f(t_0)L}{6\alpha}\left(2 - \frac{6x}{L} + \frac{3x^2}{L^2}\right)$$

$$+ \sum_{1}^{\infty} \left(A_n(t_0) - \frac{2f(t_0)L}{\alpha\pi^2 n^2}\right) e^{-k\lambda_n^2(\Delta t)} \cos \frac{n\pi x}{L} \qquad (2.41a)$$

where $\Delta t = t - t_0$ (2.41b)

and the temperature at the interface is then

$$u(0, t) = A_0(t) + \frac{f(t_0)L}{3\alpha} + \sum_{1}^{\infty} \left(A_n(t_0) - \frac{2f(t_0)L}{\alpha\pi^2 \ ^2}\right) e^{-k\lambda_n^2 \Delta t} \qquad (2.42)$$

Equation (2.41) is also useful for the numerical calculation of u as a function of time-varying forcing functions f(t). Consider Figure 2.48 in which f(t) is approximated by a series of steps Δt wide. The temperature u(x, t) may be found by updating t_0, $f(t_0)$, and $A_n(t_0)$ at the beginning of each new time step, and reapplying Equation (2.41).

Of course, it is possible to find u by solving Equation (2.37a) numerically for the first few coefficients A_n and neglecting the higher order terms. (This solution could be mechanized either be repetitive solution of Equation (2.39) across intervals Δt wide, or through the use of some more traditional integration techniques such as the HPCG package [22].) Thus we would have

$$u(x, t) \cong \sum_{1}^{N} A_n(t) \cos \frac{n\pi x}{L} \qquad (2.43)$$

and the error, E, would be

$$E(x, t) = \sum_{N+1}^{\infty} A_n(t) \cos \frac{n\pi x}{L} \qquad (2.44)$$

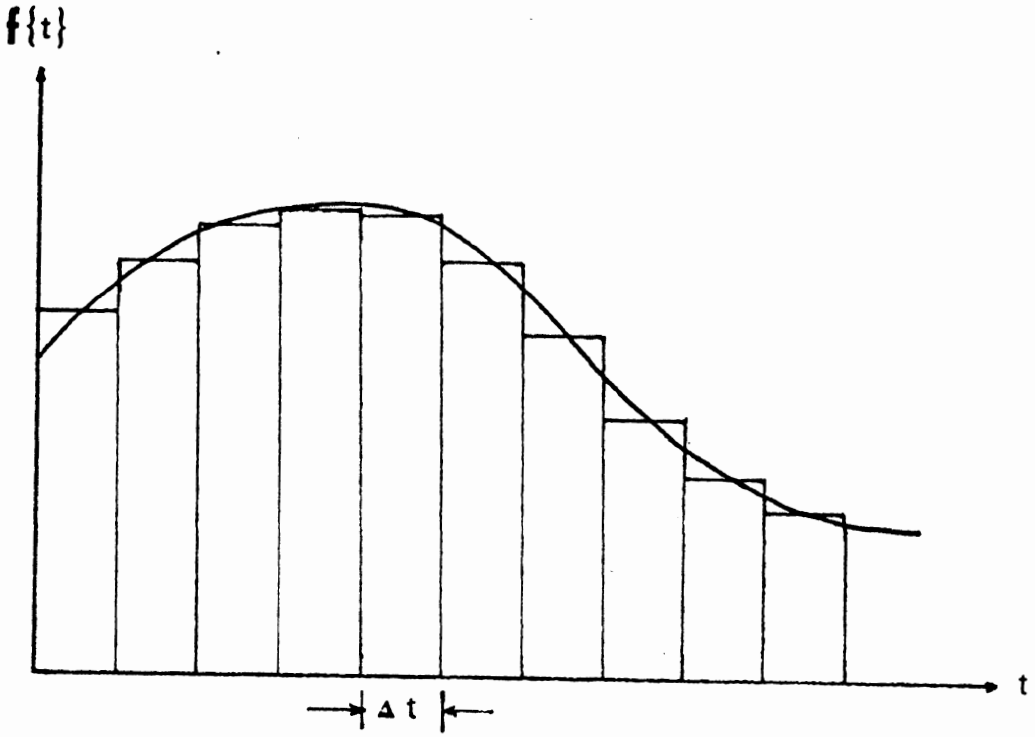

Figure 2.48. An approximation for f(t).

Use of the first N terms of Equation (2.41) rather than (2.43), however, is the far superior method, since the error is limited to the neglected exponentially decaying terms on the right-hand side of (2.43), rather than the entire sum listed in (2.44).

Confidence in this procedure has been gained by a comparison with the closed-form solutions given by Newcomb and Spurr in Reference 21, where the solution for the temperature rise at the lining-drum interface for a constant spin-down rate is presented. Computations employing only the first three terms in the sum in Equation (2.41) lead to numerical results virtually identical to those given in [21].

The Use of Brake Temperature to Predict Brake Torque

Equation (2.41) may be used to predict brake temperature as a function of arbitrarily varying brake torque and wheel spin, i.e., for any forcing function, f(t). Although f(t) may be known *a priori*, as when the torque and spin rate have been recorded as a function of time in a dynamometer test, and it is desired to compute the time-varying temperature, this is not a necessary condition. To calculate temperature, u, at the end of any Δt wide time interval, it is only necessary that f(t) be known at the beginning of the interval. Clearly, then, the solution presented in Equation (2.41) is ideal for use in the simulation where calculations take place at Δt = .0025 second intervals.

The complexity of this procedure is involved mainly in the temperature calculation—Equation (2.41) must be solved (dropping high order terms) for each brake. However, the success of the procedure also depends on the assumed relationship between the computed temperature and brake torque. Research at HSRI has led to the somewhat surprising finding that a linear relationship is extremely useful, i.e.,

$$T(t) = T_i \left[1 - \frac{u(t)}{\theta_f}\right] \tag{2.45}$$

where

t is time

T is the brake torque

T_i is called the "unfaded brake torque"

u is the computed temperature change, at the lining-drum interface, assuming a uniform initial temperature

θ_f is a user input constant called the "fade factor."

The values of T_i will be computed either from user input tables of T_i versus line pressure, or from the brake modules. This T_i value will then be modified downward to reflect the assumed linear effect of the increasing temperature at the lining-drum interface. The amount of this modification will depend on the user input "fade factor," θ_f.

As an example, consider a run in which a constant line pressure, P_i, of 60 psi is applied which results, through a table lookup calculation, in brake torque T_i = 100,000 in-lbs. In addition, assume the user has input a fade factor θ_f = 800°F. The brake torque, T(t), would then be computed using Equation (2.45), e.g., if $u_{(t)}$ reached 200°F, the brake torque would drop to 75,000 in-lbs.

Several spin-down dynamometer time traces have been examined to ascertain the range of validity of Equation (2.45). It has been found that for test data in the form given by the solid line in Figure 2.49, this model will work very well.* The constants

*Note that the torque time history shown in Figure 2.49 yields a single value of T_a at the applied pressure. Typically, dynamometer results are supplied as graphs of T_a versus pressure. The time-history data used to make these graphs are not generally available.

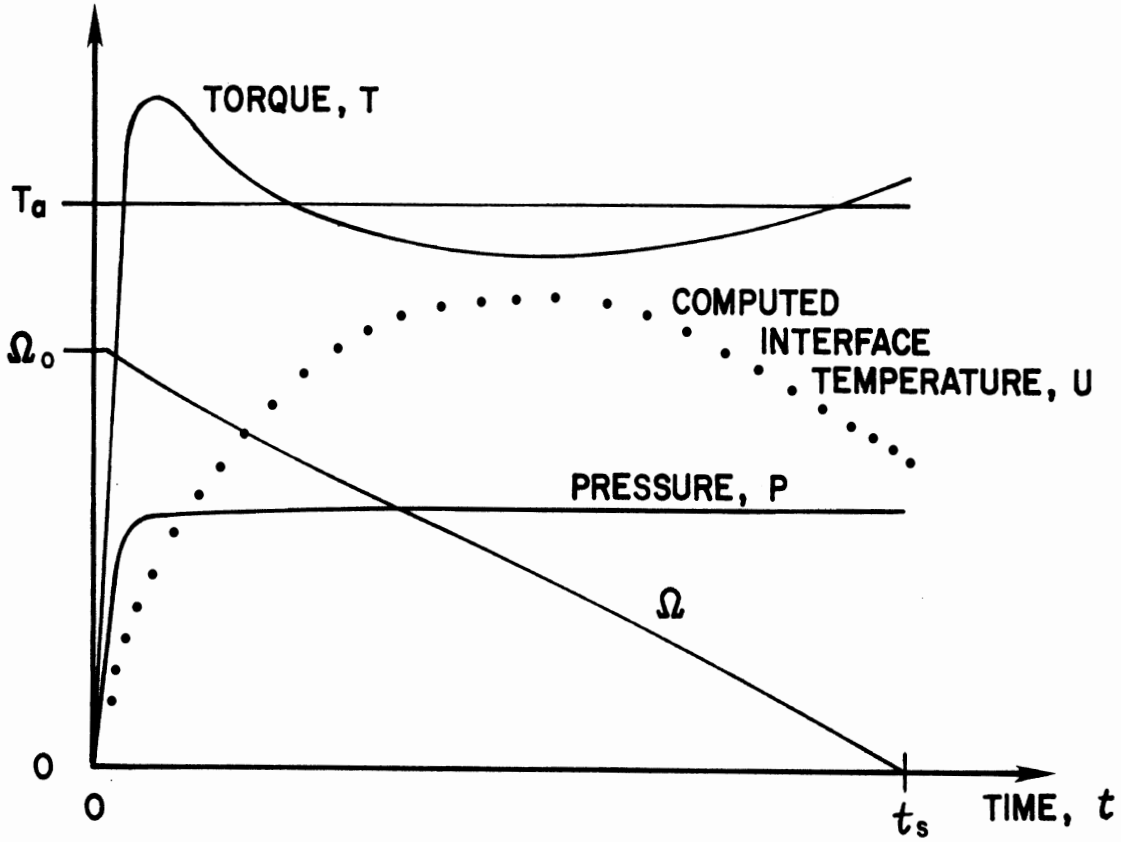

Figure 2.49. Data from a spin-down dynamometer test.

T_i and θ_f can be determined which will yield a torque-time relationship in close agreement to dynamometer results for a given initial velocity and inertial load. However, it should be noted that the value of T_i may vary with the initial speed of the spin-down test, with higher values of T_i corresponding to lower initial speeds.

Input Data for the Brake Fade Algorithm

The input data required for brake fade calculations immediately follows the last hysteresis parameter, XMAC. There are eight parameters per axle to be entered, first the initial temperature, F10.4, then seven more parameters on one record, 7F10.4. A sample data listing for a three-axle straight truck is presented in Table 2.9.

Note that if the first entry for the first axle is negative, no brake fade parameters should be entered, and temperature and brake fade calculations will not be performed. In addition, if the fade factor, θ_f, is set to zero, temperature will be calculated but fading will be neglected.

A Sample Run

The data presented in Table 2.9 were entered for use in the simulation of a 165-inch wheelbase, three-axle straight truck. The total weight of the vehicle was 45,825 lbs, with axle loads 11,936, 17,594, and 16,295, respectively. The timing parameters, TQ, were those presented in Table 2.6, and the line pressure/ brake torque relationship was taken from the tables presented in Table 2.7. The treadle valve pressure rose to 85 psi in .05 second, and the initial speed was 60 mph. The force levels generated at the tire-road interface were sufficient to prevent lockup of any wheels.

Table 2.9. Input Data to the Brake Fade Algorithm.

Data	Explanation
1.5	The last hysteresis entry
	Initial temperature, front brake, °F. (Note, if this is < 0, don't enter the rest of the data in this table.)
5.75, .95, .017, .5, 7., 7.5, 750	Front brake data, 7F10.4, in the following order:
	Drum conductivity, lb/°F sec Beta (portion of heat flux into drum) Drum diffusivity, in^2/sec Drum thickness, in. Width of rubbing area, in. Drum radius, in. Fade factor, θ_f, °F
0.	Initial temperature, leading tandem
5.75, .95, .017, .5, 7., 7.5, 750	Leading tandem brake data
0.	Initial temperature, trailing tandem
5.75, .95, .017, .5, 7., 7.5, 750	Trailing tandem brake data

Some results from this run are presented in Figure 2.50. Several comments on the figure are in order.

1) The "non-faded" brake torque is indicated by the dashed lines. Note that the front axle torque was much lower than the leading tandem axle brake torque, as would be expected from an inspection of Table 2.7. The trailing tandem axle time history, which is virtually identical to the leading tandem axle time history, is not shown in the figure.

2) Note that the calculated temperature at the lining-drum interface reached about 230°F for the front axle, and about 300°F for the leading tandem axle. (The trailing tandem also reached about 300°F.) This reflects the lower brake torque applied at the front axle.

3) The temperature at both the front axle brakes and the leading tandem axle brakes reaches a maximum about mid-way through the run. Thus brake fade, as indicated by the difference between the unfaded torque, T_i, and the brake torque, T, is a maximum at this point.

4) The shape of the deceleration trace is typical of vehicle test data. In this case, the resulting stopping distance was 290 feet.

2.4 The Tire Models

The relationship between the longitudinal forces at the tire-road interface and longitudinal slip is normally thought of as characterized by so-called "μ-slip" curves which may be expected to vary with load and speed. This may be done in either of two ways: (1) a closed-form solution based on the mechanics of the shear force generation at the tire-road interface, or (2) tabular input of μ-slip data. The closed-form solution,

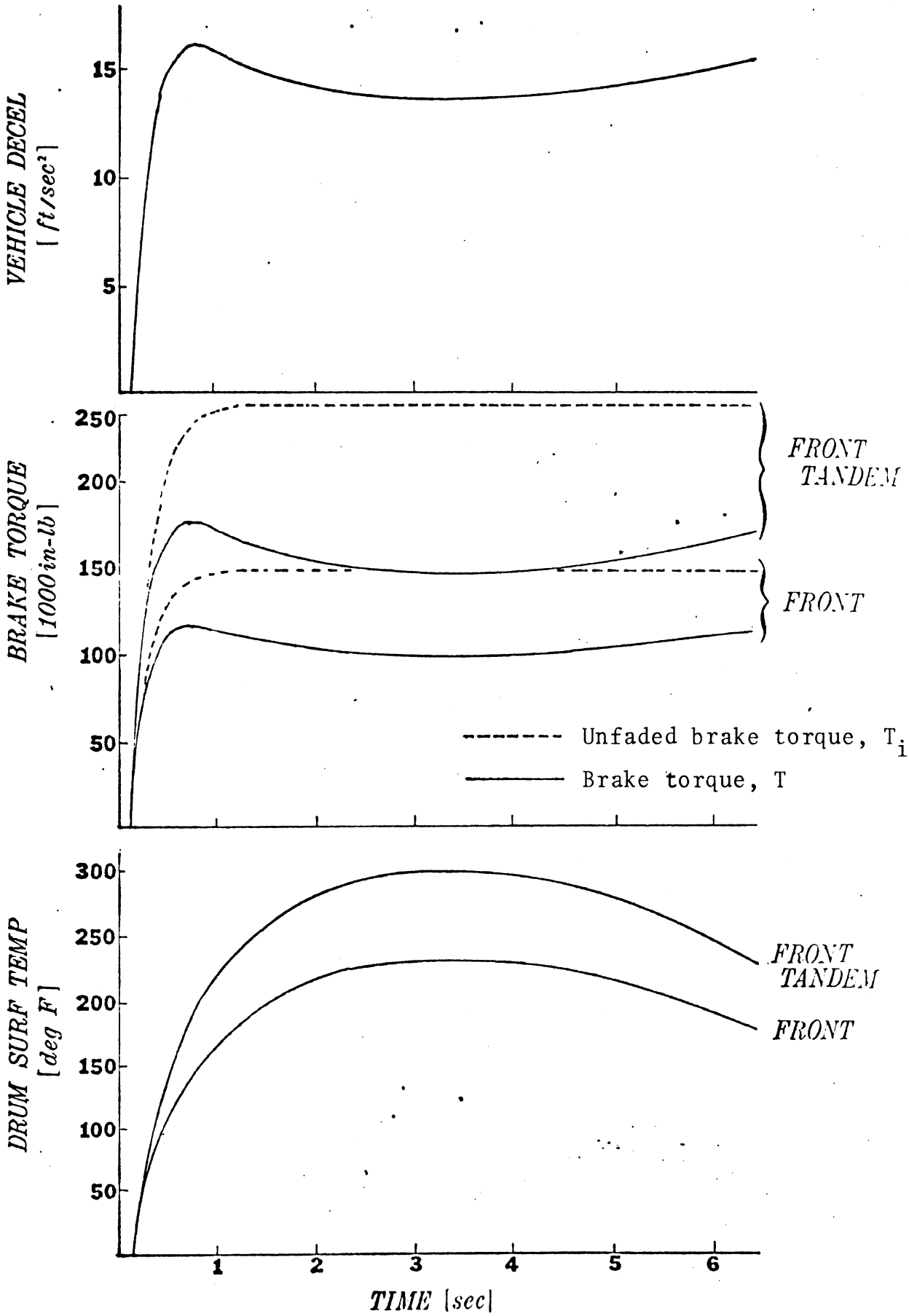

Figure 2.50. Simulated stop of a three-axle straight truck.

which was based on a well-known tire model [23], has been used with some success since the inception of the MVMA truck braking analysis. (See, for example, [1].) However, recently procured tire data [11] has indicated that the model is of limited accuracy in some cases. Thus provision has been made for direct entry of μ-slip data to the program.

In the following two subsections the use of the closed-form solution and the tabular input options are discussed.

2.4.1 The Analytical Tire Model. The analytical tire model used in this program is adapted from a more general model developed for use in a previous study. In this model, the tire-road shear force is generated on the basis of equations which approximately describe the deformation field over the tire-road contact patch. The location of the point on the tire carcass associated with the point in the contact patch where sliding starts in a braking maneuver is evaluated as a function of longitudinal slip between the tire and the road, vertical load, and sliding velocity. A thorough discussion of these equations, including comparisons of predicted tire force data to experimental data, have been reported in Reference 23. The tire parameters needed for the model (which in this program considers longitudinal and rotational motion of the tire only) are CS, the rate of change of brake force with slip at zero slip, MUZERO, the low-speed locked-wheel friction coefficient, and FA, the friction reduction parameter.

The brake force versus slip equations are summarized as follows:

$$\text{SLIP} = \frac{1 - \text{RR}(\Omega)}{\text{XDOT}} \tag{2.46}$$

$$\text{FX} = \frac{-\text{CS}(\text{SLIP})}{1 - \text{SLIP}} f(\lambda) \tag{2.47}$$

$$\begin{aligned} f(\lambda) &= (2-\lambda)\lambda \qquad \lambda < 1 \text{ (high SLIP)} \\ &= 1 \qquad\qquad \lambda > 1 \text{ (low SLIP)} \end{aligned} \tag{3.48a}$$

$$\lambda = \frac{-\text{MUZERO}\ (N)(1-\text{FA}\cdot\text{XDOT}\cdot\text{SLIP})(1-\text{SLIP})}{2\text{CS}(\text{SLIP})} \tag{2.48b}$$

where

CS is longitudinal stiffness, in pounds

FA is the friction reduction parameter, in sec/ft

MUZERO is the low-speed friction coefficient

RR is the rolling radius

N is the normal force at the tire-road interface

The normal force, N, on the tire from the road through the contact patch is a function of the static load, the tire spring rate, and viscous damping in the tire. Values for the rolling spring rates of various truck tires, as determined from experiment, have been presented in [1]. Although no similar data is available on values for truck tire viscous damping coefficients, it is reasonable to assume (for example, see References 8 and 10) that the tire damping coefficient is of the order of 2% critical. Thus the user must input only the rolling spring rate, KT; the damping at the tire-road interface is calculated based on the unsprung mass and the tire spring rate.

The normal force on the rolling tire is

$$N = NS + KT \cdot \Delta + CF \cdot \dot{\Delta} \tag{2.49}$$

where Δ is the change from the static distance between the tire and the road.

The input data related to the tires follows the last braking data. When the analytical tire model is used, the data must be input in the form shown in Table 2.10.

Table 2.10. Input Data Relating to Tires.

Parameter	Comments
ALPHA(1)	Static rolling radius, front tires (inches)
ALPHA(2)	Static rolling radius, axle 2
.	Notes: 1) enter only the radius of the tires on the lead tandem for tandem axles
.	2) enter a minus sign before the radius if dual tires are to be simulated on an axle
.	
ALPHA(N)	
CS(1)	
.	$\left.\frac{-\partial FX}{\partial S}\right\|_{S=0}$ (lbs/slip)
.	
.	
CS(N)	Note: This is a "one tire value"
FA(1)	
.	
.	Function reduction parameter
.	
FA(N)	
JS(1)	
.	Spin moment of inertia, <u>includes</u>
.	<u>both sides</u>, in lb. sec^2
.	
JS(N)	
KT(1)	
.	Tire spring rate (lbs/in)
.	Note this is a one tire value
.	
KT(N)	
$\mu_o(1)$	
.	
.	Low speed friction coefficient
.	
$\mu_o(N)$	

Several notes, called out in Table 2.10, will be elaborated upon here.

1) Since the tire model is nonlinear, brake force calculations must be made for one tire, then multiplied by the number of tires on the axle. Thus it is necessary to call out dual tires wherever they occur. The callout mechanism is the sign of the ALPHA entry; the negative sign will call for dual tires.

2) As a convenience to the user, the radius of the tires on a trailing tandem axle is assumed equal to the radius on the leading tandem. Thus an ALPHA value for a trailing tandem must not be entered.

3) It is important to note that all of the tire data entered into the Phase III simulation is data for one tire. This includes the longitudinal stiffness, C_s, and the tire spring rate, KT.

4) JS is considered an inertial parameter rather than a tire parameter. It has been grouped with the tire parameters since it fits into the wheel spin equations with the tire parameters. Thus the JS value, like all inertial descriptors in the program, includes the entire spinning mass assembly, rather than only one side.

2.4.2 Tabular Input Data. Truck tire test data recently procured in a study at HSRI [11] has indicated that a substantial peak-to-slide brake force ratio may occur at low speeds as well as high speeds. Since the analytical model assumes the peak-to-slide ratio is a function of the product of the speed and the input "friction reduction parameter," FA, the model is inadequate

in some cases. Consider, for example, Figure 2.51 in which measured data is presented along with "best fit" curves generated using the tire model to match the data gathered at 40 mph.

Since the model is of limited utility in some cases, provision has been made for the direct entry of μ-slip tables. The tabular entries, which may be a function of both speed and load, should be input in the following way:

The first CS in Table 2.10 should be set to a negative number. The remainder of the parameters for the analytical model, including CS, FA, and μ_0, should not be entered.

After the last KT entry, the tables should be entered, first for the front axle, next for axle 2, etc. The first entry in the table is the number of speeds, in I2 format. The second entry is the first speed and the number of loads at that speed, F10.4, I2. The next entry is the first load and the number of μ-slip pairs at that load, F10.4, I2. The next entries are the μ-slip pairs at that speed and load, first slip then μ, 2F10.4.

Up to five speeds and five loads may be entered for each axle, and the appropriate μ value will be found by interpolations over both load and speed. If the speed or load is below the lowest entry in the table, the μ-slip pair corresponding to the lowest value will be used. If the speed or load is higher than the highest entry in the table, the μ-slip pair corresponding to the highest pair will be used.

An example is given in Table 2.11. Note that this table is for a two-axle vehicle. The front wheels have μ-slip tables at two loads, 5,000 and 10,000 lbs, and two speeds, 10 ft/sec and 50 ft/sec. The second axle has a μ-slip curve at one speed and one load, i.e., a constant μ-slip curve. Note that the lowest speeds must be entered first and the lowest loads must be entered first.

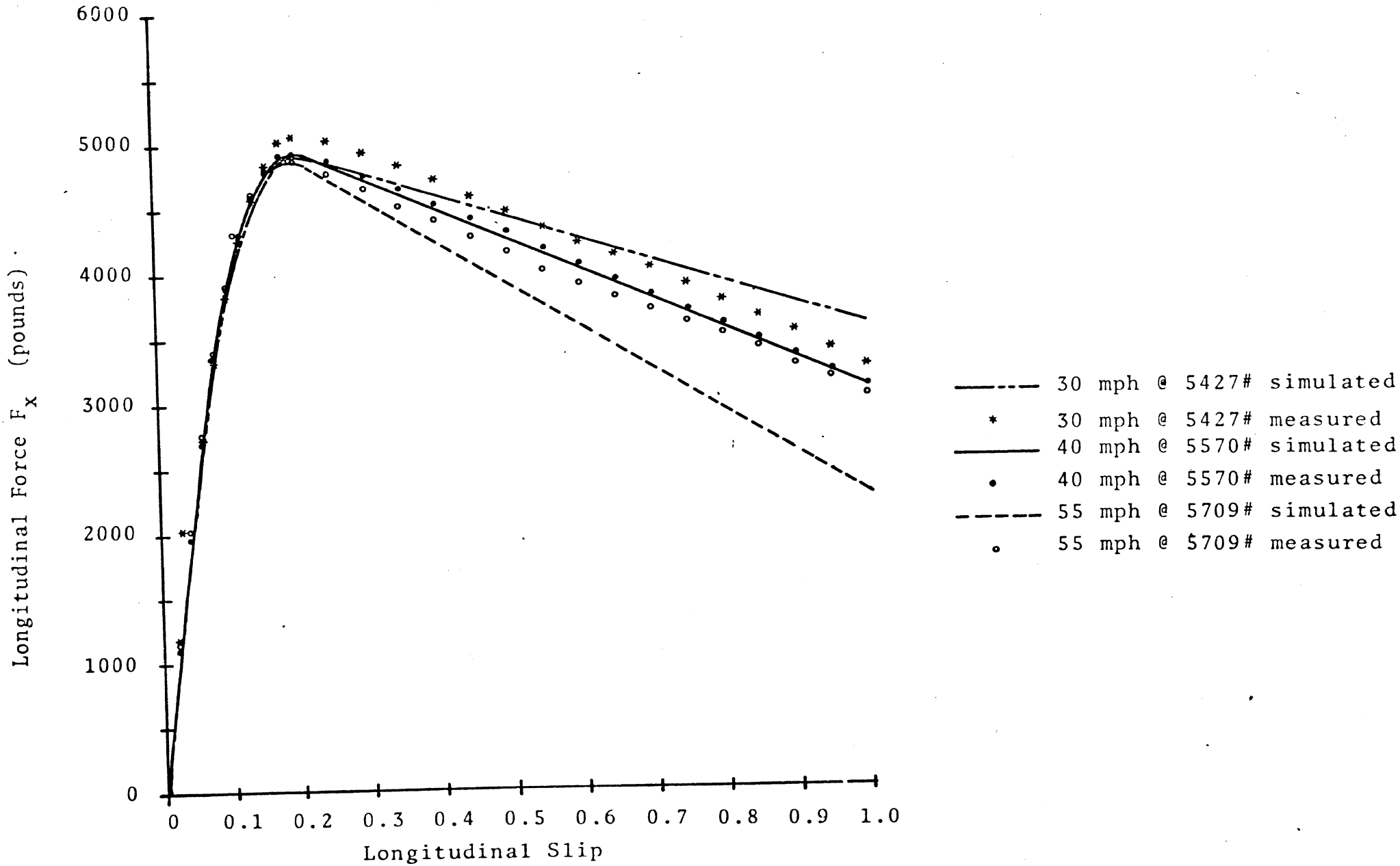

Figure 2.51. Effect of speed on force vs. slip curve for Firestone Transport 1 (10.00 x 20/F)

Table 2.11. Entry of μ-Slip Tables

Data	Comment
9500.	The last KT (see Table 2.10)
02	Two speeds in the front axle table
10. , 02	Ten ft/sec, two loads
5000. , 03	5000 lb, three pairs to come
0. , 0 .2 , .7 1. , .6	This is the μ-slip curve for 10 ft/sec, 5000 lbs.
10000. , 03	10000 lbs, three pairs to come
0. , 0. .2 , .8 1. , .7	This is the μ-slip curve for 10 ft/sec, 100000 lbs.
50. , 02	50 ft/sec, two loads
5000. , 03	5000 lbs., three pairs to come
0. , 0. .2 , .58 1. , .5	This is the μ-slip curve for 50 ft/sec, 5000 lbs.
10000. , 03	
0. , 0. .2 , .67 1. , .5	This is the μ-slip curve for 50 ft/sec, 10000 lbs.
01	One speed for axle 2
10. , 01	10 ft/sec, one load
5000. , 03	5000 lbs, three pairs to come
0. , 0. .2 , .9 1. , .6	This is the μ-slip curve for axle 2

It is apparent from Table 2.11 that the input data can become quite tedious. There is no respite from this problem if the tires on each axle require different μ-slip data. However, provision has been made to avoid unnecessary repetition of input data. If the "number of speeds entry" is set to a negative number, say -I, then the μ-slip data will be the same as the data for axle I. This option may be used for any axle number, IA, as long as IA is greater than I. Thus data for the first axle must be entered.

An explanatory example will be useful here. Consider a nine-axle vehicle with the tires on the front axle and the tires on the last four axles having identical μ-slip data, and the tires on axles 2, 3, 4, and 5 having identical μ-slip data. These data may be entered in the form shown in Table 2.12. Note we have entered μ-slip data at only one speed and one load for convenience here—up to five speeds and five loads may be used for any axle.

2.5 Antilock Simulation

The documentation presented in this section represents a major extension and revision of the previous antilock simulation used with the Phase III truck and tractor-trailer programs. The greater flexibility now available is primarily the result of the addition of a dictionary, or table, containing variables and parameters pertinent to antilock system operation. Additional features and options, such as general purpose counters and one-shots, were added for extended flexibility. The simulation concentrates on the three areas common to most antilock systems: (1) wheel speed sensor, (2) control logic module, and (3) pressure modulator. Axle-by-axle systems are allowed for, as well as three side-to-side options: (1) worst wheel, (2) best wheel, and (3) average wheel.

Table 2.12

01	
10. , 01	
5000. , 03	
0. , 0.	Axle 1 data
.2 , .7	
1. , .6	
01	
10. , 01	
5000. , 03	
0. , 0.	Axle 2 data
.2 , .9	
1. , .7	
-2	Axle 3 data = axle 2 data
-2	Axle 4 data = axle 2 data
-2	Axle 5 data = axle 2 data
-1	Axle 6 data = axle 1 data
-1	Axle 7 data = axle 1 data
-1	Axle 8 data = axle 1 data
-1	Axle 9 data = axle 1 data

A block diagram showing the relationship between the antilock elements and the main program is shown in Figure 2.52. The wheel speed signal, ω, is received from the main program and processed by the wheel sensor wherein an effective time delay occurs resulting in delayed wheel speed and acceleration signals ω_d and $\dot{\omega}_d$. These signals, along with vehicle velocity, $\dot{x}$, vehicle acceleration, $\ddot{x}$, and feedback from the pressure modulator, are input to the control logic module. The control logic module outputs an ON/OFF solenoid command signal to the pressure modulator which in turn generates the brake pressure, P, returned to the main program.

A complete description of the antilock simulation and explanation of its use is presented in the following sections. Appendix E contains three input listings and characteristic time history traces which can be used for representing basic features exhibited by three antilock systems in use today.

2.5.1 User Dictionary of Variables/Parameters. In order to offer much greater flexibility to the program user as regards variable and parameter programming choices, a table or dictionary of such variables/parameters has been added. This dictionary, as shown in Figure 2.53, is simply a listing of various variables and parameters which might be considered to be of some importance or interest to an antilock system. A user selects, for programming purposes, a particular variable/parameter by referring to its variable I.D. numeral shown in Figure 2.53. Each of these variables/parameters are defined in Table 2.13 and Figure 2.54. If a user has need for additional variables or parameters not included in the dictionary, they can be added by rather simple additions to the FORTRAN code.

The purpose of the dictionary is to allow the program user to select, from a wide variety of possible antilock variables/parameters, only those which are of interest to the particular

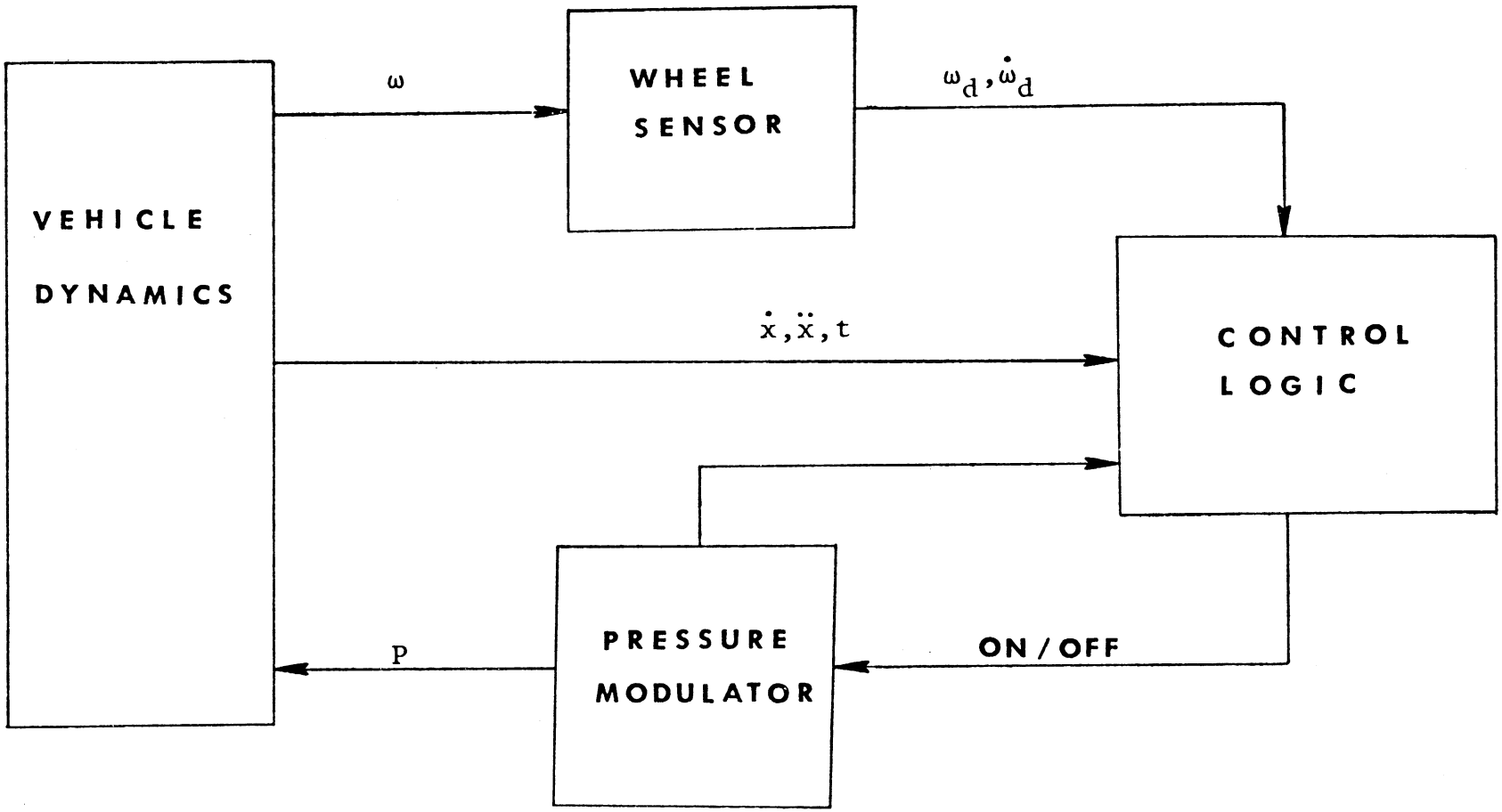

Figure 2.52. Antilock block diagram.

DICTIONARY OF ANTI-LOCK VARIABLES/PARAMÈTERS AVAILABLE TO USER.

VARIABLE I.D.	DESCRIPTION	VARIABLE I.D.	DESCRIPTION
1	1.0	45	WMAX1
2	TIME	46	WMAX2
3	OMEGA	47	TWMAX1
4	OMEGADOT	48	TWMAX2
5	XDOT	49	WMIN
6	XDDOT	50	TWMIN
7	POFF1	51	TPMAX2
8	POFF2	52	TPMIN2
9	PON1		
10	PON2		
11	TOFF1		
12	TON1		
13	XDOFF		
14	XDON		
15	WOFF		
16	WON		
17	WDOFF		
18	WDON		
19	WDMAX		
20	WDMIN		
21	TPMAX1		
22	TPMIN1		
23	WLOCK		
24	TLOCK		
25	SLON		
26	SLOFF		
27	PMAX1		
28	PMAX2		
29	PMIN1		
30	PMIN2		
31	PD		
32	ON		
33	TMOD		
34	SLIP		
35	P		
36	CYCNT		
37	SQUARE		
38	SQUARN		
39	TOFF2		
40	TON2		
41	FOS1		
42	FOS2		
43	FOS3		
44	GPCNT		

Figure 2.53

Table 2.13. Variable/Parameter Definitions

Symbol	I.D. Code	Definition	Units
1.0	1	Constant; Unity Parameter	
TIMF	2	Time in simulation	(sec)
OMEGA	3	Wheel speed at tire-road interface (expressed as an equivalent translational velocity)	(ft/sec)
OMEGADOT	4	Wheel acceleration at tire-road interface (expressed as an equivalent translational acceleration)	(ft/sec^2)
XDOT	5	Vehicle velocity	(ft/sec)
XDDOT	6	Vehicle acceleration	(ft/sec^2)
POFF1	7	Brake pressure at last "OFF" signal	(psi)
POFF2	8	Brake pressure at "OFF" signal in next to last cycle	(psi)
PON1	9	Brake pressure at last "ON" signal	(psi)
PON2	10	Brake pressure at "ON" signal in next to last cycle	(psi)
TOFF1	11	Time at last "OFF" signal	(sec)
TON1	12	Time at last "ON" signal	(sec)
XDOFF	13	Vehicle velocity at last "OFF" signal	(ft/sec)
XDON	14	Vehicle velocity at last "ON" signal	(ft/sec)
WOFF	15	Wheel speed at last "OFF" signal	(ft/sec)
WON	16	Wheel speed at last "ON" signal	(ft/sec)
WDOFF	17	Wheel acceleration at last "OFF" signal	(ft/sec^2)
WDON	18	Wheel acceleration at last "ON" signal	(ft/sec^2)
WDMAX	19	Maximum wheel acceleration in last cycle	(ft/sec^2)
WDMIN	20	Minimum wheel acceleration in last cycle	(ft/sec^2)

Table 2.13 (Cont.)

Symbol	I.D. Code	Definition	Units
TPMAX1	21	Time of maximum pressure in last cycle	(sec)
TPMIN1	22	Time of minimum pressure in last cycle	(sec)
WLOCK	23	Parameter having value 1.0 if wheel is locked; otherwise having value of 0.0	
TLOCK	24	Time ramp beginning at start of any wheel lock	(sec)
SLON	25	Wheel slip at last "ON" signal	
SLOFF	26	Wheel slip at last "OFF" signal	
PMAX1	27	Maximum pressure from last cycle	(psi)
PMAX2	28	Maximum pressure from cycle before last	(psi)
PMIN1	29	Minimum pressure from last cycle	(psi)
PMIN2	30	Minimum pressure from cycle before last	(psi)
PD	31	Treadle pressure	(psi)
ON	32	Parameter having value of 1.0 during "ON" signal; otherwise 0.0	
TMOD	33	Time of modulation for the pulse-width modulated square wave	(sec)
SLIP	34	Wheel slip	
P	35	Brake pressure	(psi)
CYCNT	36	Cycle counter beginning at 0 and incrementing its count by 1 every "OFF" signal	
SQUARE	37	Pulse-width modulated square wave having value 1.0 or 0.0	
SQUARN	38	SQUARE - 1.0	
TOFF2	39	Time of "OFF" signal in cycle before last	(sec)
TON2	40	Time of "ON" signal in cycle before last	(sec)
FOS1	41	First one-shot variable having value 1.0 during one-shot firing; otherwise having value of 0.0	

Table 2.13 (Cont.)

Symbol	I.D. Code	Definition	Units
FOS2	42	Second one-shot variable	
FOS3	43	Third one-shot variable	
GPCNT	44	General purpose counter	
WMAX1	45	Maximum wheel speed in last cycle	(ft/sec)
WMAX2	46	Maximum wheel speed in cycle before last	(ft/sec)
TWMAX1	47	Time of maximum wheel speed in last cycle	(sec)
TWMAX2	48	Time of maximum wheel speed in cycle before last	(sec)
WMIN	49	Minimum wheel speed in last cycle	(ft/sec)
TWMIN	50	Time of minimum wheel speed in last cycle	(sec)
TPMAX2	51	Time of maximum brake pressure in cycle before last	(sec)
TPMIN2	52	Time of minimum brake pressure in cycle before last	(sec)

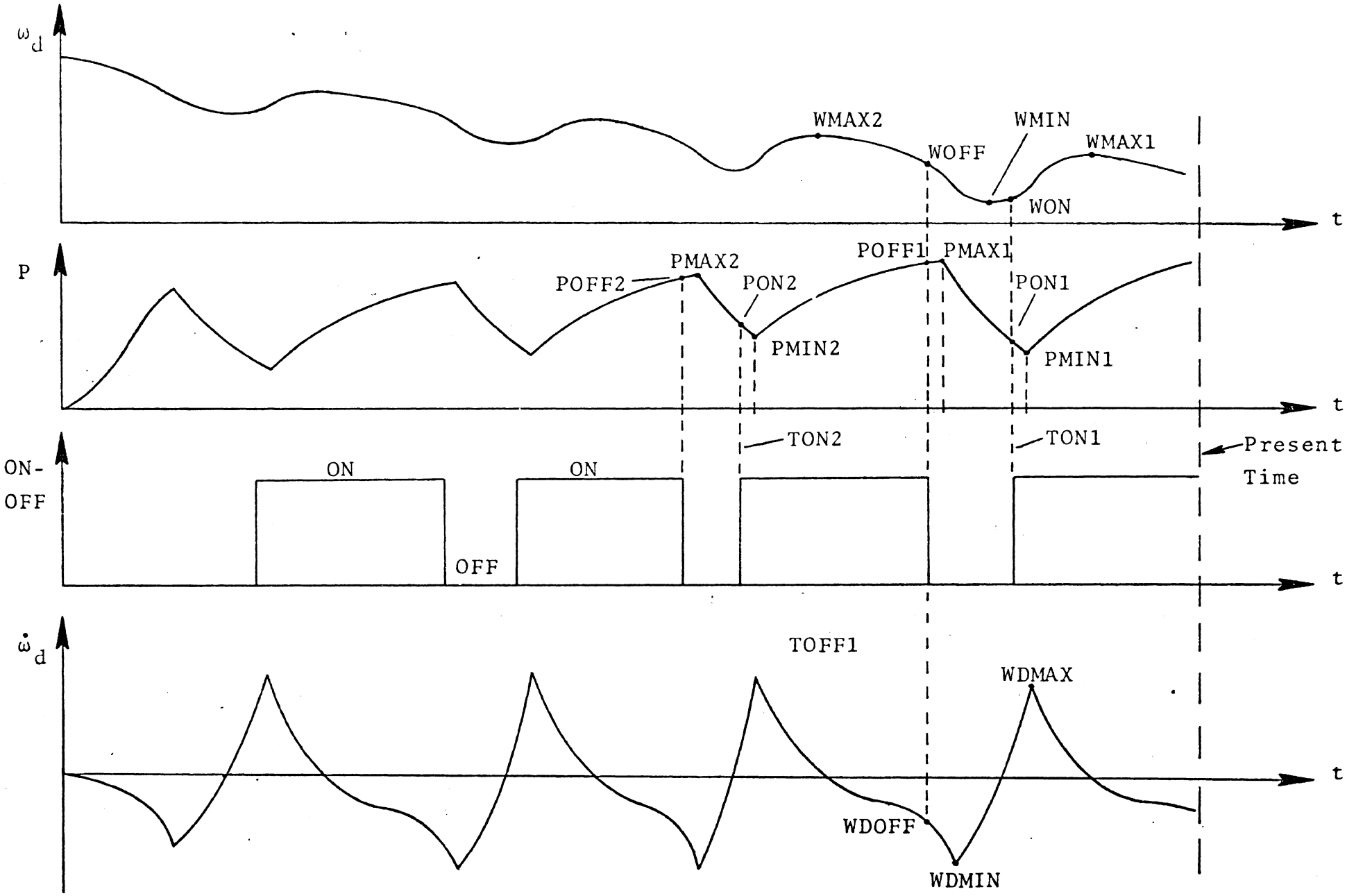
ω_d
WMAX2
WMIN
WMAX1
WOFF
WON
t
P
POFF2
PMAX2
PON2
POFF1
PMAX1
PON1
PMIN2
PMIN1
t
TON2
TON1
Present
Time
ON-
OFF
ON
ON
OFF
t
$\dot{\omega}_d$
TOFF1
WDMAX
t
WDOFF
WDMIN

Figure 2.54

system he is attempting to simulate. Those familiar with the previous antilock simulation may recall that such variable/parameter choices were fixed and limited to wheel speed, acceleration, and four or five other variables. Thus, the present approach should eliminate most problems where the user was handicapped with the previous program because a particular variable or parameter was not available.

Within the antilock variables/parameters are stored in an array of dimension 60 called VARIB(J), J=1,60. Therefore, VARIB(1) contains the constant 1.0, VARIB(2) contains the present value of the time, t, and so on as defined in Table 2.13. Variables VARIB(53) through VARIB(60) are not defined but can be used as storage locations for alternate variable/parameter definitions specified by the user and added to the FORTRAN code. Such a table or array is provided for each axle of the vehicle.

2.5.2 General Expression Form. Throughout the remainder of this chapter a particular algebraic expression will be encountered repeatedly. It would therefore be helpful beforehand to define each term in the expression and then discuss its purpose. The expression referred to is of the general form:

$$C_1x_1 + C_2x_2 + C_3x_3 + C_4x_4y_4 + C_5x_5y_5 \tag{2.50}$$

The C_i (i=1,...,5) are constant coefficients for each term. Any of these coefficients may be adaptive to as many as two different variables. This adaptive feature will be discussed in detail in Section 2.5.4. The x_i, (i=1,...,5) and y_i, (i=4,5) are variables or parameters available in the user dictionary. Note that the fourth and fifth terms are quadratic in form. During execution of the program the x_i and y_i, which the user has selected from the dictionary to form some relationship, are actually assigned values from the array VARIB(J).

The purpose of these expressions is to allow the user to form various algebraic relationships between the variables and parameters available in the dictionary, subject to the form of the general expression (2.50). A form of this general expression appears in almost every section of the program from control logic inequality expressions to evaluation of one-shot conditions. Only those terms necessary to form a desired expression are required. Some simple examples illustrating the use of these general expressions are presented in the following sections.

2.5.3 Wheel Sensor Module. The primary effect of a wheel sensor is a phase shift and/or time delay between the actual wheel rate and the derived wheel rate. This input-output relationship can often be described adequately by transfer functions of various order and/or transport time delay expressions. The present version assumes a general first-order filter of the form $1/\tau_\omega p + 1$ relating actual wheel rate to derived wheel rate, where τ_ω is the time constant of the filter and p is an operator denoting differentiation with respect to time.

Many antilock systems make use of wheel acceleration derived from the output of the wheel sensor. This normally involves additional delays along with a differentiation process. The assumed transfer function here was taken as $p/\tau_{\omega d}p + 1$ relating derived wheel rate to derived wheel acceleration. The derived wheel acceleration calculation normally takes place within the electronic control unit. However, since it, along with wheel rate, is a primary input to the control unit logic, it is included here within the wheel sensor module so that the control unit can be characterized by logical or decision-making processes only. The wheel sensor module can then be described by the input-output relationships shown in Figure 2.55.

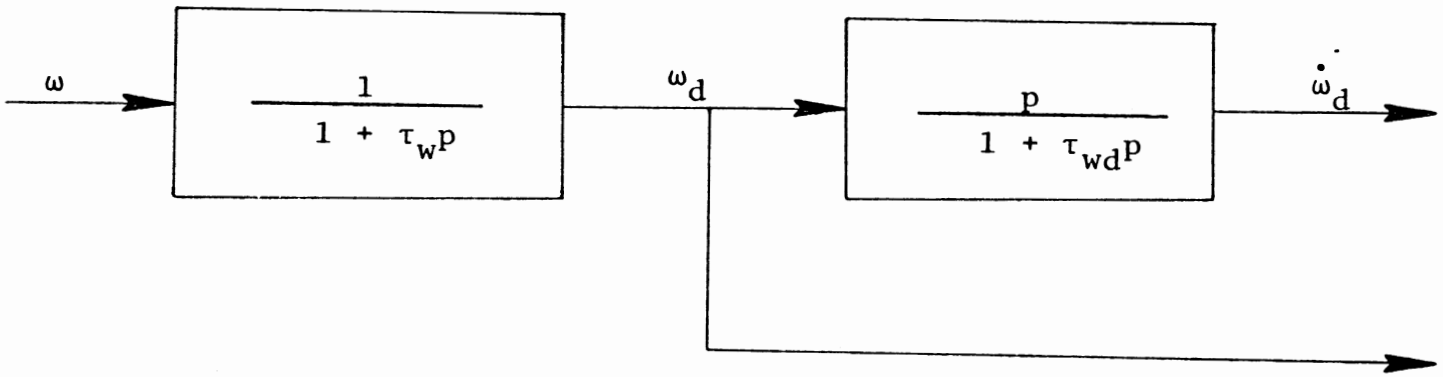

Figure 2.55. Wheel sensor module.

The delayed wheel speed and acceleration signals, ω_d and $\dot{\omega}_d$, are used as the primary inputs to the control logic module. The assumed wheel sensor and derivative circuit input-output relationships are therefore described by two input parameters, τ_ω and $\tau_{\omega d}$, which represent the first-order filter time constants of the wheel sensor and its derivative circuit. The variables, ω_d and $\dot{\omega}_d$, appear in the user dictionary as OMEGA and OMEGADOT, I.D. codes 3 and 4. (The symbols ω and $\dot{\omega}$ are used interchangeably throughout this section for ω_d and $\dot{\omega}_d$.)

Other variables are provided as possible inputs to the control logic module, however, no similar operations are attempted on these other input variables.

3.5.4 Control Logic Module. The control logic is characterized by a set of eight inequality expressions which the user forms as conditions for generating "ON" and "OFF" signals. Associated with each arithmetic inequality expression is a logical variable. These logical variables, reflecting the state or polarity of the inequality expressions, are logically combined to generate the "ON" and "OFF" signals. "ON" is defined here as air being applied to, or "ON," the brake air chambers. Figure 2.56 summarizes the overall structure of the control logic module.

Inequality Expressions.

Each of the eight arithmetic inequalities has the general form:

$$F_i \triangleq c_{i1}v_{i1} + c_{i2}v_{i2} + c_{i3}v_{i3} + c_{i4}v_{i4}w_{i4} + c_{i5}v_{i5}w_{i5} \geq 0 \quad , \quad i=1,8 \tag{2.51}$$

where

Inequality Expression	Logical Variable	Logical Operator	Solenoid Command
$F_1 \geq 0$	L_1	OP_{12}	OFF
$F_2 \geq 0$	L_2	OP_{23}	
$F_3 \geq 0$	L_3	OP_{34}	
$F_4 \geq 0$	L_4		
.	.	.	ON
.	.	.	
.	.	.	
.	.	.	
.	.	.	
		OP_{78}	
$F_8 \geq 0$	L_8		

Figure 2.56. Control logic module.

c_{ij} , (j=1,5) are the constant coefficients of each term.

v_{ij}, w_{ik} , (j=1,5; k=4,5) are the variables/ parameters selected from the user dictionary.

The first four inequalities, F_1 through F_4, are used for generating the "OFF" signal; the last four inequalities for the "ON" signal.

As an example, suppose the condition

$$\dot{\omega} \leq -100 \text{ ft/sec}^2*$$

or

$$-\dot{\omega} - 100 \geq 0$$

was used as the first "OFF" condition. Then F_1 would become

$$F_1 \triangleq (-1.0)\dot{\omega} + (-100.)1.0 \geq 0 \quad ,$$

with -1.0 and -100. required as c_{11} and c_{12}. OMEGADOT, ($\dot{\omega}$), would be selected from the user dictionary for v_{11} and the unity parameter, 1.0, would be selected as v_{12}. As will be described in detail in Section 2.5.7, five numbers would be required as program input for forming this expression: (a) the number of terms involved in the expression, (2); (b) two coefficients, (-1.0) and (-100.); and (c) two variable I.D. codes from the user dictionary, '4' and '1' for OMEGADOT and the unity parameter, respectively.

---

*See definition of OMEGADOT on page 113.

A simple description of the sequence of operations taking place within the antilock control logic module is as follows:

During a braking maneuver, the variables/parameters selected by the user are substituted in the user-defined inequality expressions. These expressions are evaluated, and based upon their polarity, OFF signals or ON signals are sent to the pressure modulator. At the beginning of the braking maneuver, evaluation of the inequalities associated with generating the "OFF" signal takes place until an "OFF" signal is generated. Attention then is focused on the inequalities associated with generating an "ON" signal until an "ON" signal is generated. This sequence continues until either the treadle valve pressure demanded by the driver falls to near zero, or until the vehicle velocity decreases to below some cut-off velocity.

Logical Variables

Each of the eight inequalities has assigned to it a logical variable that is defined as TRUE if the inequality is satisfied as shown; FALSE if not. In other words, if $F_i \geq 0$, then the logical variable L_i associated with F_i assumes the value TRUE. If $F_i < 0$, then L_i assumes the value FALSE. Since there are four inequalities for the generation of the "OFF" signal, there are four logical variables associated with the "OFF" signal. The purpose of these logical variables is to facilitate the generation of an "OFF" signal by allowing them to be "AND"-ed and "OR"-ed together by the program user. If, for example, the user had decided that F_1 and F_2 must be satisfied or else F_3 or F_4 be satisfied (F_1, F_2, F_3, and F_4 having been previously defined by the data set selected by the user), the proper "OFF" signal would be defined by the following expression:

$$\text{OFF} = (L_1 \text{ AND } L_2) \quad \text{OR} \quad (L_3 \text{ OR } L_4)$$

The same discussion applies to the "ON" signal and associated logical variables L_5, L_6, L_7, and L_8.

The user specifies the logical operations between L_1 and L_2, L_3, and L_4, and between the bracketed expressions by means of three logical operator switches, OP_{12}, OP_{34}, and OP_{23}, respectively. Input values of 0 imply logical "OR" operations; values of 1 imply logical "AND" operations. The same rules apply to logical variables L_5, L_6, L_7, L_8 and their logical operator switches OP_{56}, OP_{78}, and OP_{67}. The general forms of these logical equations are:

$$OFF = (L_1\ OP_{12}\ L_2)\ OP_{23}\ (L_3\ OP_{34}\ L_4) \tag{2.52}$$

and

$$ON = (L_5\ OP_{56}\ L_6)\ OP_{67}\ (L_7\ OP_{78}\ L_8) \tag{2.53}$$

The user is required to input data only for the number of inequality expressions needed. The details relating to data input for the inequality expressions and logical operators are explained in Section 2.5.7.

Time Delays

Four programmable time delays are available in the control logic. The first time delay, τ_1, is the delay between the evaluations of F_1 and the evaluations of either F_2, F_3, or F_4. The second time delay, τ_2, is the delay between the time of generation of the "OFF" signal and the time that F_5 may be evaluated in the generation of the next "ON" signal. τ_3 is the delay between the time of evaluation of F_5 and the time of evaluation of either F_6, F_7, or F_8. τ_4 is the delay between the time of generation of the "ON" signal and the time that F_1 may be evaluated in the generation of the next "OFF" signal. For time delay effects other than those described here, the one-shot variables (Section 3.5.6) may be employed.

Example

A brief example covering the above outlined features should prove helpful. Consider an antilock system which generates an "OFF" signal subject to the following laws:

1) $\dot{\omega} \leq -50$ ft/sec^2

and 2) at a time .05 second after (1) is satisfied, $\omega \leq .9\,\dot{x}$ must also be satisfied.

Suppose the corresponding "ON" signal must satisfy the following requirements

3) $\dot{\omega} \geq -.5$ ft/sec^2

and 4) at a time .02 second after (3) is satisfied, $\omega \geq .8\,\dot{x}$ must also be satisfied.

Suppose also that once the "ON" signal is generated during any cycle, the test for the next "OFF" signal must not take place for at least 0.1 second, guaranteeing a certain amount of brake on-time.

Rewriting (1) as

$$F_1 = -\dot{\omega} - 50 \geq 0$$

$$c_{11} = -1.0$$

$$c_{12} = -50.$$

The variable I.D. codes for v_{11} and v_{12} would be "4" and "1," corresponding to OMEGADOT and the unity parameter from the user dictionary.

Similarly, for (2),

$$F_2 = -\omega + .9\,\dot{x} \geq 0$$

$$c_{21} = -1.0$$

$$c_{22} = .90$$

The variable I.D. codes for v_{21} and v_{11} would be "3" and "5".

Since F_3 and F_4 are not required, no input for these expressions would be needed. OP_{12} should be entered as 1 since OFF = L_1 <u>AND</u> L_2. OP_{23} and OP_{24} have no meaning here and can therefore be either 0 or 1. The time delay between F_1 and F_2 implies $\tau_1 = 0.05$. Since there is no time delay specified between the generation of the "OFF" signal and the evaluation for the next "ON" signal, $\tau_2 = 0.0$.

Similarly, for the "ON" criteria, (3) may be rewritten as

$$F_5 = \dot{\omega} + 5 \geq 0$$

$$c_{51} = 1.0$$

$$c_{52} = 5.0$$

With variable I.D. codes for v_{51} and v_{52} of "4" and "1".

Likewise

$$F_6 = \omega - .8\,\dot{x} \geq 0$$

$$c_{61} = 1.0$$

$$c_{62} = -.8$$

With variable I.D. codes for v_{61} and v_{62} of "3" and "5".

Since F_7 and F_8 are not required, no input for these expressions would be needed. OP_{56} should be entered as 1 for the required "AND" operation, while OP_{67} and OP_{78} are meaningless here and can be either 0 or 1. The time delay between F_5 and F_6 requires $\tau_3 = 0.05$. The time delay between the "ON" signal and the test for the next "OFF" signal requires $\tau_4 = 0.10$.

Adaptive Coefficients

Many antilock systems possess adaptive capabilities for changing coefficients involved in their control logic. For this reason, and increased programming flexibility, an adaptive coefficient feature is provided for in this program. Each coefficient, C_{ij}, involved in the inequality expressions may be altered to change its value as a function of one or two dictionary varaibles in the manner shown in Figures 2.57 and 2.58.

In Figure 2.57, the value of C_{ij} is A_0 (its initial value), if $u_{ij} < b_1$. If u_{ij}, the adaptive variable, is greater than its breakpoint value of b_1, C_{ij} is equal to A_1.

If two adaptive variables are involved, as illustrated in Figure 2.58,

$$C_{ij} = \begin{cases} A_0 & \text{if } u_{ij} \leq b_1 \text{ and } z_{ij} \leq b_2 \\ A_1 & \text{if } u_{ij} > b_1 \text{ and } z_{ij} \leq b_2 \\ A_2 & \text{if } z_{ij} > b_2 \end{cases} \tag{2.54}$$

By including an additional numerical switch in the input, the two adaptive variable case may be altered to:

$$C_{ij} = \begin{cases} A_0 & \text{if } u_{ij} \leq b_1 \\ A_1 & \text{if } u_{ij} > b_1 \text{ and } z_{ij} \leq b_2 \\ A_2 & \text{if } u_{ij} > b_1 \text{ and } z_{ij} > b_2 \end{cases} \tag{2.55}$$

as illustrated in Figure 2.59.

The details of the numerical input format are explained in Section 2.5.7.

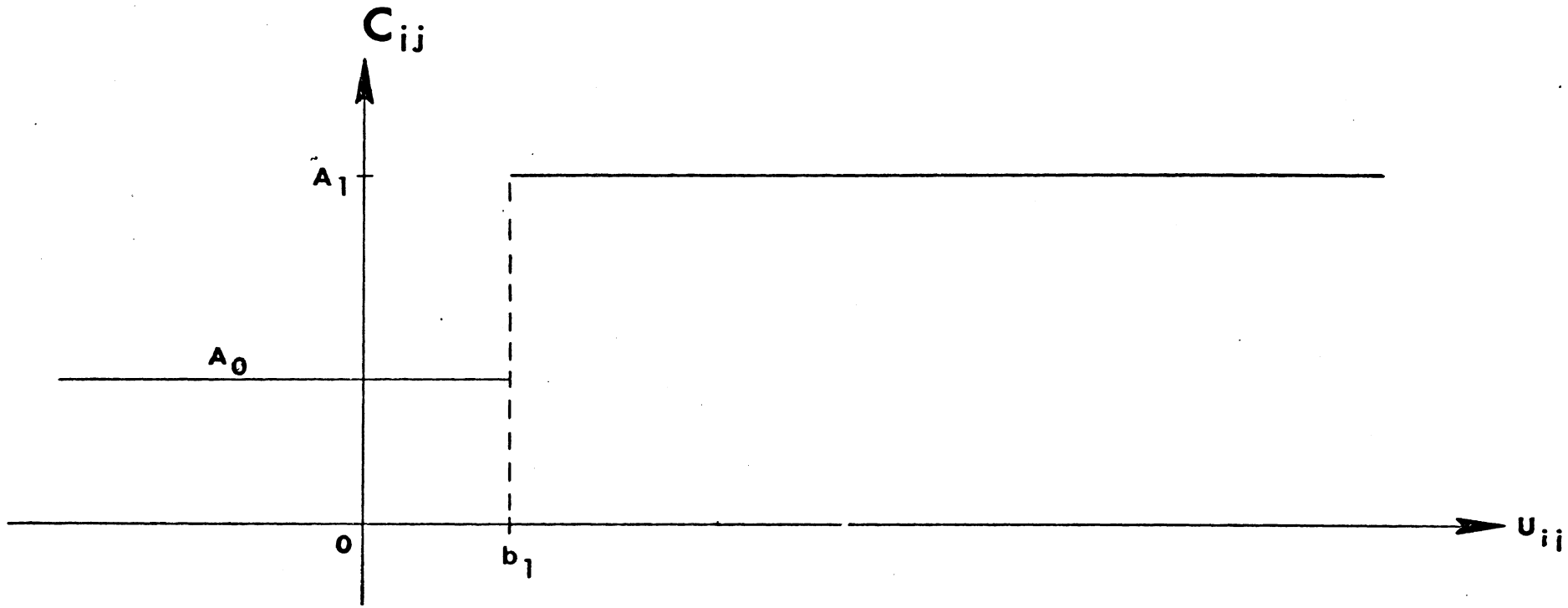

Figure 2.57

$$C_{ij} = \begin{cases} A_0 \text{ , if } u_{ij} \le b_1 \text{ and } z_{ij} \le b_2 \\ A_1 \text{ , if } u_{ij} > b_1 \text{ and } z_{ij} \le b_2 \\ A_2 \text{ , if } z_{ij} > b_2 \end{cases}$$

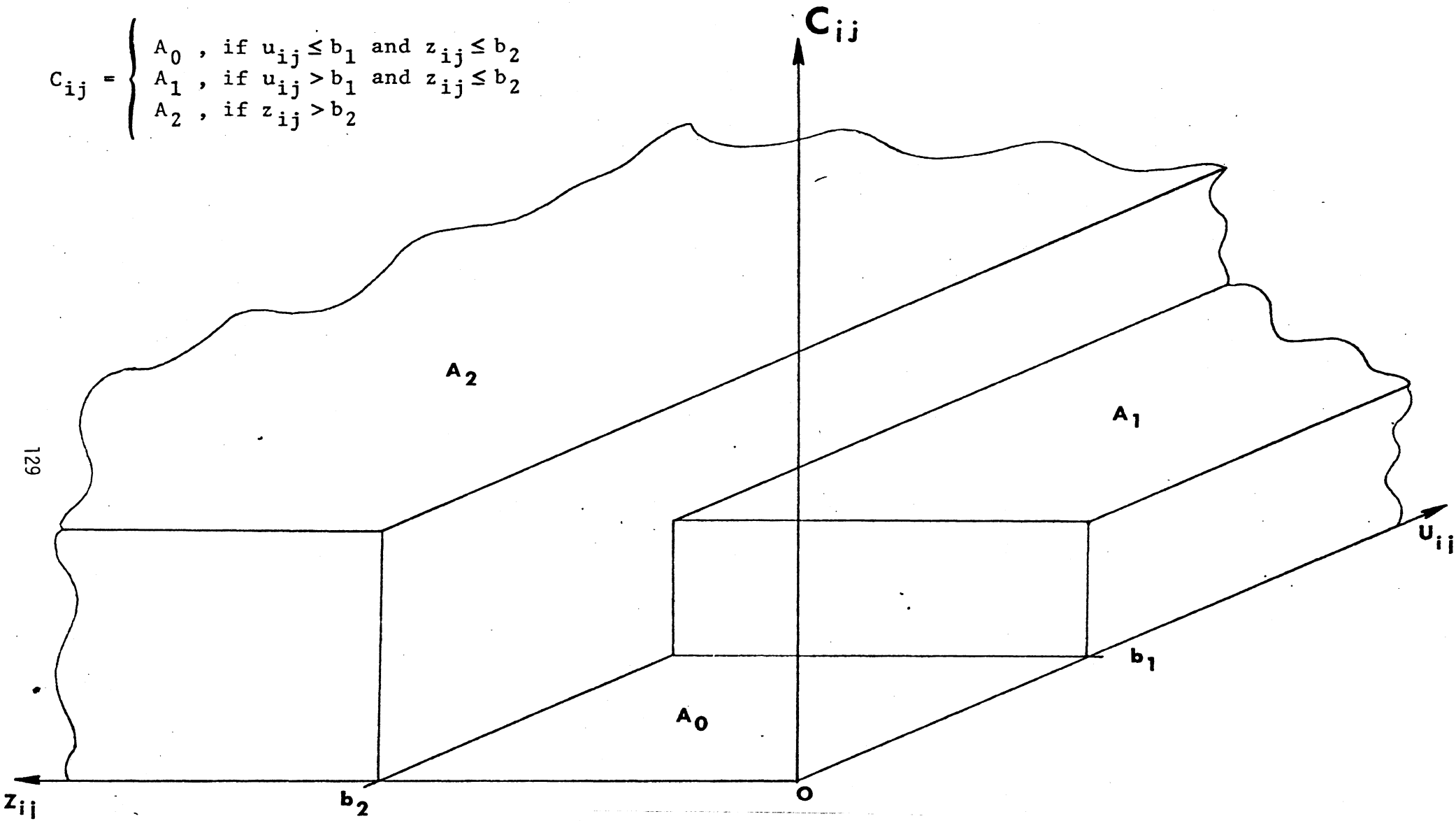

Figure 2.58. Adaptive coefficient feature.

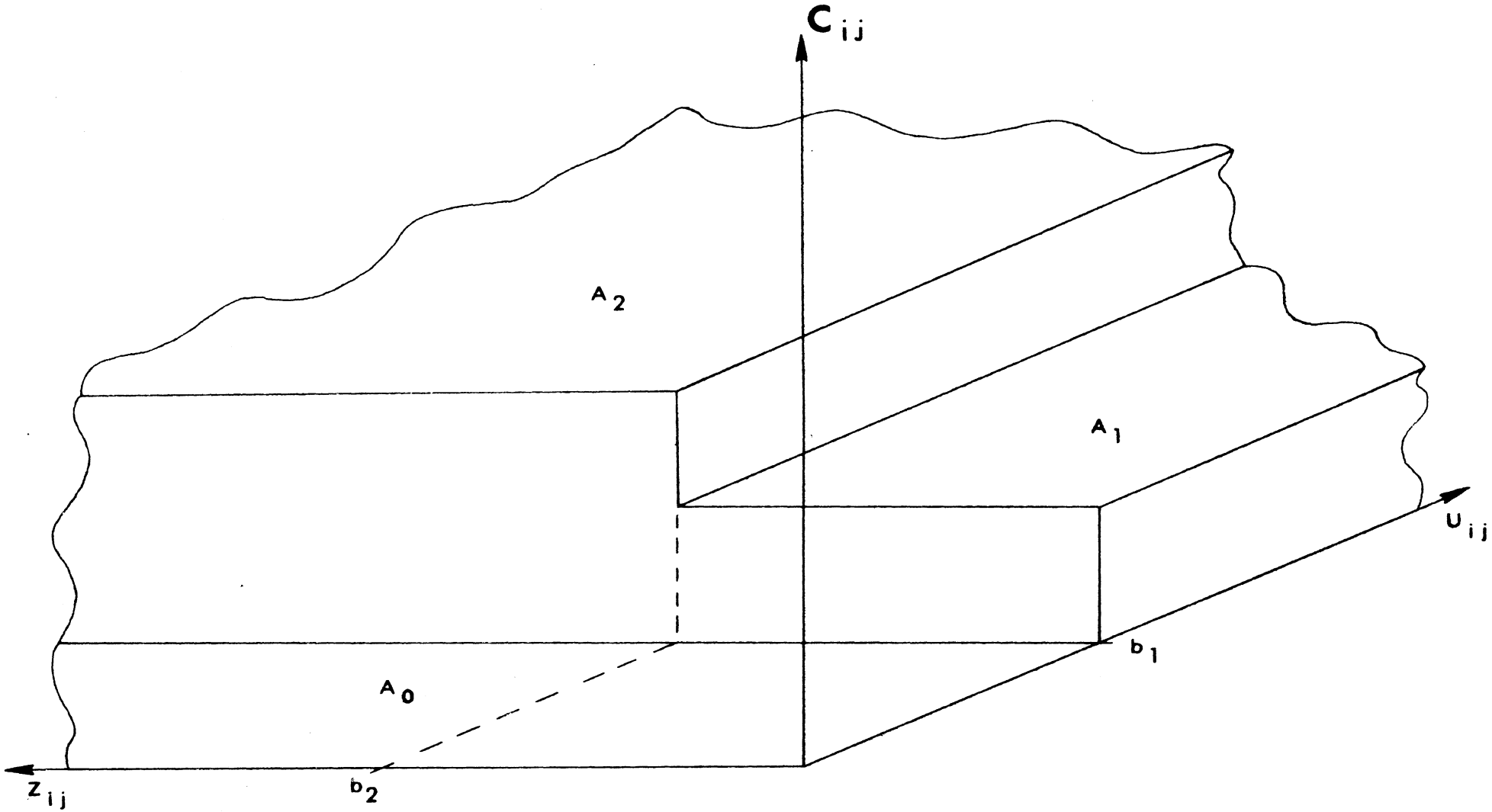

Figure 2.59

Side-to-Side Options

Three different side-to-side options per axle are available. One antilock system is allowed for each axle with the same pressure being returned to both sides for each of the available options. These are summarized below:

OPTION 1 - Worst Wheel. The wheel having the lowest rotational rate (omega) for a given axle is selected by the control logic as its input. The same pressure is returned to both sides based on this input.

OPTION 2 - Best Wheel. Same as Option 1 except that the wheel with the highest rotational rate is selected as input.

OPTION 3 - Average Wheel. Both wheel rates are averaged by the control logic module and used as input. The same pressure is returned to both sides.

See Section 2.5.7 for the numerical input and format required for each option.

Logic Sampling Rate Control

The program user is asked to specify a logic sampling period, TSMPLE, which controls the rate at which the antilock logic is interrogated. If TSMPLE is specified to be less than or equal to the digital simulation time step, then no sampling rate control is in effect. If, however, a logic sampling period greater than the digital simulation time step is called for, all control logic and special option features pertaining to the control logic module are interrogated at time intervals set by the logic sampling period, TSMPLE. Wheel sensor computations and pressure modulator activities are not affected.

For vehicle velocities less than 7 ft/sec, the antilock simulation is inactivated and line pressures will follow the treadle pressure.

2.5.5 Pressure Modulator. The pressure modulator valve is simulated by two time delays and several programmable rise and fall rates for both exponential and linear characteristics. The programmable rise and fall rates make possible the simulation of relatively complex pressure modulator activity including designs involving pneumatic logic or pulse-width modulators.

Time Delays

The input received by the pressure modulator is simply the "ON" and "OFF" signals generated in the control logic module. Once a control signal is received there is normally a time delay before actual pressure reduction or increase takes place. These time lags are denoted in the simulation as τ_{ON} and τ_{OFF} and are program inputs specified by the user.

Exponential Fall and Rise Rates

The pressure rise is defined to be exponential in time with the upper pressure limit set by the treadle valve output or by a programmable limit PDRSE offered as a special option and explained in Section 2.5.6. Likewise, the pressure fall is exponential in time with its lower limit as zero pressure or by a programmable lower limit, PDFALL, offered as a special option and defined in Section 2.5.6. As many as three pressure fall rates and three rise rates can be programmed. The fall and rise rates referred to are defined as the inverse of the time constants associated with the exponential pressure rise and fall.

The three exponential fall rates are denoted as PFE_i, (i=1,3); the three exponential rise rates are defined as PRE_i, (i=1,3). For reasons of flexibility these fall and rise rates are defined to be functions of variables denoted as ε_1 and ε_2, respectively. ε_1 and ε_2 are defined by the general form expressions:

$$\varepsilon_1 \triangleq H_1v_1 + H_2v_2 + H_3v_3 + H_4v_4w_4 + H_5v_5w_5$$

$$\varepsilon_2 \triangleq G_1v_1 + G_2v_2 + G_3v_3 + G_4v_4w_4 + G_5v_5w_5$$

where H_i and G_i, (i=1,5) are the constant coefficients of each term, and v_j and w_k, (j=1,5; k=4,5) are variables/parameters available in the user dictionary.

These relationships are shown in Figures 2.60 and 2.61. The break-points X_1, X_2, X_3, and X_4 along the ε_1 and ε_2 axes separate the fall and rise rate regions.

In terms of transfer function notation, the above relationships can be expressed as:

<u>Pressure Fall</u>:

PDFALL or

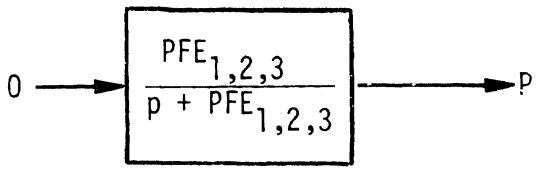

<u>Pressure Rise</u>:

PDRISE or

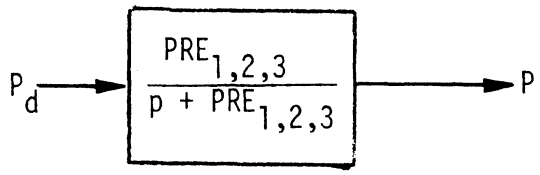

where $PFE_{1,2,3}$ and $PRE_{1,2,3}$ defined above are functions of ε_1 and ε_2, respectively, and p is an operator denoting differentiation with respect to time.

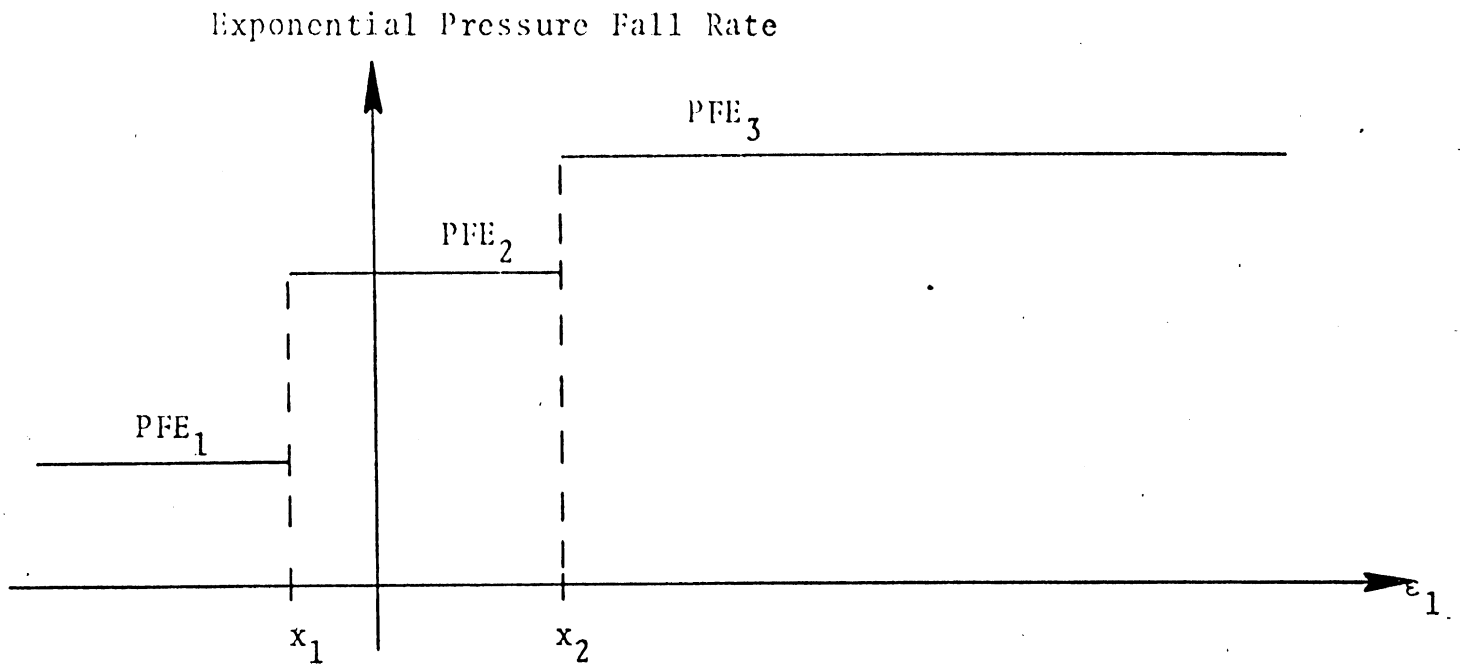

Figure 2.60

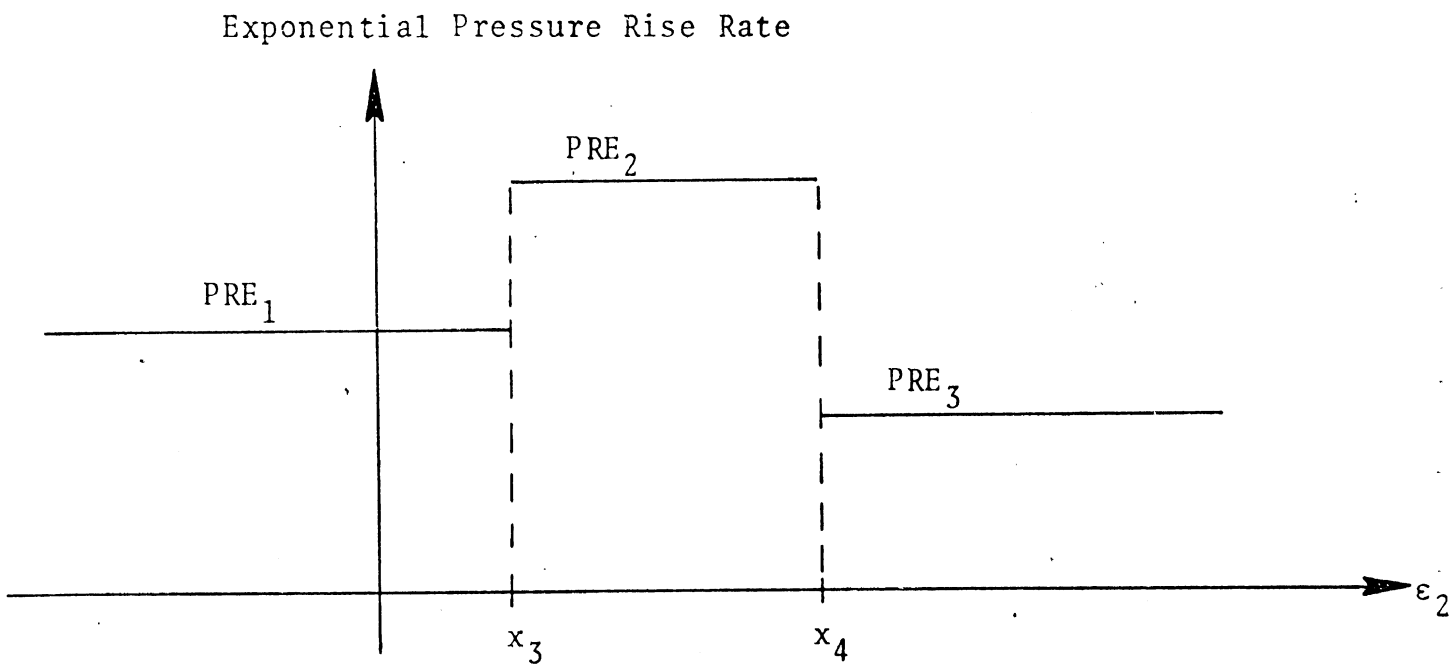

Figure 2.61

Linear Fall and Rise Rates

The pressure fall and rise, under this option, is linear in time with an upper limit as treadle pressure, P_d, and a lower limit as zero pressure. Three fall rates and three rise rates may be specified as in the exponential case. The linear fall and rise rates are denoted as PFL_i and PRL_i , (i=1,3), respectively. Again, for programming flexibility, the linear fall and rise rates are defined as functions of variables denoted as ε_3 and ε_4, respectively. ε_3 and ε_4 are defined by the general form expressions:

$$\varepsilon_3 \triangleq R_1v_1 + R_2v_2 + R_3v_3 + R_4v_4w_4 + R_5v_5w_5$$

$$\varepsilon_4 \triangleq S_1v_1 + S_2v_2 + S_3v_3 + S_4v_4w_4 + S_5v_5w_5$$

where R_j and S_j , (j=1,5) are the constant coefficients of each term, and v_j w_k , (j=1,5; k=4,5) are variables/parameters available in the user dictionary. These relationships are illustrated in Figures 2.62 and 2.63. The pressure returned is given simply by the following two equations:

$$P(t-t_0) = [PFL_i(\varepsilon_3)] \cdot (t-t_0) + P(t_0) \quad ; \quad \text{(fall)}$$

$$P(t-t_0) = [PRL_i(\varepsilon_4)] \cdot (t-t_0) + P(t_0) \quad ; \quad \text{(rise)}$$

X_5, X_6, X_7, and X_8 are the associated break-points similar to the exponential case.

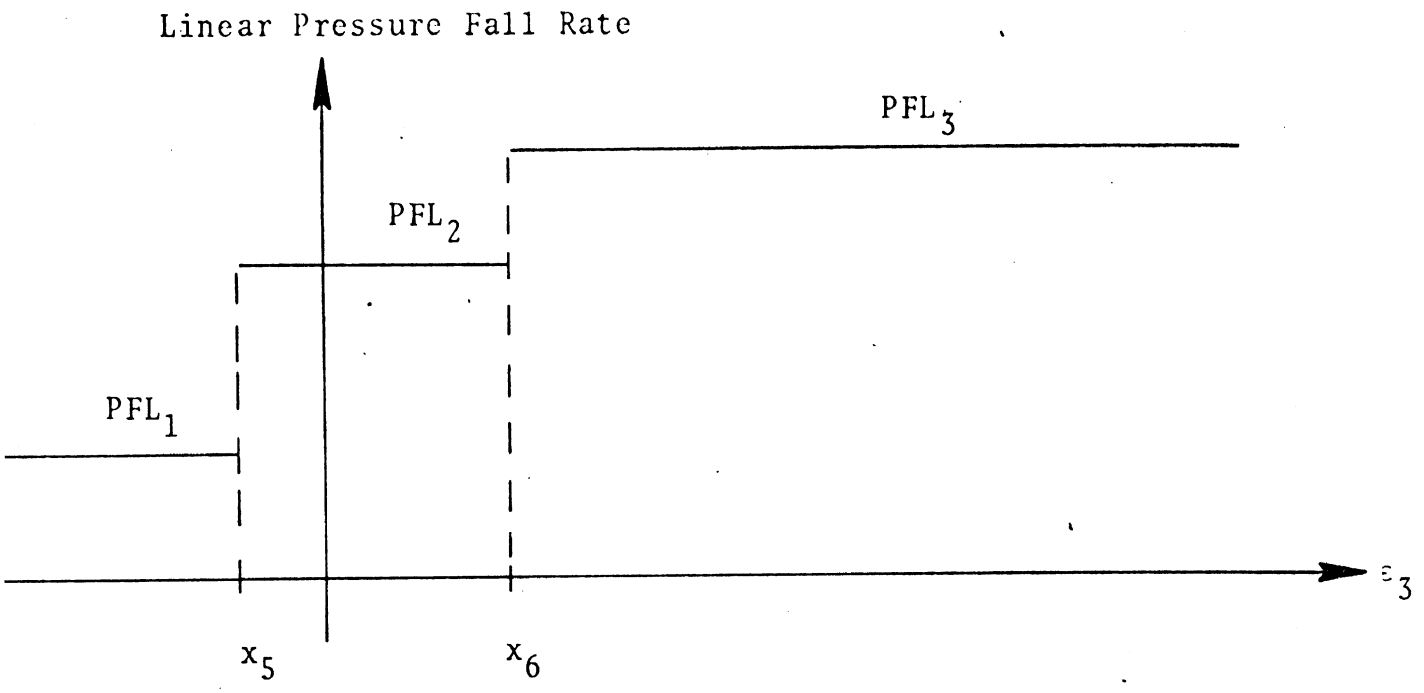

Figure 2.62

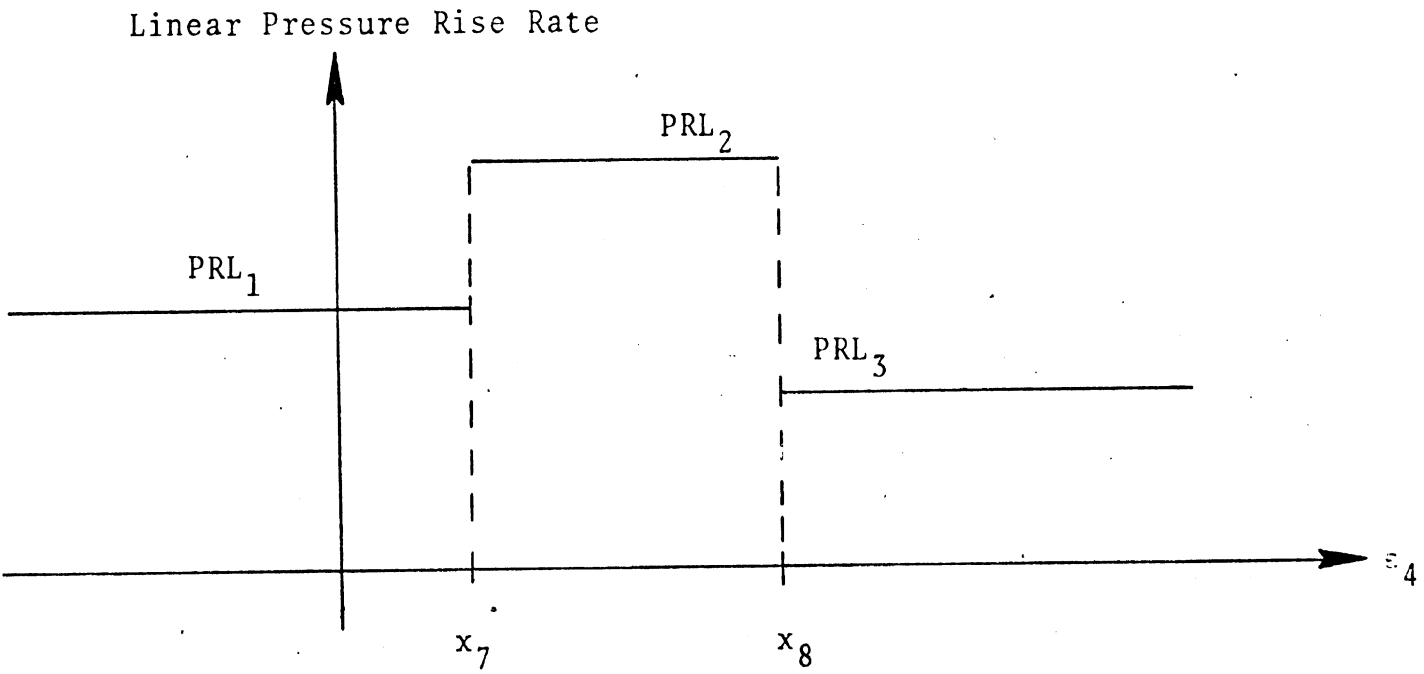

Figure 2.63

Pressure Modulator Key

A pressure modulator key, IPKEY, is read during input just prior to any data related to the pressure modulator. The value of this key distinguishes for the program whether exponential, linear, or both exponential and linear characteristics will be computed. The following key defines the IPKEY values required for each case:

$$\text{IPKEY} = \begin{cases} 0 \quad , & \text{exponential} \\ 1 \quad , & \text{linear} \\ 2 \quad , & \text{exponential and linear} \end{cases}$$

The exponential and linear option (IPKEY=2) returns a pressure representing the summation of the exponential and linear pressure computations.

Finally, all coefficients appearing in the general form expressions for the pressure modulator possess the adaptive coefficient feature.

Example

Consider the following example of a certain pressure modulator having only exponential pressure fall and rise characteristics:

1) "ON" delay = "OFF" delay = 0.05 seconds.

2) The exponential pressure rise rate assumes an approximate value of $(0.2)^{-1} = 5.0$ for differences between treadle valve output pressure and line pressure of 50 psi or more, and an approximate exponential rise rate of $(0.33)^{-1} = 3.0$ for pressure differences of less than 50 psi.

3) The exponential pressure fall rate is approximately constant for all line pressure values with a fall rate equal to $(0.25)^{-1} = 4.0$.

This could be simulated by the following choice of input parameters:

IPKEY = 0

τ_{ON} = 0.05

τ_{OFF} = 0.05

H_1 = 1.0 } => $\varepsilon_1 = 1.0$

G_1 = -1.0 , G_2 = 1.0 } => $\varepsilon_2 = P_d - P$

Variable I.D. code for P_d = 31.

Variable I.D. code for P = 35.

See User Diectionary

$X_1 = X_2 = 0.0$

$PFE_1 = PFE_2 = PFE_3 = 4.0$

$X_3 = 0.0$, $X_4 = 50.0$

$PRE_1 = PRE_2 = 3.0$, $PRE_3 = 5.0$

The number of terms required for ε_1, (1 term) and ε_2 (2 terms) would also be required as input as explained in Section 2.5.7.

2.5.6 Special Options. Four special options have been included in the model in order to facilitate simulation of certain features displayed in some actual antilock systems while also providing increased programming flexibility. The four options referred to are: (1) treadle pressure modulation/programming, (2) pulse-width modulated square wave, (3) three programmable one-shots, and (4) general purpose counter. Each of these options will be explained in the following sections.

Treadle Pressure Modulation/Programming

Most pressure valves operating without antilock interruption, and many under antilock cycling, follow or are limited above by the treadle pressure application; while similarly, the output pressure of these valves fall to treadle pressure or zero

pressure when treadle pressure is decreased or removed. However, in some valves, during antilock cycling, pressure may rise to some limiting pressure less than treadle and/or fall to some pressure greater than zero. Such treadle modulation or programming of demanded pressure is a feature which is allowed for under this option.

Prior to any input for this option, a key, IPDKEY, for treadle pressure modulation, is read. A value of -1 or less negates the use of this option, while values greater than or equal to 0 activate the option. Variables PDFALL and PDRISE become the demanded pressure during pressure fall and rise periods, respectively. These variables are defined by the following general form expressions:

$$\text{PDFALL} \triangleq V_1v_1 + V_2v_2 + V_3v_3 + V_4v_4w_4 + V_5v_5w_5$$

$$\text{PDRISE} \triangleq W_1v_1 + W_2v_2 + W_3v_3 + W_4v_4w_4 + W_5v_5w_5$$

where,

V_j and W_j , (j=1,5) are constant coefficients for each term. The adaptive coefficient feature is provided for these coefficients.

v_j, w_k , (j=1,5; k=4,5) are variables/parameters selected from the user dictionary.

As an example, suppose an antilock system operated so as to always rise to the maximum pressure attained in the previous cycle rather than to treadle pressure. PDRSE would then be defined as simply

$$\text{PDRSE} = (1.0)\ \text{POFF1}$$

where 1.0 is W_1 and POFF1, the maximum pressure from the last cycle, is selected from the user dictionary for v_1. In this case, the coefficient, 1.0, and the variable I.D. code for POFF1, 7, would be required as input for the option.

Pulse-Width Modulated Square Wave

A time, or pulse-width, modulated square wave is provided as an option for general use. This option was motivated by a particular antilock system known to possess such a feature for purposes of treadle pressure modulation. The square wave generated under this option can be used in any portion of the program and is available in the user dictionary under the name SQUARE. Figure 2.64 illustrates the parameter and variable relationships which define the square wave. The period of the suqare wave, PERIOD, is constant. The amount of time modulation, represented by TMOD, may be variable and programmable. This is accomplished in the program by allowing the ratio, TMOD/PERIOD, to be a tabular function of a variable, ε_5, as shown in Figure 2.65. ε_5 is defined as a general form expression:

$$\varepsilon_5 = PW_1v_1 + PW_2v_2 + PW_3v_3 + PW_4v_4w_4 + PW_5v_5w_5$$

where

PW_i , (i=1,5) are constant coefficients for each term. The adaptive coefficient feature is provided for these coefficients.

v_i, w_k , (i=1,5; k=4,5) are variables/parameters selected from the user dictionary.

Note that the FZ_i values in the TMOD/PERIOD table should not be greater than 1.0 or less than 0.0. Values of 1.0 ideally signify 100% modulation; values of 0.0, no modulation. (In

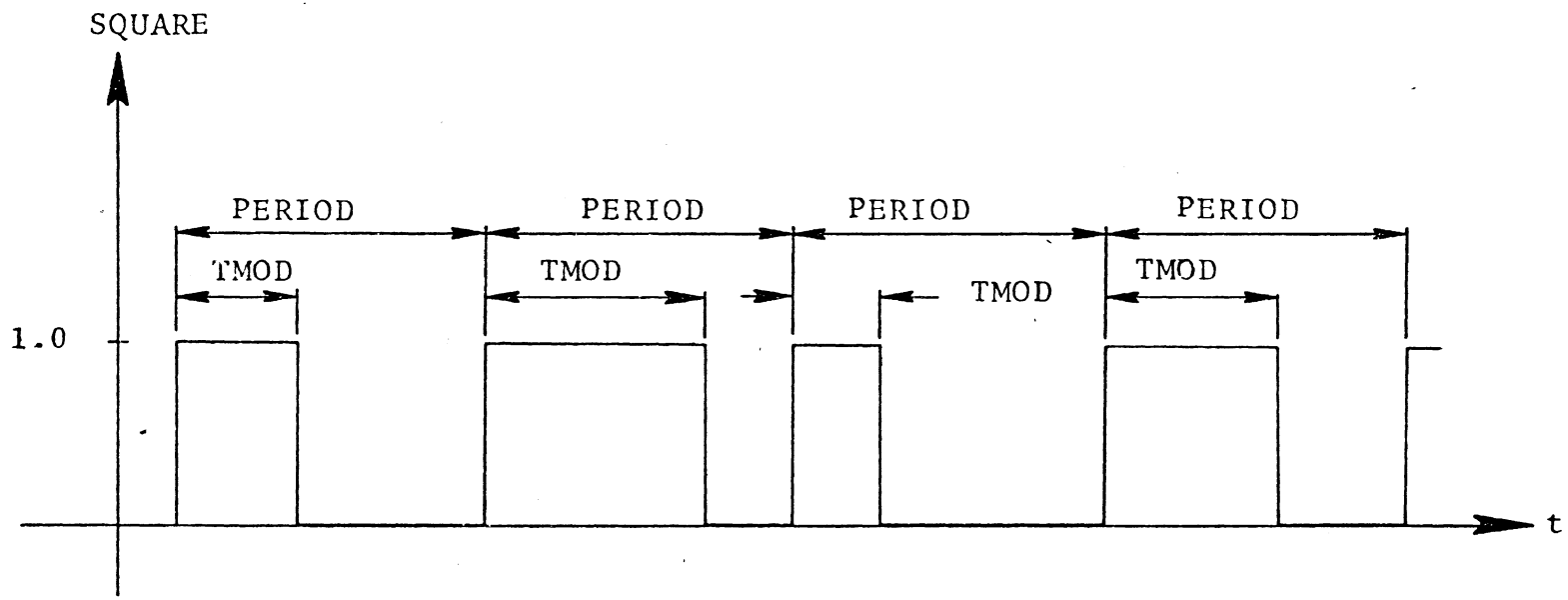

Figure 2.64. Pulse-width modulated square wave.

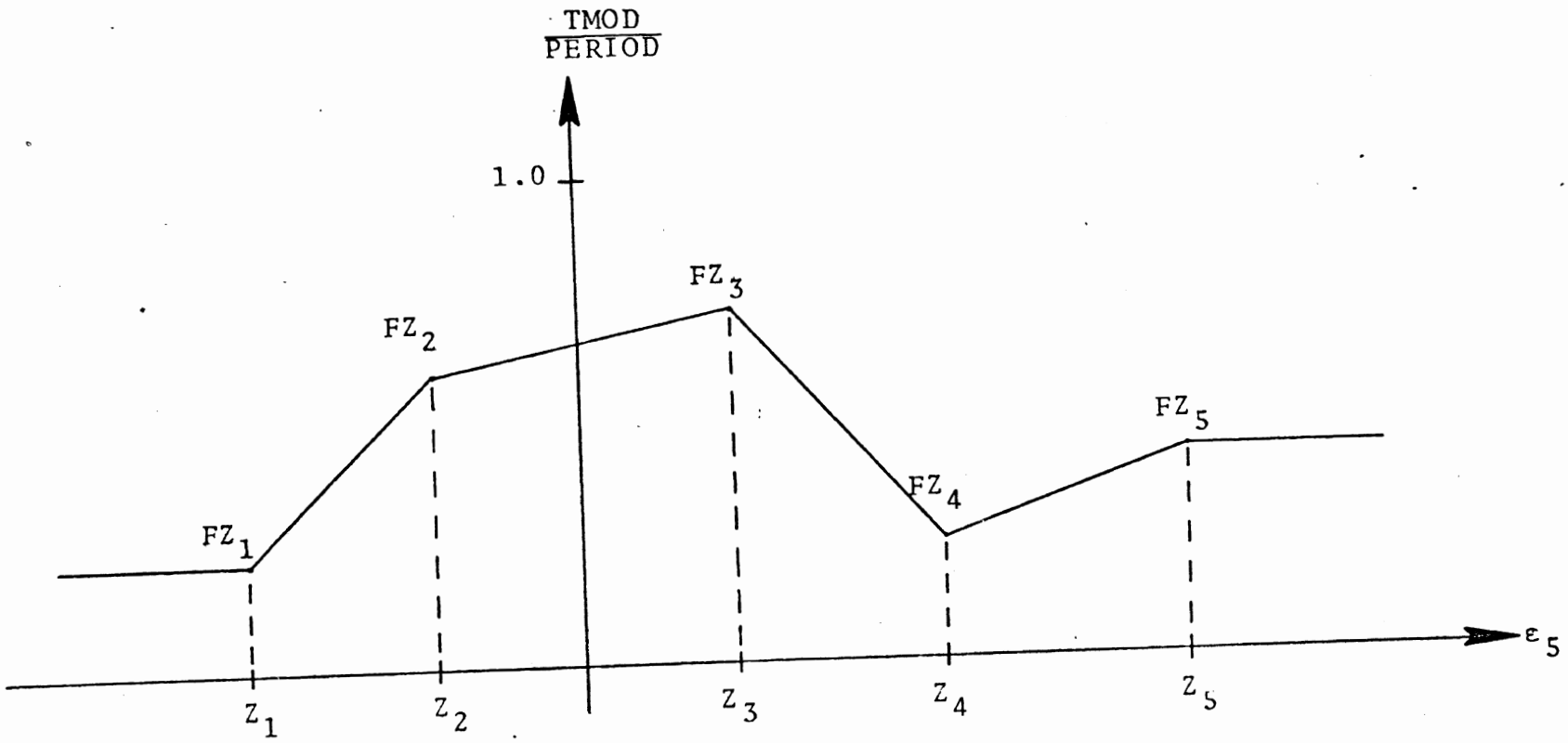

Figure 2.65. Pulse-width table.

actuality, the degree of modulation attainable depends on the simulation time step used and the period chosen for the square wave.)

Input data required for this option includes: (a) five pairs of FZ_i and Z_i, (b) PERIOD, and (c) coefficient values and variable I.D. codes used in the general form expression for ε_5. As before, a key for the pulse-width modulation option, IPWMKY, is read prior to any input for this option. IPWMKY values greater than or equal to 0 enable the option.

If desired, two additional sets of FZ_i values may be input. Each set is associated with a specific variable/parameter chosen by the user from the dictionary and a break-point for that variable/parameter. If the specified variable exceeds the break-point value for the given FZ_i set, that FZ_i set replaces the original or previous set used by the program. The purpose of this is to allow for some adaptive capability within the FZ_i table, if desired. The details of the numerical input for this adaptive option are explained in Section 2.5.7.

One-Shots

Three programmable one-shots are provided under this option and can be used for several different purposes. Two common uses are: (1) simulating time delay effects and (2) as auxiliary binary variables for use in any general purpose expressions. The three one-shots, as defined in this document, are binary variables having the numerical value of 1.0 or 0.0. These are available in the user dictionary under the names FOS1, FOS2, and FOS3.

The one-shots used in the program operate according to the following rule: If a trigger or input condition (inequality) changes from negative to positive, the one-shot will change its value from 0.0 to 1.0 for a fixed length of time, specified by the user, then return to 0.0. During a one-shot firing (1.0

value), the trigger input is disabled and cannot effect recurrent firings from this state. The one-shot is reset for another firing by two necessary occurrences: (1) the time duration of the present one-shot firing has been exceeded, followed by or concurrent with, (2) the trigger condition being negative. A trigger condition value of 0.0 is interpreted by the program as positive. See Figure 2.66.

The trigger condition is defined by the general form expression:

$$OS_1v_1 + OS_2v_2 + OS_3v_3 + OS_4v_4w_4 + OS_5v_5w_5 \geq 0$$

where

OS_i (i=1,5) are constant coefficients for each term and possess the adaptive coefficient feature.

v_i, w_k (i=1,5; k=4,5) are variables/parameters from the user dictionary.

Each one-shot trigger is programmable by a general form expression as shown above. The one-shot time durations are denoted as TOS1, TOS2, and TOS3 and are required as input for each one-shot used.

General Purpose Counter

This option allows the user to generate a count sequence by incrementing a counter by 1 every digital time step, if a particular inequality expression is greater than or equal to 0. The variable containing the count is called GPCNT and is in the user dictionary with the I.D. code 44. The general form expression is given by

$$GP_1v_1 + GP_2v_2 + GP_3v_3 + GP_4v_4w_4 + GP_5v_5w_5 \geq 0$$

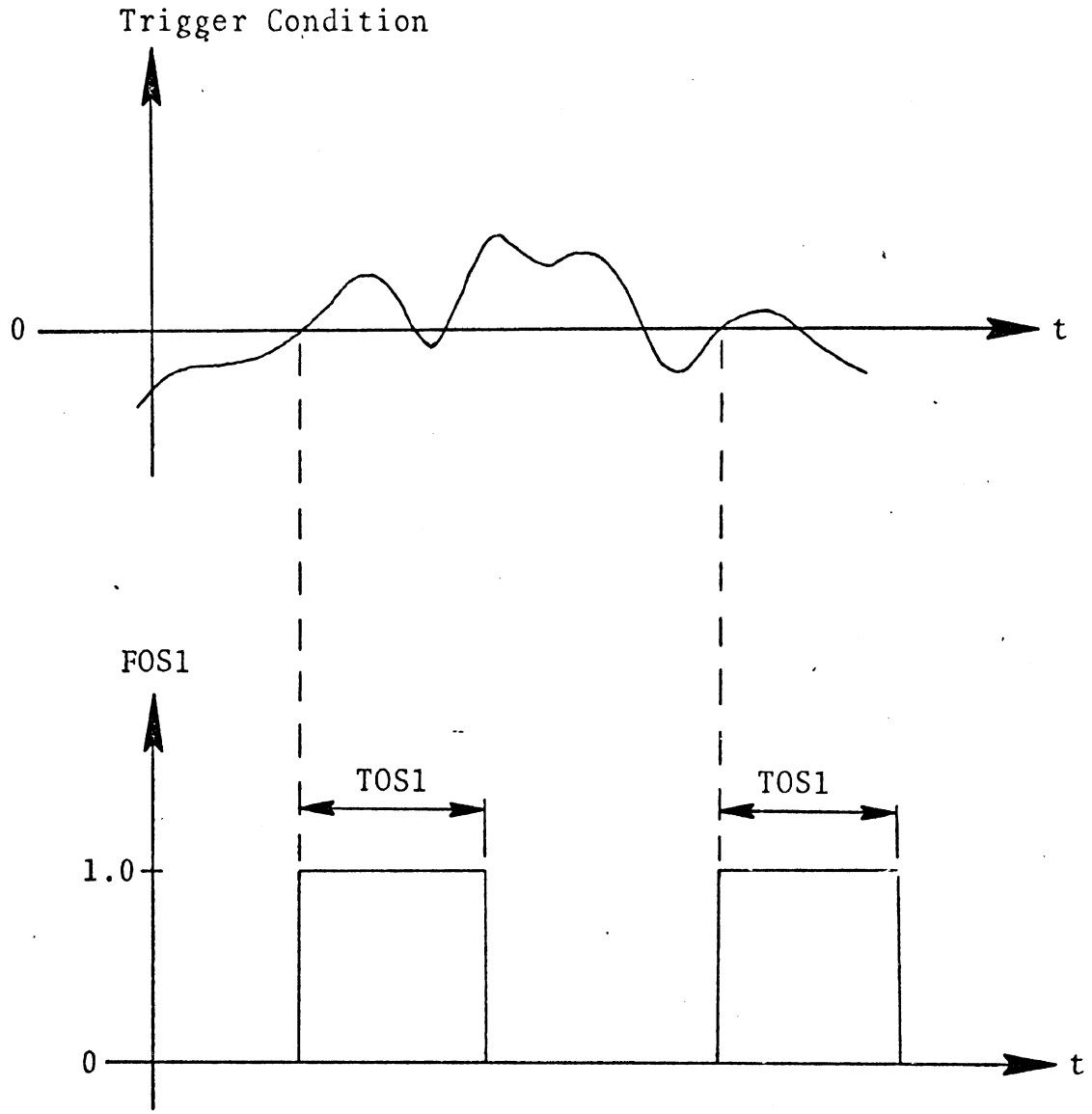

Figure 2.66. One-shct operation.

where

GP_i , (i=1,5) are constant coefficients for each term and can be adaptive.

v_i, w_k , (i=1,5; k=4,5) are variables/parameters from the user dictionary.

If the above inequality is satisfied, the GPCNT count is incremented <u>each time step</u>. If only a one count increment is desired whenever a particular condition is satisfied, then a one-shot could be fired for a time period equal to or less than the digital time step, with the general purpose counter incrementing itself every one-shot firing.

The above discussion applies whenever the logic sampling period is specified as less than or equal to the digital simulation time step. If the user specifies a larger logic sampling period (slower sampling rate), then the general purpose counter will be incremented only each <u>logic sampling period</u>.

The counter can be reset to zero by allowing the inequality expression to become less than or equal to -10,000.

2.5.7 <u>Input Data Format - General Form Expressions</u>. The most frequently occurring form encountered by the program user is the general form expression which appears in almost every program segment and special option. As discussed in Section 2.5.2, it has the form

$$C_1x_1 + C_2x_2 + C_3x_3 + C_4x_4y_4 + C_5x_5y_5$$

where

C_i (i=1,5) are the constant coefficients of each term.

x_i, y_k (i=1,5; k=4,5) are variables/parameters available in the user dictionary.

The user defines a given general form expression for the program by inputting three different pieces of information: (1) the number of terms in the expression required (1 to 5), (2) the variable I.D. codes corresponding to the x_i, y_k from the user dictionary for each variable/parameter used in constructing the expression, and (3) the coefficients of each term, C_i, used in the expression. The following data input sequence is what would be required for defining a general form expression:

NT	, number of terms	; I1 format
(I.D. code of x_1)		; F10.4 format
(I.D. code of x_2)		; F10.4 format
(I.D. code of x_3)		; F10.4 format
(I.D. code of x_4),(I.D. code of y_4)		; 2F10.4 format
(I.D. code of x_5),(I.D. code of y_5)		; 2F10.4 format
Coefficient of x_1		; F10.4 format
Coefficient of x_2		; F10.4 format
Coefficient of x_3		; F10.4 format
Coefficient of x_4y_4		; F10.4 format
Coefficient of x_5y_5		; F10.4 format

If NT is 5, the above format is used. If NT = M $\leq$ 5, only M I.D. code cards and M coefficient cards are required. Note that the second fields of the I.D. code cards are used only for the 4th and 5th terms. The 4th and 5th terms allow for quadratic representations, but can be linear if one of the two variable I.D. codes is selected as 1.0 (unity parameter).

Constant terms are represented by the unity parameter, 1.0, and the desired constant coefficient.

As an example, consider the general form expression, $\dot{x} - \omega - 10$. The required input for this would be:

3	number of terms required; I1 format
5.	variable I.D. codes from the user
3.	dictionary corresponding to $\dot{x}$, ω,
1.	and the constant; F10.4 format
1.	the C_i coefficients for each of
-1.	the terms; F10.4 format
-10.	

Adaptive Coefficient Input Format

As explained in Section 3.5.4, an adaptive coefficient feature exists to allow the coefficients appearing in the general form expressions to change value as a function of one or two variables from the user dictionary and their associated break-points. The third and fourth fields (columns 21-30, 31-40) of each variable I.D. input card are used to identify the variable(s) to which the corresponding term's coefficient is adaptive. Similarly, the fourth and fifth fields (columns 31-40, 41-50) of each coefficient card are used for specifying their associated break-points. The alternate coefficients are specified in the second and third fields (columns 11-20, 21-30) of each coefficient card. Consider the example from the previous section and suppose it was desired to alter the coefficient of $\dot{x}$, i.e., 1., to values of .5, and .2 according to the following rule:

$$\text{Coefficient of } \dot{x} = \begin{cases} 1.0 & \text{initial or nominal value} \\ 0.5 & \text{whenever } \dot{\omega} > 25 \text{ and } t \leq 2.0 \\ 0.2 & \text{if } t > 2.0 \end{cases}$$

The input required would now become:

```
3
5.        ,      ,      4.      ,      2.      ,
3.
1.
1.        , 0.5  , 0.2        , 25.        ,      2.0      ,
-1.
-10.
```

where the numbers 4. and 2. are the I.D. codes for $\dot{\omega}$ and t, respectively, and occur on the I.D. card for $\dot{x}$ in fields 3 and 4.

If only one adaptive variable is required, then field 4 of the I.D. code card and fields 3 and 5 of the coefficient card should not be used. Negative I.D. codes are permitted for the adaptive variables. This will cause the program to invert the sign of the adaptive variable. It would be used if one found it more convenient to have the adaptive condition, $u_{ij} > b_1$, interpreted as

$$-u_{ij} > -b_1 \quad , \quad (u_{ij} < b_1).$$

Reference was made in Section 2.5.4 to a numerical switch which allows the adaptive coefficient feature to be defined by Equation (2.55) rather than by Equation (2.54). If this optional

definition is desired, any negative number should be entered in field 2 (columns 11-20) of the variable I.D. card. Normally, this field is not used except when 4 or 5 terms are needed in a general form expression. In the case of a 4th or 5th term and the optional definition, the negative of the variable I.D. code should be used in field 2.

Pulse-Width Modulation Table - Adaptive Capability

The adaptive capability for the FZ_i table is implemented by the following numerical input procedure: If field 6 (column 51-60) of the first FZ_i card is non-zero, two more FZ_i cards are read. Each of these cards maintain the same five fields for the alternate FZ_i input. However, two additional fields are included (columns 51-60, 61-70) and are used to specify the adaptive variable I.D. code and its associated break-point for that card (alternate table). The second alternate card takes precedence over the first alternate in the event both break-points are exceeded. The following sample input is an example:

Z_i card:	-30.	-10.	0.	10.	50.		
1st FZ_i card:	0.	.10	.20	.50	.90	99.	
1st alternate FZ_i card:	0.	.05	.10	.25	.45	5.	50.
2nd alternate FZ_i card:	0.	.025	.05	.12	.22	5.	70.

The number 99. in field 6 for the 1st FZ_i card simply causes the next two cards to be read. Both alternate cards are adaptive in this case to the same variable, vehicle velocity (I.D. code 5; field 6). The respective break-points are 50. ft/sec and 70. ft/sec. The effect of this input is to cause the program to use table 3 for speeds above 70 ft/sec, table 2 for speeds between 70 ft/sec and 50 ft/sec, and table 1 for speeds less than 50 ft/sec. The adaptive variables do not have to be the same, as in the example.

Antilock Input Stream

Before any input data for the antilock subroutine is read, a key parameter (ILOCK) is read which determines whether or not any axle of the vehicle possesses an antilock system. If any or all axles do, the key parameter (ILOCK) in the input stream should be set to 01 (I2 format). If no antilock system at all is desired, ILOCK should be set to 0. No antilock data should follow ILOCK if ILOCK is 0. For ILOCK set to 01, the following key and input parameter discussion applies for each axle.

$IALOPT_i$ is a key which must be entered for each axle on the vehicle. A value of less than zero implies that a new antilock system follows. All of the parameters described below must be entered for this axle. A value of zero implies there will be no antilock for axle i. A positive value, for example, j, entered for $IALOPT_i$ implies that axle j will have the same system as axle 3. Note that i must be greater than j. Thus, if $IALOPT_3$ = 01, axle 3 will have the same antilock system as axle 1.

The numerical inputs for OPTION, the side-to-side option key, are as follows:

OPTION

01 => Worst Wheel

02 => Best Wheel

03 => Average Wheel

(I2 Format)

The following list defines all the input parameters available for each antilock system used (one or none per axle). The parameters required should be entered in the order given below.

It should be noted that this complete listing is presented to define the order and format of any required input data. The program, however, requires as input only that quantity of data needed to define a particular system.

Input	Description	Format
ILOCK	global antilock key	I2
$IALOPT_1$	IALOPT for axle 1	I2
$OPTION_1$	side-to-side option, axle 1	I2
$NOFF_1$	No. of 'OFF' inequalities to follow	I1
M1	No. of terms in 1st inequality	I1
ID_1 . . . ID_{M1}	M1 variable I.D. code cards for logic inequality 1	4F10.4
$C_{1,1}$ . . . $C_{1,M1}$	M1 coefficient cards	5F10.4
M2	No. of terms in 2nd inequality	I1
ID_1 . . . ID_{M2}	M2 variable I.D. code cards for logic inequality 2	4F10.4
$C_{2,1}$ . . . $C_{2,M2}$	M2 coefficient cards	5F10.4
M_3	No. of terms in 3rd inequality	I1

For $NOFF_1$ inequality expressions, $NOFF_1 \leq 4$.

NON_1	No. of 'ON' inequalities to follow	I1
M5	No. of terms in 5th inequality	I1
ID_1 ⋮ ID_{M5}	M5 variable I.D. code cards for logic inequality 5	4F10.4
$C_{5,1}$ ⋮ $C_{5,M5}$	M5 coefficient cards	5F10.4
M6 ⋮	No. of terms in 6th inequality ⋮	I1

For NON_1 inequality expressions, $NON_1 \leq 4$.

$\tau_1, \tau_2, \tau_3, \tau_4$	Logic time delays	4F10.4
IPKEY	Pressure modulator key	I1
N1	No. of terms in ε_1 expression (IPKEY=0,2)	I1
ID_1 ⋮ ID_{N1}	N1 variable I.D. code cards	4F10.4
H_1 ⋮ H_{N1}	N1 coefficient cards	5F10.4

N2	No. of terms in the ε_2 expressions	I1
ID_1 . . . ID_{N2}	N2 variable I.D. code cards	4F10.4
G_1 . . . G_{N2}	N2 coefficient cards	5F10.4
X_1 X_2	ε_1 break-points	2F10.4
X_3 X_4	ε_2 break-points	2F10.4
PFE1 PFE2 PFE3	exponential fall rates	3F10.4
PRE1 PRE2 PRE3	exponential rise rates	3F10.4
N3	No. of terms in ε_3 expression (IPKEY=1,2)	I1
ID_1 . . . ID_{N3}	N3 variable I.D. code cards	4F10.4
R_1 . . . R_{N3}	N3 coefficient cards	5F10.4
N4	No. of terms in ε_4 expression	I1
ID_1 . . . ID_{N4}	N4 variable I.D. code cards	4F10.4

S_1 ⋮ S_{N4}	N4 coefficient cards	5F10.4
X_5 X_6	ε_3 break-points	2F10.4
X_7 X_8	ε_4 break-points	2F10.4
PFL1 PFL2 PFL3	linear fall rates	3F10.4
PRL1 PRL2 PRL3	linear rise rates	3F10.4
τ_{ON}, τ_{OFF}	pressure modulator time delays	2F10.4
τ_W, τ_{WD}	wheel rate, acceleration time constants	2F10.4
OP_{12}, OP_{23}, OP_{34}	logical operator switches	3I1
OP_{56}, OP_{67}, OP_{78}	logical operator switches	3I1
IPDKEY	treadle pressure modulator key	I2
N5	No. of terms for PDRISE	I1
ID_1 ⋮ ID_{N5}	N5 variable I.D. code cards	4F10.4
W_1 ⋮ W_{N5}	N5 coefficient cards	5F10.4
N6	No. of terms in PDFALL expression	I1
ID_1 ⋮ ID_{N6}	N6 variable I.D. code cards	4F10.4

V_1 . . . V_{N6}	N6 coefficient cards	5F10.4
IPWMKY	pulse-width modulation key	I2
PERIOD	period of pulse-width modulated square wave	F10.4
N7	No. of terms in ε_5 expression	I1
ID_1 . . . ID_{N7}	N7 variable I.D. code cards	4F10.4
PW_1 . . . PW_{N7}	N7 coefficient cards	5F10.4
Z_1, Z_2, Z_3, Z_4, Z_5	$\frac{TMOD}{PERIOD}$ table break-points	5F10.4
$FZ_1, FZ_2, FZ_3, FZ_4, FZ_5$	$\frac{TMOD}{PERIOD}$ table input	6F10.4
	alternate/adaptive FZ_i input (see Section)	7F10.4 7F10.4
IOSKEY	one-shot option key	I2
N1	No. of terms for 1st one-shot expression	I1
ID_1 . . . ID_{N1}	N1 variable I.D. code cards	4F10.4

OS_1 . . . OS_{N1}	N1 coefficient cards	5F10.4
TOS1	time duration of 1st one-shot	F10.4
N2	No. of terms in 2nd one-shot expression	I1
ID_1 . . . ID_{N2}	N2 variable I.D. code cards	4F10.4
OS_1 . . . OS_{N2}	N2 coefficient cards	5F10.4
TOS2	time duration of 2nd one-shot expression	F10.4
N3	No. of terms in 3rd one-shot expression	I1
ID_1 . . . ID_{N3}	N3 variable I.D. code cards	4F10.4
OS_1 . . . OS_{N3}	N3 coefficient cards	5F10.4
TOS3	time duration of 3rd one-shot	F10.4

(N3 and/or N2 must be entered (as 0) if only the first or second one-shots are used.)

IGPKEY	general purpose counter key	I2
NG	No. of terms in general purpose counter expression	I1
ID_1 . . . ID_{NG}	NG variable I.D. code cards	4F10.4
GP_1 . . . GP_{NG}	NG coefficient cards	5F10.4
TSMPLE	control logic sampling period	F10.4
$IALOPT_2$	IALOPT for axle 2	I2
$OPTION_2$	OPTION for axle 2	I2
	Same input format as for axle 1	
$IALOPT_3$	IALOPT for axle 3	I2
$OPTION_3$	OPTION for axle 3	I2
	Same input format as for axle 1	
. . .	. . .	

End of antilock input

TINC
TRUCK

The following section provides two example problems and their associated input lists. Appendix E contains three antilock data sets which exhibit pressure and wheel slip characteristics similar to those depicted in Figures E.1 through E.3.

Example Problems

EXAMPLE 1.

Suppose an antilock system possesses the following features: (1) a wheel sensor time delay effect of 10 ms. and another 20 ms. delay in the derivation of wheel acceleration; (2) control logic which generates an "OFF" signal once the wheel acceleration falls below -50.0 ft/sec^2 and an "ON" signal for wheel accelerations greater than -10.0 ft/sec^2; (3) pressure modulator time delays of 40 ms. for "OFF" signals and 60 ms. for "ON" signals. The supposed exponential pressure rates are functions of wheel acceleration defined as follows:

$$\text{Pressure Fall Rate} \equiv \begin{cases} (0.1)^{-1} = 10.0 \text{ for } \dot{\omega} \leq -100 \text{ ft/sec}^2 \\ (0.2)^{-1} = 5.0 \text{ for } \dot{\omega} > -100 \text{ ft/sec}^2 \end{cases}$$

$$\text{Pressure Rise Rate} \equiv \begin{cases} (0.2)^{-1} = 5.0 \text{ for } \dot{\omega} \leq 50 \text{ ft/sec}^2 \\ (0.1)^{-1} = 10.0 \text{ for } \dot{\omega} > 50 \text{ ft/sec}^2 \end{cases}$$

The following choice of input parameters would satisfy the above antilock system:

$\tau_\omega = 0.01$

$\tau_{\omega d} = 0.02$

$C_{11} = -1.0$

$C_{12} = -50.0$ $\rightarrow F_1 = -\dot{\omega} - 50.0 \geq 0$

$C_{51} = 1.0$

$C_{52} = 10.0$ $\rightarrow F_5 = \dot{\omega} + 10.0 \geq 0$

I.D. Code for $\dot{\omega}$ = 4.

I.D. Code for 1.0 = 1.

$\tau_1 = \tau_3 = \tau_4 = 0.0$

$\tau_2 = 0.2$

$H_1 = 1.0$

$H_2 = 100.0$ $\rightarrow \varepsilon_1 = \dot{\omega} + 100$

$X_1 = -10000.0$

$X_2 = 0.0$

PFE1 = 10.0

PFE2 = 5.0

$G_1 = 1.0$

$G_2 = -50.0$ $\rightarrow \varepsilon_2 = \dot{\omega} - 50.0$

$X_3 = -10000.0$

$X_4 = 0.0$

$PRE1 = 5.0$

$PRE2 = 10.0$

$OP_{12} = OP_{23} = OP_{34} = OP_{56} = OP_{67} = OP_{78} =$ either 0 or 1

$\tau_{ON} = 0.06$

$\tau_{OFF} = 0.04$

The following input list would be required:

01					ILOCK
-1					IALOPT
01					worst-wheel side-to-side option
1					NOFF1
2					M1
4.					I.D. code for $\dot{\omega}$
1.					I.D. code for 1.0
-1.					1st term coefficient, C_{11}
-50.					2nd term coefficient, C_{12}
1					NON_1
2					M5
4.					I.D. code for $\dot{\omega}$
1.					I.D. code for 1.0
1.					1st term coefficient, C_{51}
10.					2nd term coefficient, C_{52}
0.	0.	0.	0.		τ_i
0					IPKEY
2					N1
4.					I.D. for $\dot{\omega}$
1.					I.D. for 1.0
1.		ε_1			1st term coefficient for ε_1
100.					2nd term coefficient for ε_1
2					N2
4.					I.D. for $\dot{\omega}$
1.		ε_2			I.D. for 1.0
1.					1st term coefficient for ε_2
-50.					2nd term coefficient for ε_2
-10000.		0.			X_1, X_2
-10000.		0.			X_3, X_4

10.	10.	5.	PFE1, PFE2, PFE3
5.	5.	10.	PRE1, PRE2, PRE3
.06	.04		τ_{ON}, τ_{OFF}
.01	.02		τ_{W}, τ_{WD}
000			OP_{12}, OP_{23}, OP_{34}
000			OP_{56}, OP_{67}, OP_{78}
-1			IPDKEY
-1			IPWMKY
-1			IOSKEY
-1			IGPKEY
.0001			TSMPLE
01			$IALOPT_2$
01			$IALOPT_3$
.			.
.			.
.			.
TINC			
TRUCK			

EXAMPLE 2.

Simulation of an antilock system having the following features:

Wheel Sensor: $\tau_\omega \quad \tau_{\omega d} = .010$ seconds

Control Logic:

OFF signal given by

$$F_1 = \dot{x} - \omega - 14 \geq 0, \quad \text{for } \dot{X} > 50 \text{ ft/sec}$$
$$= \dot{x} - \omega - 11 \geq 0, \quad \text{for } \dot{X} \leq 50$$

<u>AND</u>

$$F_2 = -\dot{\omega} - 12 \geq 0$$

<u>OR</u>

$$F_3 = \text{SLIP} - .50 \geq 0$$

ON signal generated when

$$F_5 = -\dot{x} + \omega + 10 \geq 0$$

<u>AND</u>

$$F_6 = \dot{\omega} - 20. \geq 0$$

<u>OR</u>

$$F_7 = \dot{\omega} - 250. \geq 0$$

Pressure Modulator:

a) τ_{ON} = .015 sec. ; τ_{OFF} = .010 sec.

b) One exponential fall rate of 14. sec^{-1}.

c) One exponential rise rate of 14. sec^{-1}.
and one linear rise rate of 45. sec^{-1}.

The exponential and linear pressure rise regions are determined by a decaying time ramp from the maximum pressure in the previous cycle. For pressure below this time ramp, the pressure rise is exponential; for pressure greater than the time ramp, the pressure rise is linear (see Figure 2.67). The decaying time ramp can be written as

$$PMAX1 - 85. \ (t - TPMAX1)$$

where

PMAX1 is the maximum pressure in the last cycle

t is time

TPMAX1 is the time of the maximum pressure in the last cycle

and 85. is the rate of decay.

By subtracting the above expression from brake pressure, P, the ε_2 and ε_4 general expressions become:

$$\varepsilon_2 = P - PMAX1 + 85\ T - 85\ TPMAX1$$

and

$$\varepsilon_4 = P - PMAX1 + 85\ T - 85\ TPMAX1,$$

the switching point occurring at $\varepsilon_2 = \varepsilon_4 = 0$. Therefore, the desired rise characteristic can be simulated by the following set of pressure inputs:

$$X_3 = X_4 = X_7 = X_8 = 0$$

$$PRE1 = PRE2 = 14. \quad , \quad PRE3 = 0$$

$$PRL1 = PRL2 = 0. \quad , \quad PRL3 = 45.$$

The following input list would be required:

01	ILOCK
-1	$IALOPT_1$
01	$OPTION_1$
3	$NOFF_1$
3	M1
5.	
3.	
1. , , 5. , ,	
1.	C_{11}
-1.	C_{12}
-11. , -14. , , 50., ,	C_{13}
2	M2
4.	
1.	
-1.	C_{21}
-120.	C_{22}
2	M3
34.	
1.	
1.	C_{31}
-.50	C_{32}
3	NON_1
3	M5
5.	
3.	
1.	

-1.				C_{51}
1.				C_{52}
10.				C_{53}
2				M6
4.				
1.				
1.				C_{61}
-20.				C_{62}
2				M7
4.				
1.				
1.				C_{71}
-250.				C_{72}
0.	0.	0.	0.	τ_i
2				IPKEY
1				N1
1.				ε_1
5.				
4				N2
35.				ε_2
27.				
2.				
21.	1.			
1.				
-1.				
85.				
85.				

0.	0.			X_1, X_2
0.	0.			X_3, X_4
14.	14.	14.		PFE1, PFE2, PFE3
14.	14.	0.		PRE1, PRE2, PRE3
1				N3
1.			ε_3	
5.				
4				N4
35.			ε_4	
27.				
2.				
21.	1.			
1.				
-1.				
85.				
85.				
0.	0.			X_5, X_6
0.	0.			X_7, X_8
0.	0.	0.		PFL1, PFL2, PFL3
0.	0.	45.		PRL1, PRL2, PRL3
.015	.010			τ_{ON}, τ_{OFF}
.010	.010			τ_{ω} , $\tau_{\omega D}$
100				OP_{12}, OP_{23}, OP_{34}
100				OP_{56}, OP_{67}, OP_{78}
-1				IPDKEY
-1				IPWMKY
-1				IOSKEY

-1	IGPKEY
.0001	TSMPLE
01	$IALOPT_2$
01	$IALOPT_3$
.	.
.	.
.	.
.	.
TINC	
TRUCK	

Output-Echo Format

Figures 2.68 through 2.71 show an example output-echo from the antilock subroutine. The first output page is simply the user dictionary of variables/parameters. The succeeding pages represent a computer echo of the input. The "First" and "Second Adaptive Value" columns refer to the alternate coefficients available with the adaptive coefficient feature. The "First" and "Second Adaptive Variable" columns echo the variable I.D. codes for the two adaptive variables, while the columns labeled "First" and "Second Break-Point" contain their associated break-points. If the secondary adaptive coefficient definition (Figure 2.59) is used, the word "AND" appears between the First and Second Adaptive Variable columns in the output echo for that coefficient. Any input not associated with a general form expression is listed under "Non-Adaptive Antilock Parameters."

The echo shown in Figures 2.68 through 2.71 is for the second antilock data set of Appendix E.

DICTIONARY OF ANTI-LOCK VARIABLES/PARAMETERS AVAILABLE TO USER.

VARIABLE I.D.	DESCRIPTION	VARIABLE I.D.	DESCRIPTION
1	1.0	45	WMAX1
2	TIME	46	WMAX2
3	OMEGA	47	TWMAX1
4	OMEGADOT	48	TWMAX2
5	XDOT	49	WMIN
6	XDDOT	50	TWMIN
7	POFF1	51	TPMAX2
8	POFF2	52	TPMIN2
9	PON1		
10	PON2		
11	TOFF1		
12	TON1		
13	XDOFF		
14	XDON		
15	WOFF		
16	WON		
17	WDOFF		
18	WDON		
19	WDMAX		
20	WDMIN		
21	TPMAX1		
22	TPMIN1		
23	WLOCK		
24	TLOCK		
25	SLON		
26	SLOFF		
27	PMAX1		
28	PMAX2		
29	PMIN1		
30	PMIN2		
31	PD		
32	ON		
33	TMOD		
34	SLIP		
35	P		
36	CYCNT		
37	SQUARE		
38	SQUARN		
39	TOFF2		
40	TON2		
41	POS1		
42	POS2		
43	POS3		
44	GPCNT		

Figure 2.68. Antilock output echo.

*** ANTI-LOCK SUBROUTINE INPUT PARAMETER TABLE --- AXLE 1. ***

SYMBOL	DESCRIPTION	INITIAL VALUE	FIRST ADAPTIVE VALUE	SECOND ADAPTIVE VALUE	INITIAL VALUE VARIABLE	FIRST ADAPTIVE VARIABLE	SECOND ADAPTIVE VARIABLE	FIRST BREAK-PT	SECOND BREAK-PT
INEQUALITY EXPRESSION: 1									
C(1)	COEFFICIENT(1)	-1.0000			3				
C(2)	COEFFICIENT(2)	1.0000			45				
C(3)	COEFFICIENT(3)	-20.0000	-10.0000		2	6		-16.000	
C(4)	COEFFICIENT(4)	20.0000	10.0000		47, 1	6		-16.000	
C(5)	COEFFICIENT(5)	-4.0000	-7.0000		1, 1	36		0.500	
INEQUALITY EXPRESSION: 2									
C(1)	COEFFICIENT(1)	-1.0000			4				
C(2)	COEFFICIENT(2)	-70.0000			1				
INEQUALITY EXPRESSION: 3									
C(1)	COEFFICIENT(1)	1.0000			42				
C(2)	COEFFICIENT(2)	-0.1000			1				
C(3)	COEFFICIENT(3)	1000.0000			23				
INEQUALITY EXPRESSION: 5									
C(1)	COEFFICIENT(1)	1.0000			3				
C(2)	COEFFICIENT(2)	-1.0000			45				
C(3)	COEFFICIENT(3)	20.0000	10.0000		2	6		-16.000	
C(4)	COEFFICIENT(4)	-20.0000	-10.0000		47, 1	6		-16.000	
C(5)	COEFFICIENT(5)	7.0000			1, 1				
INEQUALITY EXPRESSION: 6									
C(1)	COEFFICIENT(1)	1.0000			4				
C(2)	COEFFICIENT(2)	-20.0000			1				
INEQUALITY EXPRESSION: 7									
C(1)	COEFFICIENT(1)	1.0000			42				
C(2)	COEFFICIENT(2)	-0.1000			1				

EPSILION 1:

Figure 2.69. Antilock output echo.

```
  F(1)            COEFFICIENT(1) .        5.0000                          1

EPSILION 2:

  G(1)            COEFFICIENT(1)          1.0000                         35
  G(2)            COEFFICIENT(2)         -1.0000                         27
  G(3)            COEFFICIENT(3)        200.0000     100.0000            2          36                1.500
  G(4)            COEFFICIENT(4)       -200.0000    -100.0000           21,  1      36                1.500

EPSILION 3:

  R(1)            COEFFICIENT(1)          5.0000                          1

EPSILION 4:

  S(1)            COEFFICIENT(1)          1.0000                         35
  S(2)            COEFFICIENT(2)         -1.0000                         27
  S(3)            COEFFICIENT(3)        200.0000     100.0000            2          36                1.500
  S(4)            COEFFICIENT(4)       -200.0000    -100.0000           21,  1      36                1.500

ONE-SHOT 1:

OS1(1)            COEFFICIENT(1)         -1.0000                          3
OS1(2)            COEFFICIENT(2)          1.0000                         45
OS1(3)            COEFFICIENT(3)        -20.0000     -10.0000            2           6              -16.000
OS1(4)            COEFFICIENT(4)         20.0000      10.0000           47,  1       6              -16.000
OS1(5)            COEFFICIENT(5)         -6.0000                          1,  1

ONE-SHOT 2:

OS2(1)            COEFFICIENT(1)          0.0                             1
OS2(2)            COEFFICIENT(2)         -0.1000                          1
OS2(3)            COEFFICIENT(3)         50.0000                         41
OS2(4)            COEFFICIENT(4)          1.0000                         41,  4

** NON-ADAPTIVE ANTI-LOCK PARAMETERS. **

 TAU1             LOGIC TIME DELAY         0.0
 TAU2                   "                  0.0
 TAU3                   "                  0.0
 TAU4                   "                  0.0
 X1               EPSILON 1 BREAK-PT       0.0
 X2                     "                 50.0000
 X3               EPSILON 2 BREAK-PT      -5.0000
 X4                     "                  2.5000
 PFE1        EXP. PRESSURE FALL RATE      12.5000
 PFE2                   "                 12.5000
 PFE3                   "                 12.5000
 PRE1        EXP. PRESSURE RISE RATE      14.0000
 PRE2                   "                 14.0000
 PRE3                   "                  0.0
 X5               EPSILON 3 BREAK-PT       0.0
 X6                     "                 50.0000
 X7               EPSILON 4 BREAK-PT      -5.0000
```

Figure 2.70. Antilock output echo.

```
X8                    "                    2.5000
PFL1        LIN. PRESSURE FALL RATE        0.0
PFL2                  "                    0.0
PFL3                  "                    0.0
PRL1        LIN. PRESSURE RISE RATE        0.0
PRL2                  "                    0.0
PRL3                  "                   40.0000
TAUON       PRESSURE-ON TIME DELAY         0.0150
TAUOFF      PRESSURE-OFF TIME DELAY        0.0100
TAUW        TIME CONSTANT-WHEEL RATE       0.0100
TAUWD       TIME CONSTANT-WHEEL ACCEL.     0.0100
OP12        LOGICAL OPERATOR SWITCH             1
OP23                  "                         0
OP34                  "                         0
OP56        LOGICAL OPERATOR SWITCH             1
OP67                  "                         0
OP78                  "                         0
TOS1        ONE-SHOT TIME DURATION         0.0200
TOS2        ONE-SHOT TIME DURATION         0.0200
TSAMPLE     ANTI-LOCK SAMPLING RATE        0.0010
OPTION      SIDE-TO-SIDE                        1

*** AXLE 2 WILL HAVE THE SAME ANTI-LOCK SYSTEM AS AXLE 1

*** AXLE 3 WILL HAVE THE SAME ANTI-LOCK SYSTEM AS AXLE 1

    *** END INPUT ***
```

Figure 2.71. Antilock output echo.

2.6 Rough Road

The preceding subsections of Section 2 have discussed all the major areas of the Phase III simulations. The programs also contain a variety of minor options. These include:

1. Rough Road
2. Mechanical Actuation of the Parking Brake
3. Brake Torque Applied to the Drive Shaft
4. Proportioning Valves

Of this list, the last three options have been documented in the Phase I report [1]. The rough road option will be covered here.

In the Phase III program, the user is given the option of simulating vehicle performance on either a smooth or rough road. As was discussed in Section 2.1, the "Rough Road" option may be called into play by the entry of a -1 value for the ROAD KEY. A smooth road is employed by the simulation if the KEY is deleted from the input flow.

A rough road may be of any profile chosen by the user. To input the desired road profile, the user must modify the ROAD subroutine appropriately. The ROAD subroutine subprogram which has been supplied to the user is listed in Figure 2.72. Notice that there are three entry points to the subprogram, viz.:

1. the SUBROUTINE ROAD statement
2. the ENTRY ROADS statement
3. the ENTRY ROAD2 statement

The SUBROUTINE ROAD and ENTRY ROADS statements are both "initialization" entry points which come into play prior to the actual calculation of vehicle performance. The ENTRY ROAD2 statement is the active entry point which is used during simulation. The initialization portion of the program

```
      SUBROUTINE ROAD(A1,A2,A3,A4,A5,A6,A7,A8,BB1,BB2)
      DIMENSION CNST(9),ROADZ(9)
      IW=2
      ICOUNT=1
      RETURN
      ENTRY ROADS(D1,D2)
      GO TO (1,2,3,4),ICOUNT
    1 CNST(1)=A1
      CNST(2)=-A2+D1
      CNST(3)=-A2-D2
      GO TO 5
    2 CNST(IW)=-A2+BB1-A3-A4+D1
      CNST(IW+1)=-A2+BB1-A3-A4-D2
      GO TO 5
    3 CNST(IW)=-A2+BB1-A5-A8-BB2+D1
      CNST(IW+1)=-A2+BB1-A5-A8-BB2-D2
      GO TO 5
    4 CNST(IW)=-A2+BB1-A5-A6-A7-A8+D1
      CNST(IW+1)=-A2+BB1-A5-A6-A7-A8-D2
    5 IW=IW+1
      IF (D2 .NE. 0.) IW=IW+1
      ICOUNT=ICOUNT+1
      RETURN
      ENTRY ROAD2(X,ROADZ,KAXLE)
      DO 1001 I=1,KAXLE
      AXLEX=X+CNST(I)
      IF (AXLEX .GT. 45.) ROADZ(I)=.1
      IF (AXLEX .GT. 50.) ROADZ(I)=0.
 1001 CONTINUE
      RETURN
      END
```

Figure 2.72. Subroutine ROAD listing.

establishes the relative positions of the various axles of the vehicle with respect to the vehicle's sprung mass c.g. (the tractor sprung mass for articulated vehicles). These relative positions are expressed by the values of the parameters CNST(I) where I=1,2... no. of axles on the vehicle, counting from front to rear. (If an axle is forward of the c.g., its CNST value is positive; if aft, its CNST is negative.)

In the active portion of the program, the simulation passes the longitudinal position of the sprung mass c.g., X (in earth coordinates), to ROAD. With this value, the values of the CNST parameter, and the user-supplied road profile, ROAD, calculates the vertical height of the road under each axle, i.e., ROADZ(I) where I=1,2,... no. of axles on the vehicle, counting from front to rear.

To input the desired road profile, the user need only provide a statement (or statements) which describe the profile in the form:

ROADZ(I) = f(AXLEX)

where

ROADZ(I) is the vertical dimension of the road in feet with the positive direction upwards

AXLEX is the horizontal dimension of the road in feet with the positive direction forward and the zero position directly below the sprung mass c.g. (of the tractor for articulated vehicles) at time = zero.

The correct position for such a statement (or statements) is shown by the shaded area of Figure 2.72. <u>This shaded area is the only portion of the supplied program which the user need alter</u>.

Two examples of road profiles and the appropriate "user-supplied" statements appear in Figures 2.73 and 2.74. Figure 2.73 indicates the road profile defined in the ROAD program supplied (Figure 2.72). A road of sinusoidal profile is shown in Figure 2.74.

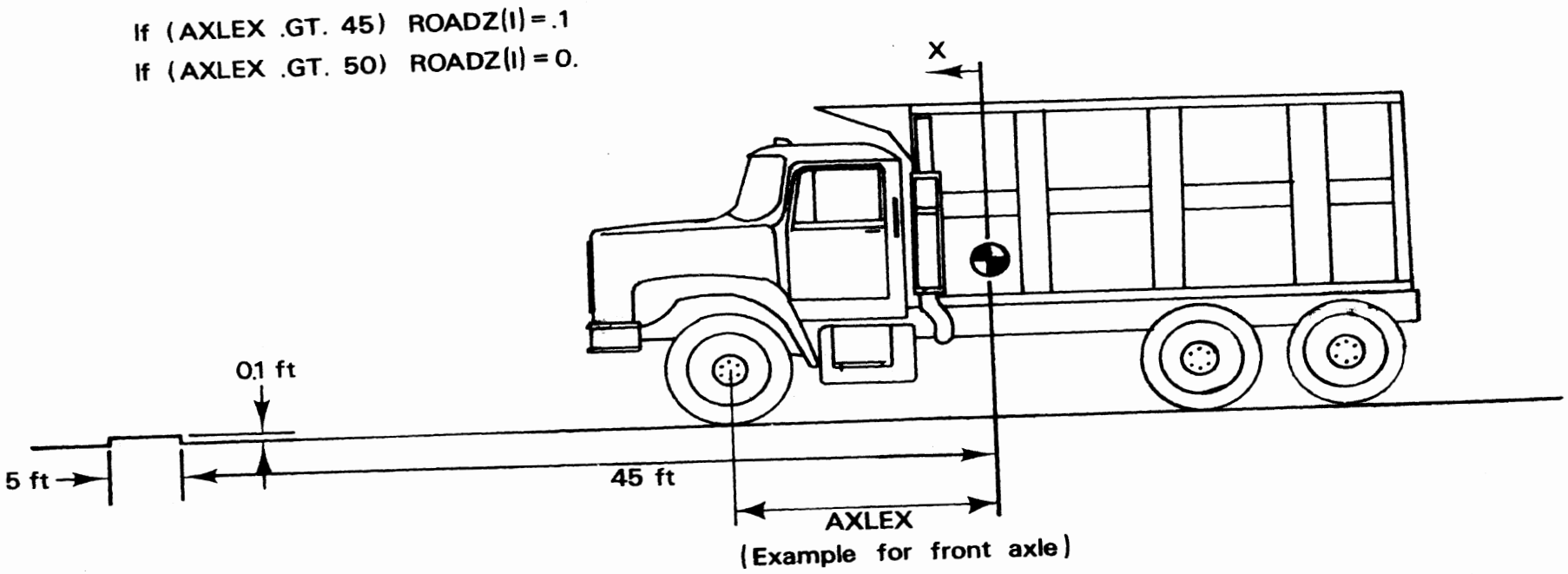

Figure 2.73. Step disturbance ROAD example.

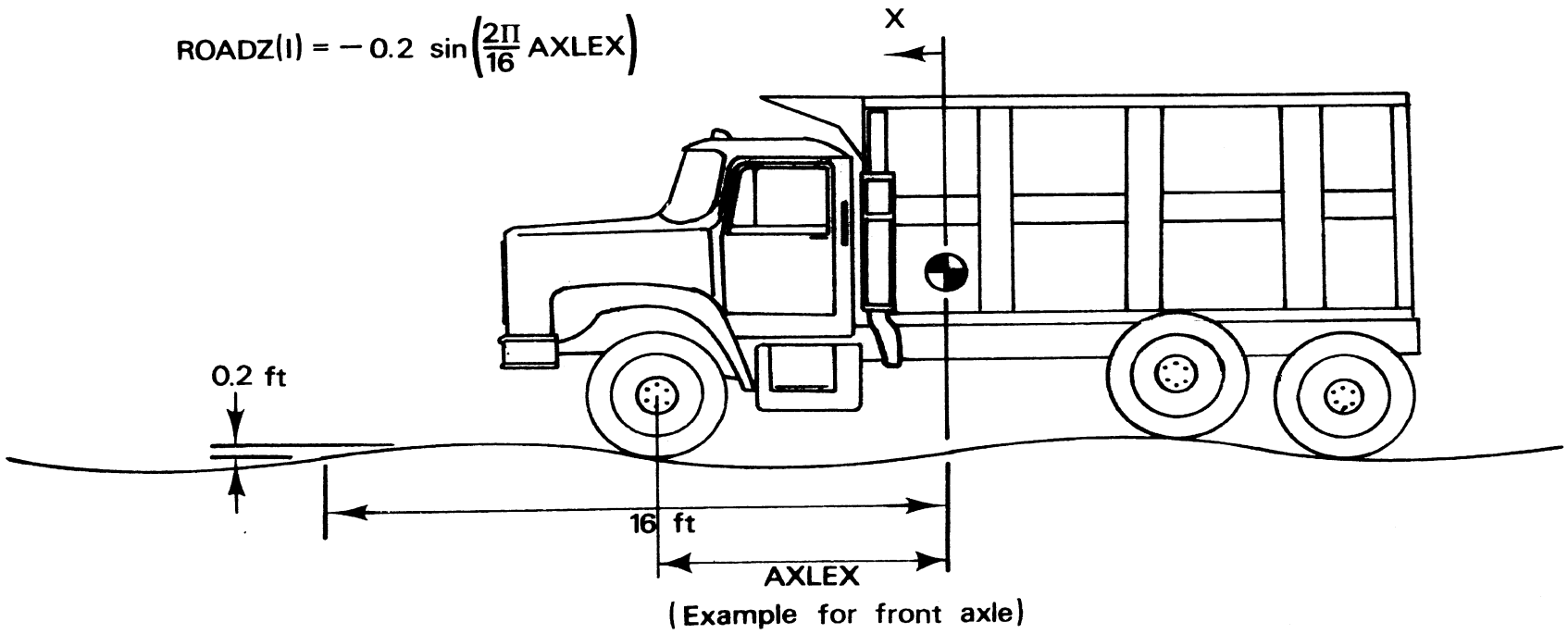

Figure 2.74. Sine wave ROAD example.

3.0 APPLICATIONS, CONCLUSIONS, AND RECOMMENDED RESEARCH

A computer simulation for analyzing the braking performance of commercial vehicles equipped with antilock systems was described in detail in Section 2 of this report. The use of this simulation requires an extensive set of parametric data to represent a motor truck. Apparatus and techniques for measuring the needed parametric data are described in References 1, 2, 6 through 11, and 15 through 17. In particular, methods and special devices for measuring (1) the shear force performance of truck tires, (2) the torque response of pneumatic brakes, and (3) the pressure modulation characteristics of antilock braking systems are presented in References 15, 16, and 17, respectively.

The comprehensiveness of the mathematical model used in this simulation can be either an advantage or a disadvantage, depending upon the application. Clearly, the simulation can be used to investigate the influence of changes in suspension design, brake characteristics, tire properties, and antilock system design on the braking performance of a specific vehicle. However, simpler vehicle models [24, 30] requiring much less parametric data, can be used to advantage in certain applications where general results or trends are of interest.

In the remainder of this section three topics are discussed: (1) application studies based on the capabilities of this simulation, (2) conclusions concerning this approach to the simulation (prediction) problem, and (3) areas for further research investigations.

3.1 Applications

An initial version of this computer program has been used to aid in predicting compliance with FMVSS 121. Reference 14 presents data showing good agreement between simulation and test results for a truck which was equipped with an antilock system to study braking performance in the tests specified in FMVSS 121. Certainly, the prime application of this computer program has been to aid in developing and evaluating vehicles that will meet the requirements of FMVSS 121.

Since the prediction of the braking performance of a current model of commercial vehicles is a complex problem with many interacting elements, it is very difficult to be sure that the simulation will perform accurately in every case under every set of circumstances. Until the simulation has been used successfully in an extensive number of well understood cases, the user should proceed with caution. To start with, it is envisioned that simulation and test results for a baseline configuration of a particular vehicle model will be obtained and compared. After all significant discrepancies between simulation and test results have been analyzed and corrected to obtain satisfactory agreement between simulation and test, the simulation may be used to predict the influence of changes in vehicle components or service factors (loading, inflation pressure, wear, etc.) on braking performance. (An example of the use of the procedure described above is given in Reference 29.)

Since trucks are often tailored to the buyer's needs and desires, many different configurations of a basic vehicle type may be produced. The simulation provides a tool for evaluating the influence of these configuration changes on stopping performance.

Vehicle components, for example, commercial vehicle brakes, are known to have differing characteristics from sample to

sample of the same type of component. Estimates of the range of variability of the mechanical properties of basic vehicle components can be used to define parameter variations for use in the simulation. Once the parameter variations are defined, the simulation can be used to study the influence of component variability on stopping distance.

Although this is a straight-line braking model, side-to-side differences in brake torque properties (brake imbalance) are allowed. It is assumed that the driver steers to correct for the moment produced by any imbalanced brake forces and that the steering-induced side forces have a negligibly small effect on braking performance. The reason for allowing a brake imbalance option is that current antilock systems control both wheels on an axle based on the wheel which is closest to locking. Consequently, the wheel which is not close to locking may be producing a level of braking force which is considerably less than optimum if the brake imbalance is large. Clearly, this effect can have an undesirable influence on stopping distance, and it needs to be considered in predicting brake performance.

The paragraph above provides an example of the detailed, specific type of problem which can be addressed with this simulation. Other typical applications of the simulation include the effect on wheels-unlocked stopping distance of:

(1) brake proportioning front to rear

(2) axle loads as a function of loading, suspension type, and vehicle geometry (wheelbase, center of gravity location, and axle position)

(3) variation of tire characteristics from axle to axle (in particular, variations in peak and slide braking force values)

(4) changes in antilock system design for the entire vehicle or from axle to axle

(5) changes in brake operating characteristics such as fade, effectiveness, and hysteresis.

An example set of results covering effects (1) through (5) for a particular vehicle is given in Reference 29.

3.2 Conclusions Concerning the Simulation Problem

The simulation approach described in this report provides a direct, albeit complex, method for obtaining quantitative predictions of vehicle braking response. Operating this simulation is in many ways analogous to conducting a vehicle response test. The control input, brake pressure, is selected before the test (or simulation run) and then used in the test (or simulation run). Vehicle response to the control input is measured (or computed). Thus, if the vehicle parameters are accurate and the equations describe the vehicle adequately, then operating the simulation is nearly equivalent to conducting skid pad tests.

Operating the simulation has several advantages over vehicle testing. It is inexpensive and safe. The influence of changes in vehicle components can be determined without fabricating and installing new components. The simulation output contains data on many more variables than can be measured with a reasonable amount of instrumentation on the test vehicle.

The main disadvantage of the simulation is the need to obtain parametric data. The effort, cost, and time required to measure vehicle parameters may be as large as the effort, cost, and time required to instrument an existing vehicle and make a few vehicle tests. However, the cost of testing will exceed the cost of simulating as the number of specified test conditions increases.

Other approaches to the problem of simulating (predicting) braking performance exist. A simplified program [24] has been developed to complement this program. The simplified program

provides preliminary results which can be very helpful in planning simulation studies and in understanding the results from the complex computer program. Another approach is the indirect, or so-called "inverse," approach in which the stopping time history is chosen, and the brake pressure required for this time history is calculated by the computer. This type of approach appears to be more useful in directional response studies of driver demand than in braking performance studies.

The simplified program described in [24] has an option which allows the user to select various brake proportioning arrangements. With a few trial runs the user can find a satisfactory proportioning arrangement. Clearly, programs can be written which will find an optimum proportioning for a given vehicle configuration. That type of program is aimed at the vehicle design (synthesis) problem. The large simulation described in this report is an analysis tool. To use it in the design context, the user can analyze a number of design possibilities and pick the best design, but this program does not find an optimum design automatically (i.e., by itself).

3.3 Recommended Research

Recent state-of-the-art reviews [25, 26, 27, 28] are in total agreement in two areas: (1) the scarcity of experimental work performed to validate predictive models, and (2) the need for accurately characterizing truck tire mechanics. It seems clear that more vehicle test programs are needed to verify that our understanding of truck mechanics (as represented by our simulation models) is sufficient to predict vehicle performance. Equally clear is the need to obtain truck tire shear force performance data. Further studies of truck tire mechanics should be performed now that appropriate tire testers have been developed for truck tires.

The commercial vehicle brake does not appear to be well understood at this time. The presence of brake variability hinders attempts to use a limited number of test runs to determine vehicle stopping performance. Further studies are needed to examine the variability, fade, and hysteresis exhibited by air-actuated brakes.

The use of antilock systems on commercial vehicles increases the complexity of the simulation problem. Efficient, simple means for representing antilock systems are needed.

And finally, once validated against vehicle test results, the simulation programs should be used to conduct large-scale parameter sensitivity studies for

(a) providing aids to vehicle design, and

(b) studying the importance of modeling simplifications and assumptions.

4.0 REFERENCES

1. Murphy, R.W., Bernard, J.E., and Winkler, C.B., A Computer Based Mathematical Method for Predicting the Braking Performance of Trucks and Tractor-Trailers, Phase I Report, Motor Truck Braking and Handling Performance Study, Highway Safety Research Institute, The Univ. of Michigan, Ann Arbor, September 15, 1972. (Available from the National Technical Information Service, Springfield, Va., 22151; Report PB-212-805.)

2. Bernard, J.E., Winkler, C.B., and Fancher, P.S., A Computer Based Mathematical Method for Predicting the Directional Response of Trucks and Tractor-Trailers, Phase II Technical Report, Motor Truck Braking and Handling Performance Study, Highway Safety Research Institute, Univ. of Michigan, Ann Arbor, June 1, 1973. (Available from the National Technical Information Service, Springfield, Va., 22151; Report PB-221-630.)

3. Bernard, J.E., "A Digital Computer Method for the Prediction of Braking Performance of Trucks and Tractor-Trailers, SAE Paper No. 730181, January 1975.

4. Fancher, P.S., Winkler, C.B., and Bernard, J.E., "Computer Simulation of the Braking and Handling Performance of Trucks and Tractor-Trailers," HIT Lab Reports, Vol. 3, No. 5, January 1973.

5. Bernard J.E., "A Digital Computer Method for the Prediction of the Braking and Handling Performance of Trucks and Tractor-Trailers," SAE Paper No. 740138, Feb.-Mar., 1974.

6. Winkler, C.B., "Measurement of Inertial Properties and Suspension Parameters of Heavy Highway Vehicles," SAE Paper No. 730182, January 1973.

7. Tielking, J.T., Fancher, P.S., and Wild, R.E., "Mechanical Properties of Truck Tires," SAE Paper No. 730183, January 1973.

8. Winkler, C.B., "Analysis and Computer Simulation of the Four Elliptical Leaf Spring Tandem Suspension," SAE Paper No. 740136, Feb.-Mar., 1974.

9. Ervin, R.D. and Fancher, P.S., "Preliminary Measurements of the Longitudinal Traction Properties of Truck Tires," SAE Paper No. 741139, November 1974.

10. Post, T.M., Fancher, P.S., and Bernard, J.E., "Torque Characteristics of Commercial Vehicle Brakes," SAE Paper No. 750210, February 1975.

11. Ervin, R.D., MacAdam, C.C., and Fancher, P.S., The Longitudinal Traction Characteristics of Truck Tires as Measured on Dry Pavements, Highway Safety Research Institute, Univ. of Michigan, Report No. UM-HSRI-PF-75-3, February 1975.

12. Bernard, J.E., "Some Time-Saving Methods for the Digital Simulation of Highway Vehicles," Simulation, Vol. 21, No. 6, December 1973.

13. Bernard, J.E., "Articulated Vehicle Simulation—A Fresh Approach to Some Recurring Problems," Proceedings of the 1974 Winter Simulation Conference, Washington, D.C., January 14-16, 1974.

14. Gurney, J.W. and Bernard, J.E., "Utilization of a Computer Simulation as an Aid to Predict Compliance with FMVSS 121," SAE Paper No. 740137, March, 1974.

15. Ervin, R.D., "Mobile Measurements of Truck Tire Traction," Proceedings, The Symposium on Commercial Vehicle Braking and Handling, Highway Safety Research Institute, Univ. of Michigan, May 5-7, 1975.

16. Post, T.M., "Measurement and Prediction of Commercial Vehicle Brake Torque," Proceedings, The Symposium on Commercial Vehicle Braking and Handling, Highway Safety Research Institute, Univ. of Michigan, May 5-7, 1975.

17. MacAdam, C.C., "A General Purpose Simulation for Antilock Braking Systems," Proceedings, The Symposium on Commercial Vehicle Braking and Handling, Highway Safety Research Institute, Univ. of Michigan, May 5-7, 1975.

18. Fancher, P.S., "Prediction of Braking and Directional Responses of Commercial Vehicles," Proceedings, The Symposium on Commercial Vehicle Braking and Handling, Highway Safety Research Institute, Univ. of Michigan, May 5-7, 1975.

19. Commercial Brochure, "Actuate Isolate Ride," Firestone Industrial Products Company.

20. Millner, N. and Parsaus, B., "Effects of Contact Geometry and Elastic Deformation on the Torque Characteristics of a Drum," Proceedings, Inst. of Mech. Engrs., 1973.

21. Newcomb, C.P. and Spurr, R.T., Braking of Road Vehicles, Chapman and Hall, London, 1967.

22. System/360 Scientific Subroutine Package, Version III, Programmers Manual, IBM.

23. Dugoff, H., Fancher, P.S., and Segel, L., Tire Performance Characteristics Affecting Vehicle Response to Steering and Braking Control Inputs, Final Report for DOT, Contract FH-11-7290, Highway Safety Research Institute, Univ. of Michigan, March 1971.

24. Moncarz, H.T. and Bernard, J.E., An Interactive Computer Program for the Prediction of Commercial Vehicle Braking Performance, Highway Safety Research Institute, Univ. of Michigan, Report No. UM-HSRI-PF-75-4, April 1975.

25. Dugoff, H. and Murphy, R.W., "The Dynamic Performance of Articulated Highway Vehicles—A Review of the State-of-the-Art," SAE Paper No. 710223, January 1971.

26. Eshleman, R.L., "Particular Handling Safety Problems of Trucks and Articulated Vehicles," Vehicle Safety Research Integration Symposium Proceedings, U.S. Dept. of Transportation, DOT-HS-820-306, May 1973.

27. Smith, N.P. and Barker, D., The Operational Safety of Articulated Vehicles, First Report: Literature Survey on Articulated Vehicle Stability and Proposals for Further Research, Report No. AFC.9/1, Motor Industry Research Association, Lindley, England, August 1974.

28. Marples, V., Safety in Trucking Operations, Department of Mech. Eng., Report No. ME/A 75-1, Carleton Univ., Ottawa, Canada, January 1975.

29. Fancher, P. and MacAdam, C., "Computer Analysis of Antilock System Performance in the Braking of Commercial Vehicles," Proceedings of Conference on Braking of Road Vehicles, The Inst. of Mech. Engrs., March 23,25, 1976.

30. Moncarz, H., Bernard, J., and Fancher, P., A Simplified Interactive Simulation for Predicting the Braking and Steering Response of Commercial Vehicles, Highway Safety Research Institute, Univ. of Michigan, August 1975.